UNIVERSITÉ DU QUÉBEC

ÉTUDE DES VARIATIONS SPATIALES ET TEMPORELLES DU

PHYTOPLANCTON EN MER DE BEAUFORT : BIOMASSE, PRODUCTION ET

STRUCTURE DE TAILLE DES COMMUNAUTÉS

THÈSE

PRÉSENTÉE À

L'UNIVERSITÉ DU QUÉBEC À RIMOUSKI

comme exigence partielle du programme de doctorat conjoint en Océanographie
à l'obtention du grade de

PHILOSOPHIAE DOCTOR (OCÉANOGRAPHIE)

PAR

SONIA BRUGEL

Septembre 2009

UNIVERSITÉ DU QUÉBEC À RIMOUSKI
Service de la bibliothèque

Avertissement

AVANT-PROPOS

L'objet de cette thèse de doctorat est l'étude des variations spatiales et temporelles du phytoplancton en mer de Beaufort, englobant le plateau continental du Mackenzie et le golfe d'Amundsen, au cours de la période libre de glace. Ce doctorat a été réalisé dans le cadre du programme CASES (Canadian Arctic Shelf Exchange Study).

Le cœur de la thèse est constitué de trois chapitres, présentés sous forme d'articles scientifiques rédigés en anglais. Le premier chapitre a été accepté pour publication dans la revue Marine Ecology Progress Series avec corrections mineures : « Phytoplankton biomass and production in the southeastern Beaufort Sea in fall 2002 and 2003 » Brugel S, Nozais C, Poulin M, Tremblay J-E, Miller LA, Simpson KG, Gratton Y, Demers S.

Les résultats rapportés dans cette thèse ont fait l'objet de trois affiches et de deux présentations orales présentées au cours de plusieurs congrès : CASES general meetings, Montréal - 2004, Winnipeg - 2006 et Québec - 2007, ASLO Summer Meeting, Santiago de Compostela – 2005.

REMERCIEMENTS

Je me dois de remercier mon directeur Serge Demers et mon co-directeur Christian Nozais pour m'avoir permis de travailler sur ce projet de doctorat. Merci également aux membres ayant accepté de prendre part à mon comité de thèse Bruno Zakardjian et Jean-Éric Tremblay.

Je remercie Michel Gosselin, qui a accepté de présider mon jury de thèse, et Susana Agustí officiant en tant que membre externe du jury de thèse.

Cette thèse a été réalisée avec le support financier du Conseil de recherche en science et en génie du Canada (CRSNG) et de l'Institut des sciences de la mer de Rimouski (ISMER).

Cette thèse s'intégrait dans le programme de recherche CASES sous la direction de Louis Fortier, j'en remercie donc les acteurs : les capitaines et équipages de la Garde côtière canadienne à bord du Radisson et de l'Amundsen, les chefs de mission successifs, Martin Fortier, Dave Barber, Lisa Miller, Jody Deming, Tim Papakyriakou, Louis Fortier, Yves Gratton, Dave Scott, et André Rochon.

J'ai également bénéficié de l'utilisation de certaines données. Merci à Yves Gratton, Pascal Guillot et Marie-Emmanuelle Rail pour les données de CTD, à Lisa Miller pour les concentrations de carbone inorganique dissous, à Neil Price, Jean-Eric Tremblay et Kyle Simpson pour les éléments nutritifs, à Michel Poulin, Lyse Bérard-Therriault et Sylvie Lessard pour les identifications taxonomiques, et à Dave Barber et Wayn Chan pour les concentrations de glace.

RESUME

Cette thèse de doctorat est consacrée à l'étude des variations spatiales et temporelles du phytoplancton du sud-est de la mer de Beaufort, comprenant le plateau continental du Mackenzie et le golfe d'Amundsen, au cours de la période libre de glace. La communauté phytoplanctonique a été caractérisée par la biomasse, la production primaire et la structure de taille du phytoplancton <20 µm.

En automne en 2002 et 2003, la biomasse phytoplanctonique et la contribution des cellules >5 µm étaient plus élevées dans le golfe d'Amundsen que sur le plateau continental du Mackenzie. Au début de l'automne 2003, la communauté phytoplanctonique du golfe d'Amundsen présentait les caractéristiques d'une efflorescence automnale, qui aurait possiblement culminé à la fin du mois de septembre. Les proportions élevées de production primaire par rapport à la biomasse et la dominance générale des cellules <5 µm suggéraient que la production automnale en mer de Beaufort était entretenue par un recyclage actif. En automne 2003, la diminution de la biomasse phytoplanctonique et de la production primaire au cours du temps était probablement due à la diminution de la disponibilité en lumière.

Au printemps et en été 2004, les différences de distribution spatiale étaient également marquées. En juin, la communauté phytoplanctonique était dans une situation de pré-bloom dans le sud du golfe d'Amundsen, et en situation de post-bloom au centre du golfe, en raison de l'ouverture précoce de la polynie du Cap Bathurst. Dans le golfe d'Amundsen, la biomasse chlorophyllienne, ainsi que la contribution des cellules >5 µm, restaient faibles du printemps à l'été. Par contre, sur le plateau continental du Mackenzie,

les phénomènes d'upwelling liés au vent et l'extension du panache des eaux du fleuve Mackenzie favorisaient la production phytoplanctonique, en augmentant la biomasse chlorophyllienne due aux cellules >20 μm et l'export potentiel de production primaire en profondeur. En général, les proportions élevées de production primaire par rapport à la biomasse, ainsi que l'absence d'accumulation de cellules >5 μm dans le golfe d'Amundsen, suggéraient une forte pression de broutage sur le phytoplancton et un recyclage actif. Dans le golfe d'Amundsen, la production primaire annuelle a été estimée à 21 g C m^{-2} a^{-1}. Cette faible valeur résulte probablement d'une sous-estimation liée à l'extrapolation, mais également du faible niveau hivernal de nitrates, qui pré-conditionnait vraisemblablement faible production phytoplanctonique annuelle.

La structure de taille du phytoplancton <20 μm a été étudiée en automne 2003 et au printemps et en été 2004. Le picophytoplancton (<3 μm) dominait le phytoplancton <20 μm en abondance pendant toutes les saisons. Dans le golfe d'Amundsen, le picophytoplancton répondait plus rapidement que le nanophytoplancton au retrait printanier des glaces. De plus, les conditions de retrait des glaces modelaient la structure de taille du phytoplancton <20 μm. En outre, en été, la circulation et la fonte de glace mobile favorisaient la croissance du pico- et du nanophytoplancton de 3-10 μm. En automne, la diminution de la disponibilité en lumière était probablement responsable de la chute de l'abondance du phytoplancton <20 μm. Sur le plateau continental du Mackenzie, le phytoplancton <20 μm était dominé, au large, par le picophytoplancton en été et en automne, alors que, près de la côte, le picophytoplancton était moins dominant en été qu'en automne. Le panache des eaux du fleuve Mackenzie était probablement une source de cellules de plus grande taille en

été (nanophytoplancton) qu'à la fin de l'automne (pico- et nanophytoplancton de 3-10 μm). En général, les cellules picophytoplanctoniques étaient fortement retenues dans les eaux de surface, et entretenaient probablement un réseau trophique microbien très actif.

Cette étude souligne l'importance des cellules phytoplanctoniques de petite taille (<3-5 μm) dans le réseau trophique de la mer de Beaufort. Ces cellules dominaient la biomasse et la production pour la plus grande partie de la période libre de glace, notamment dans le golfe d'Amundsen où la dynamique du couvert de glace semble être le principal facteur de variations spatio-temporelles. Par contre, sur le plateau continental du Mackenzie les apports d'eaux douces du fleuve Mackenzie et les phénomènes d'upwelling le long du talus continental favoriseraient épisodiquement la production de cellules phytoplanctoniques de grande taille.

TABLE DES MATIERES

LISTE DES FIGURES

CHAPITRE II

CHAPITRE III

LISTE DES TABLEAUX

INTRODUCTION GENERALE

L'océan Arctique

Depuis la seconde moitié du XIXième siècle, les activités humaines ont conduit à une augmentation considérable des concentrations en dioxyde de carbone (CO_2) atmosphérique, de l'ordre de 31 % (IPCC 2001), qui a engendré des perturbations climatiques et notamment l'augmentation de la température globale. La température globale a augmenté de 1,5°C depuis 150 ans (Overpeck et al. 1997). Les régions situées aux hautes latitudes, comme l'océan Arctique, sont plus vulnérables au phénomène de réchauffement climatique (Vinnikov et al. 1999, ACIA 2005). En effet, au cours du XXième siècle la température atmosphérique en Arctique a augmenté de 5°C au-dessus des terres (IPCC 2001), et ce, à un rythme deux fois élevé que pour le reste du globe (ACIA 2005). Des modèles climatiques prévoient une augmentation de température de 3,9 à 4,5°C pour l'Arctique d'ici 2050, alors qu'elle ne serait que de 1,7 à 2,2°C au niveau global (Dixon et al. 2003). De surcroît, un rétrécissement et un amincissement du couvert de la glace de mer ont été observés en Arctique (Cavalieri et al. 1997, Johannessen et al. 1999, Rothrock et al. 1999, Vinnikov et al. 1999). L'étendue du couvert de glace estival s'est réduite de 15-20 % ces trois dernières décennies (ACIA 2005), et son épaisseur a diminué de 12 % en moyenne (Holloway & Sou 2002). Depuis 2001, la réduction du couvert de glace estival s'est accélérée atteignant un taux de 10 % par décennie, et l'année 2007 a enregistré la plus faible étendue de glace estivale de 4,28x10^6 km² (NSIDC 2007). Selon les projections climatiques dans un contexte

de réchauffement global, l'océan Arctique serait totalement libre de glace en été à la fin du XXIième siècle (ACIA 2005, Serreze et al. 2007) ou dès 2040 (Holland et al. 2006). La réduction du couvert de glace et l'augmentation de température observées ces dernières années seraient également dues aux variations naturelles de la circulation atmosphérique, i.e. l'oscillation arctique (Deser et al. 2000), dont l'effet pourrait être amplifié par les changements provoqués par les activités humaines (Shindell et al. 1999). Quelles que soient les causes de la réduction de couvert de glace, à terme, l'océan Arctique deviendrait un océan à couvert de glace saisonnier (Arzel et al. 2006, Zhang & Walsh 2006). En outre, la fonte hâtive des glaces au printemps, ainsi que la formation tardive du couvert de glace en automne, allongeraient la période libre de glace (Stroeve et al. 2006).

Au-delà de son couvert de glace, l'océan Arctique est également caractérisé par une très forte stratification, qui est principalement due à des apports fluviaux très importants (Macdonald et al. 2004a). En effet, alors que l'océan Arctique ne représente que 1 % du volume total des océans, il reçoit 11 % des apports fluviaux globaux (Dittmar & Kattner 2003). Les apports d'eau douce maintiennent la faible densité de la couche de surface (~0-50 m) au-dessus de l'halocline permanente formée par des eaux plus denses d'origine pacifique ou atlantique, ce qui limite les échanges entre les eaux de surface et les eaux plus profondes (Macdonald et al. 1987, McLaughlin et al. 1996). Dans l'océan Arctique, les plateaux continentaux couvrent 52,7 % de la superficie (Jakobsson et al. 2004). Ces régions soutiennent une forte production primaire (AMAP 1998, Sakshaug 2004), qui atteint 80 % de la production primaire totale de l'océan Arctique (Hill & Cota 2005). Les variations

saisonnières y sont particulièrement marquées par la superposition des fluctuations du débit des fleuves au cycle de formation et fonte des glaces (Jakobsson et al. 2004). Dans un contexte de changement climatique, l'accroissement des précipitations sur les bassins versants des fleuves arctiques augmenterait leur débit (Peterson et al. 2002, 2006, ACIA 2005). Par conséquent, les plateaux continentaux arctiques, qui sont des environnements très variables et encore peu étudiés (Carmack et al. 2006), seraient particulièrement vulnérables au changement climatique.

Dans les régions polaires, les zones d'eau libre entourées de glace sont appelées des polynies. Ces polynies peuvent être libre de glace toute l'année ou recouvertes pendant les périodes les plus froides (Smith et al. 1990). La réduction précoce de l'étendue et de l'épaisseur de la glace favorise la production primaire, qui est généralement plus forte dans les polynies que dans les régions adjacentes (Pesant et al. 1996, Klein et al. 2002, Tremblay & Smith 2007). Ces zones très productives ont également un grand intérêt écologique en Arctique, puisqu'elles représentent des aires primordiales de reproduction et d'alimentation pour de nombreux oiseaux et mammifères marins (Stirling 1980, 1997). De plus, les polynies sont libres de glace pour de plus longues périodes que les régions adjacentes, et représenteraient de ce fait des modèles pour l'étude des mers arctiques dont la période d'englacement diminuerait (Tremblay et al. 2006).

Importance et dynamique saisonniere du phytoplancton

Le phytoplancton constitue la première voie d'incorporation du carbone inorganique dans les écosystèmes marins à travers le processus de photosynthèse ; le carbone biogénique phytoplanctonique est ensuite transféré vers les niveaux trophiques supérieurs par broutage (Legendre 1990). Le carbone phytoplanctonique peut être exporté en profondeur vers les réseaux trophiques benthiques et conduire à la séquestration de carbone à long terme (Legendre & Le Fèvre 1995). Le transfert du phytoplancton à travers l'écosystème pélagique est fonction de la taille des cellules phytoplanctoniques. Selon la taille des cellules, le phytoplancton est divisé en picophytoplancton (<2 ou 3 µm), nanophytoplancton (2-3 à 20 µm) et microphytoplancton (>20 µm) (Sieburth et al. 1978, Li 1986). Les cellules de grande taille du nano- et du microphytoplancton (généralement >5 µm) sont préférablement exportées en profondeur (Chisholm 1992), par sédimentation de cellules intactes, de pelotes fécales issue du broutage par le meso- et macrozooplancton ou de neige marine (Legendre 1990). Les cellules de plus petite taille (pico- et nanophytoplancton <5 µm), quant à elles, sont retenues dans les eaux de surface et sont broutées par le microzooplancton, alimentant ainsi le réseau trophique microbien (Legendre & Le Fèvre 1995).

La production primaire est régie par de nombreux mécanismes physiques et chimiques, dont l'intensité du mélange vertical, l'intensité lumineuse et la disponibilité en éléments nutritifs (Smith & Sakshaug 1990). Dans les milieux marins où l'azote est l'élément nutritif qui limite la production phytoplanctonique, comme dans l'océan Arctique

(Wheeler et al. 1997), l'azote nouvellement disponible dans la zone euphotique sous forme de nitrate, provenant du mélange vertical, de remontée d'eaux profondes ou d'apports continentaux et atmosphériques, favorise la production de cellules de grande taille (Dugdale & Goering 1967), alors que l'azote provenant de la minéralisation bactérienne ou de l'excrétion animale sous forme d'ammonium implique des cellules de petite taille (Harrison & Wood 1988, Agawin et al. 2000).

Dans l'océan Arctique, les variations du couvert de glace influencent la production phytoplanctonique (Smith & Sakshaug 1990). La présence de glace diminue fortement la pénétration de lumière dans la colonne d'eau (Palmisano et al. 1987), et le cycle de formation et de fonte de la glace contraint la période production phytoplanctonique à quelques mois (Sakshaug 2004). La saisonnalité induite par la glace est couplée à celle de l'inclinaison solaire ; les régions au-delà de 66,7°N sont soumises à l'absence totale de lumière autour du solstice d'hiver et à des périodes d'éclairement continu autour du solstice d'été (Smith & Sakshaug 1990). L'efficacité photosynthétique ainsi que le taux de croissance du phytoplancton sont fortement dépendants de l'intensité lumineuse (Sakshaug & Slagstad 1991). Dans l'océan Arctique, outre les variations saisonnières, la disponibilité en lumière est très variable, en raison de la formation importante de nuages et de brouillard, notamment lorsque les eaux sont libres de glace, et de la dérive des glaces flottantes, qui diminuent la quantité de lumière dans la colonne d'eau (Sakshaug & Slagstad 1991). L'intensité du mélange vertical influence également l'efficacité photosynthétique du phytoplancton en exposant les cellules plus ou moins rapidement à différentes intensités

lumineuses. Or les mécanismes de photoacclimatation se mettent généralement en place à des échelles de temps qui peuvent être plus importantes que celles des variations du mélange vertical ou de l'éclairement incident, générant des processus de photoinhibition (Harrison & Platt 1986). La stabilité de la colonne d'eau est également dictée par le cycle de formation et de fonte de la glace (Carmack & Macdonald 2002). Typiquement au printemps, des efflorescences algales se développent suite à l'augmentation de l'éclairement incident, à la pénétration accrue de la lumière dans la colonne d'eau et à la stratification induite par la fonte des glaces, et ce, jusqu'à épuisement des sels nutritifs disponibles dans la zone euphotique (Sakshaug 2004). D'autres efflorescences peuvent se produire à la suite d'un réapprovisionnement de la couche de surface en éléments nutritifs (remontée d'eaux profondes, mélange vertical induit par le vent, apports continentaux…) jusqu'en automne.

Jusqu'à récemment, il était considéré que le nano- et le microphytoplancton (>5 µm) dominaient les communautés phytoplanctoniques de l'océan Arctique (von Quillfeldt 1997, Sakshaug 2004). Cependant, des travaux plus récents se sont intéressé aux formes phytoplanctoniques de plus petite taille (Wassmann et al. 2006) et ont souligné l'importance du phytoplancton de petit taille (<5 µm) dans l'océan Arctique en terme d'abondance (Mostajir et al. 2001, Lovejoy et al. 2002, Sherr et al. 2003, Not et al. 2005, Schloss et al. 2008, Tremblay 2008), de biomasse (Lovejoy et al. 2002, 2007, Sherr et al. 2003) et de production primaire (Gosselin et al. 1997, Lee & Whitledge 2005). Dans un contexte de changement climatique, la réduction du couvert de glace allongerait la période

de production, favorisant ainsi la production phytoplanctonique. Cependant, l'effet d'une modification du mélange vertical (intensité et profondeur de mélange), due à l'exposition de la couche de surface aux vents, pourrait avoir un impact difficilement prévisible sur la structure des communautés phytoplanctoniques (Sakshaug 2004).

La mer de Beaufort

La mer de Beaufort borde l'Alaska et les Territoires du Nord-Ouest, et s'étend au-dessus du bassin Canadien. La partie canadienne de la mer de Beaufort comprend le plateau continental du Mackenzie et le golfe d'Amundsen (Fig. 1). Le plateau continental du Mackenzie est relativement étroit (~120km) et sillonné par le canyon Mackenzie sur la bordure ouest et le canyon Kugmallit au centre (Macdonald et al. 2004b). Le golfe d'Amundsen est situé entre la bordure est du plateau continental et l'île de Banks, et abrite la polynie du Cap Bathurst (Topham et al. 1983).

En mer de Beaufort, la circulation générale est gouvernée par le gyre de Beaufort qui impose une circulation anticyclonique aux eaux de surface et au pack de glace pluriannuelle. Le long de la côte, la circulation est dictée par les vents (AMAP 1998). En sub-surface (50-75 m), le contre-courant de Beaufort impose une circulation cyclonique, qui déplace les eaux vers l'est le long du plateau continental (Aagaard 1984). Les eaux de surface de la couche de mélange s'étalent sur les 50 premiers mètres ; en dessous se trouvent les eaux d'origine pacifique issues du détroit de Bering ; plus en profondeur (sous ~220 m) les eaux sont d'origine atlantique (Carmack et al. 2004). La très forte stratification

empêche le plus souvent un apport de sels nutritifs dans la couche de surface à partir des eaux pacifiques riches en éléments nutritifs. Cependant, des phénomènes d'upwelling sont souvent observés le long du plateau ainsi qu'au niveau des canyons Mackenzie et Kugmallit (Williams et al. 2006, 2008), permettant ainsi un apport de nutriments dans la couche de surface (Macdonald et al. 1987).

En mer de Beaufort, la glace se forme en octobre suite à la baisse de température. Sur le plateau continental, la banquise s'étend jusqu'au chenal de séparation qui fait partie du système de chenaux de séparation circum-arctique. Au-delà du chenal de séparation, le couvert de glace est constitué par un mélange de glace nouvellement formée et de glace pluriannuelle, puis par le pack de glace pluriannuelle (Barber & Hanesiak 2004). Le mouvement du pack de glace pluriannuelle est dicté par la circulation du gyre de Beaufort, et la limite du pack de glace s'étend plus ou moins au sud selon les champs de pression atmosphérique. La période de débâcle est variable d'année en année, mais se produit généralement fin mai. La disparition de la glace peut être lente, ainsi en juillet et août les glaces peuvent persister, alors qu'en septembre la zone est totalement libre de glace (Barber & Hanesiak 2004).
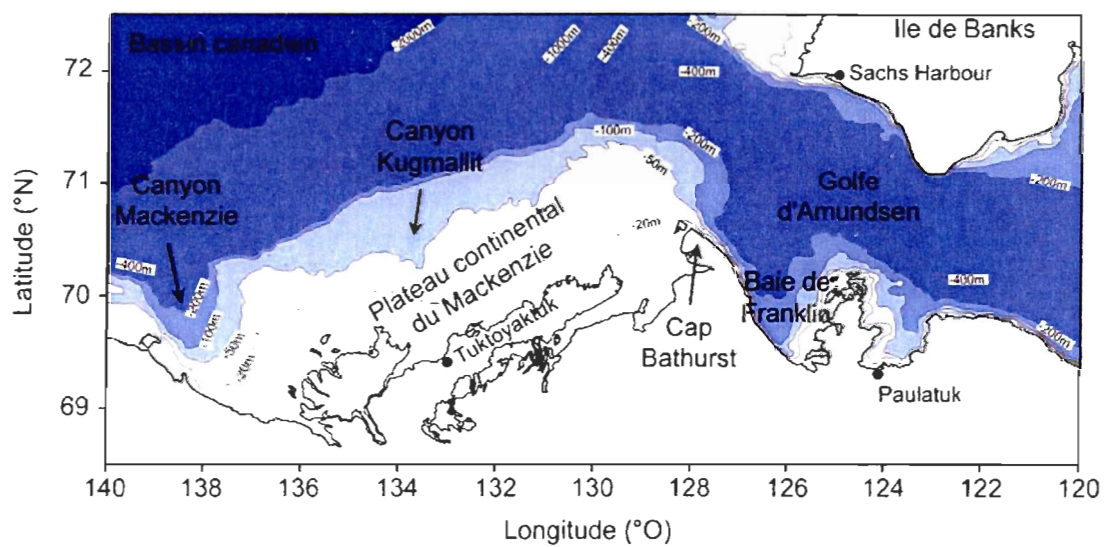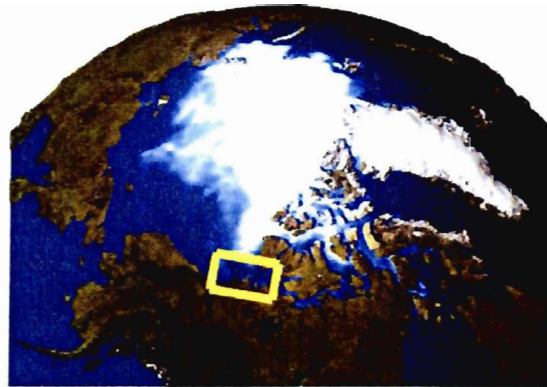
Figure 1 : Situation et particularités géographiques de la mer de Beaufort (adaptée de http://earthobservatory.nasa.gov/Newsroom/NewImages/images.php3?img_id=16340).

Les dernières études publiées portant sur l'écosystème pélagique et notamment sur le phytoplancton en mer de Beaufort ont été conduites dans les années 70-80, essentiellement en zone très côtière (Alexander 1974, Horner & Schrader 1982, Horner 1984, Parsons et al. 1988) et sur le plateau continental (Hsiao et al. 1977, Parsons et al. 1989, Carmack et al. 2004), le golfe d'Amundsen n'ayant fait l'objet d'échantillonnage qu'à partir de 2002 (Lee & Whitledge 2005). De plus, seule la période estivale a été étudiée en raison des conditions de glace rendant l'accès difficile et de l'absence de logistique adéquate. Considérant la variabilité actuelle du couvert de glace et les prévisions futures quant à son étendue, le programme CASES (Canadian Arctic Shelf Exchange Study) a été mis en place afin d'étudier l'effet de la variabilité du couvert de glace sur le système de la mer de Beaufort en terme de flux biogéochimiques et d'échanges entre le plateau continental et le bassin profond.

Le fleuve Mackenzie se déverse sur le plateau continental du Mackenzie. En termes de débit, le Mackenzie est le quatrième fleuve en Arctique, et déverse annuellement 330 km^3 d'eau douce sur le plateau (Macdonald et al. 1998). Ce fleuve est le plus important en considérant la charge sédimentaire qui peut atteindre 124x10^6 tonnes par an (Holmes et al. 2002). Soixante dix pour cent des eaux sont déversés entre mai et septembre, les débits les plus forts étant observés entre mai et juin (Carmack & Macdonald 2002). Les eaux déversées sur le plateau influencent la production phytoplanctonique, puisqu'elles constituent une source importante d'éléments nutritifs mais aussi de particules, qui diminuent la pénétration de la lumière dans la colonne d'eau (Parsons et al. 1989, Carmack

et al. 2004). La production primaire annuelle sur le plateau est estimée entre 20 et 28 g C m^{-2} (Macdonald et al. 1987, Lavoie et al. 2008).

Dans le golfe d'Amundsen, la polynie du Cap Bathurst est formée par advection de la glace sous l'influence des vents (Carmack & Macdonald 2002), elle s'ouvre le plus souvent en juin jusqu'à ce que la glace se reforme en octobre (Arrigo & Van Dijken 2004). Selon les données satellitaires de chlorophylle, le cycle saisonnier de production phytoplanctonique semble relié à la dynamique du couvert de glace et notamment à la période et à la vitesse d'ouverture de la polynie (Arrigo & Van Dijken 2004). De plus, la période de production phytoplanctonique semble marquée par deux périodes d'efflorescence, la première à la fin du printemps ou début de l'été, et la deuxième à la fin de l'été ou début d'automne. La production annuelle estimée par Arrigo et Van Dijken (2004) est très variable, entre 90 et 175 g C m^{-2}, ce qui placerait la polynie du Cap Bathurst parmi les écosystèmes pélagiques les plus productifs de l'océan Arctique.

Objectifs

Dans le contexte climatique actuel, l'océan Arctique semble condamné au changement. Des études récentes ont déjà rapporté des modifications des écosystèmes pélagiques arctiques (Hegseth et al. 2008, Wassmann et al. 2008), cependant de nombreuses données nécessaires à la compréhension du fonctionnement des écosystèmes marins arctiques manquent encore dans certaines régions (Carmack et al. 2006). L'objet de ce travail est l'étude la communauté phytoplanctonique, notamment en termes de biomasse, de production primaire et de structure de taille, en relation avec les forçages

environnementaux dans la mer de Beaufort au cours de la période libre de glace. Cette étude était articulée autour de plusieurs hypothèses, abordées dans les différents chapitres, selon lesquelles : (1) hors des périodes d'efflorescence, la communauté phytoplanctonique serait dominée par les cellules de petite taille, (2) la disponibilité en lumière et le couvert de glace modèleraient la dynamique saisonnière des communautés et de la production phytoplanctonique, (3) la forte stratification de la colonne d'eau limiterait la production primaire au cours de la période libre de glace en empêchant de nouveaux apports d'éléments nutritifs dans la zone euphotique, (4) les eaux du fleuve Mackenzie influenceraient les communautés phytoplanctoniques par le biais des apports d'eau douce, d'éléments nutritifs et de particules, et (5) les phénomènes d'upwelling le long du plateau continental favoriseraient le développement du phytoplancton.

Le premier chapitre traite plus particulièrement de la biomasse et de la production phytoplanctonique au cours de la période automnale. La fin de la période productive a été très peu étudiée dans l'océan Arctique en général, en raison des contraintes logistiques liées aux conditions climatiques (Hegseth 1997). Le programme CASES a permis d'étudier la transition d'une période favorable à la production phytoplanctonique à une période de forçages environnementaux extrêmes (diminution de la lumière incidente et des températures jusqu'au point de congélation, et la formation de glace). De plus, des campagnes d'échantillonnage, couvrant une même période au cours de deux années successives, a permis une comparaison interannuelle. La distribution spatiale, ainsi que la

dynamique temporelle, de la biomasse phytoplanctonique ont été mises en relation avec facteurs environnementaux.

Le deuxième chapitre correspond à l'étude de la biomasse et de la production phytoplanctonique au cours du printemps et de l'été, après dislocation du couvert de glace. La dynamique saisonnière du phytoplancton a été plus particulièrement étudiée dans le golfe d'Amundsen, alors que les variations de la distribution spatiale du phytoplancton ont été considérées dans le golfe d'Amundsen et au niveau du plateau continental de Mackenzie, sous l'influence de forts débits du fleuve Mackenzie. De plus, la production primaire annuelle a été estimée pour le golfe d'Amundsen à partir d'un cycle saisonnier composite de production primaire.

Le troisième chapitre a été consacré à la caractérisation de la structure de taille des communautés phytoplanctoniques <20 µm. Dans l'océan Arctique, les populations du picophytoplancton et du nanophytoplancton de petite taille ne sont étudiées que depuis quelques années, malgré leur grande importance au sein des communautés phytoplanctoniques (Mostajir et al. 2001, Not et al. 2005, Lovejoy et al. 2006, 2007). Les variations saisonnières et spatiales de la distribution du pico- et du nanophytoplancton ont été examinées en relation avec les forçages environnementaux, tels que la dynamique du couvert de glace et les apports du fleuve Mackenzie.

CHAPITRE I

PHYTOPLANKTON BIOMASS AND PRODUCTION IN THE SOUTHEASTERN

BEAUFORT SEA IN FALL 2002 AND 2003

RESUME

Les communautés phytoplanctoniques du plateau continental du Mackenzie et du golfe d'Amundsen (mer de Beaufort) ont été caractérisées (biomasse chlorophyllienne, production primaire et taxonomie) en automne en 2002 et en 2003. Les différences spatiales étaient marquées, et ce, particulièrement en début d'automne. La biomasse phytoplanctonique totale et la contribution des grandes cellules (>5 μm) à la biomasse étaient plus élevées dans le golfe d'Amundsen que sur le plateau continental du Mackenzie. La communauté des cellules autotrophes (>10 μm) était dominée en abondance par les diatomées dans le golfe d'Amundsen et par les dinoflagellés sur le plateau continental du Mackenzie. L'abondance des chlorophycées mettait en évidence l'influence du fleuve Mackenzie sur le plateau continental du Mackenzie. Contrairement à l'année 2002, lorsque tous les échantillons provenaient du début de l'automne, la communauté phytoplanctonique du golfe d'Amundsen, en 2003, présentait les caractéristiques d'une efflorescence automnale, qui aurait possiblement culminé à la fin du mois de septembre. Cependant, en début d'automne, les taux de production primaire étaient similaires pour les deux années, atteignant une moyenne de 75 mg C m^{-2} j^{-1}. Les proportions élevées de production primaire par rapport à la biomasse et la dominance générale des cellules de petite taille (<5 μm) suggèrent que la production en mer de Beaufort était entretenue par un recyclage actif. En automne 2003, la diminution de la biomasse phytoplanctonique et de la production primaire au cours du temps était probablement due à la diminution de la disponibilité en lumière. Enfin, la production primaire estimée, dans cette étude, pour la période automnale, de la mi-septembre à la fin du mois d'octobre, pourrait augmenter de 15 % l'estimation de production primaire annuelle précédente pour la mer de Beaufort.

ABSTRACT

The phytoplankton community of the Mackenzie shelf and the Amundsen Gulf (southeastern Beaufort Sea) was characterized (e.g. chlorophyll *a* biomass, primary production and taxonomy) during fall 2002 and 2003. Spatial differences were evident, particularly in early fall. Total phytoplankton biomass and the contribution of large cells (>5 µm) to biomass where higher in the Amundsen Gulf than on the Mackenzie shelf. The community of autotrophic cells (>10 µm) was numerically dominated by diatoms in the Amundsen Gulf and by dinoflagellates on the Mackenzie shelf. The abundance of chlorophytes revealed the influence of the Mackenzie River on the Mackenzie shelf. Contrary to 2002, when all measurements were from early fall, the phytoplankton community of the Amundsen Gulf in 2003 presented the characteristics of a late bloom, which presumably peaked in late September. In early fall, however, rates of primary production were similar for both years, averaging 75 mg C m^{-2} d^{-1}. High primary production-to-biomass ratios and overall dominance of small cells (<5 µm) suggest that pelagic production in the southeastern Beaufort Sea was sustained by active recycling. During fall 2003, a temporal decrease in phytoplankton biomass and primary production likely resulted from decreasing light availability. Overall, the fall primary production estimated in this study, from mid-September to the end of October, could increase the annual primary production previously estimated for the Beaufort Sea by 15 %.

INTRODUCTION

The increasing impacts of climate change at northern latitudes make arctic ecosystems a major environmental concern (ACIA 2005). Field studies, as well as numerical simulations, indicate that the Arctic Ocean and more particularly its marginal seas are warming faster than other oceans (Rigor et al. 2000, Comiso 2003). The arctic sea ice minimum extent (i.e. summer) decreased of about $8x10^5$ km^2 over the 1978-2003 period (Johannessen et al. 2004), and numerical models predict that the Arctic Ocean could be free of ice in summer by the end of the 21st century (Serreze et al. 2007) or as early as 2040 (Holland et al. 2006). Since 2002, the Arctic Ocean has experienced minimal sea ice extent records, with a new maximum in summer open water in September 2007 (NSIDC 2007, Comiso et al. 2008), suggesting the acceleration of sea ice cover shrinking. The Arctic Ocean is also strongly influenced by large river inflow (Macdonald et al. 2004a), and the freshwater inputs will likely increase through the intensification of the hydrological cycle (Peterson et al. 2002); therefore its marginal seas would be even more sensitive to climate change impact (ACIA 2005). Arctic ecosystems are expected to be affected by climate changes, e.g., shifts in the biodiversity and the food web structure (Gradinger & Bluhm 2005); though it is unclear how these changes will impact the components and pathways of carbon cycling (Walsh et al. 2004, Wassmann 2004). Analysis of climate-related changes in arctic ecosystems and model validation need to be based on historical measurements, in order to identify where the impacts of climate change are most likely to be observed.

However such data are still missing in some biologically active regions and seasons in the Arctic Ocean (Carmack & Wassmann 2006).

Arctic marine environments are characterized by large seasonal variations in solar radiation and sea ice cover (Sakshaug & Slagstad 1991). Indeed, pelagic phytoplankton production is usually constrained to the summer months between sea ice melting in spring and the freeze-up in fall, and high phytoplankton production and standing stocks are restricted to relatively short periods of the ice-free season (Sakshaug 2004). Moreover, phytoplankton is the most important mediator of carbon flow in pelagic ecosystems, and phytoplankton cell size is a critical factor in the fate of carbon through the food web (Legendre & Le Fèvre 1995). For example, carbon export and transfer to higher trophic levels are favoured by large cell production (Legendre & Le Fèvre 1991). However, blooms of large microphytoplankton cells are often constrained to a couple of weeks and smaller cells, i.e. nano- and picophytoplankton, often dominate outside these periods (Not et al. 2005).

The highest rates of primary production in the Arctic Ocean are observed on continental shelves and in polynyas (Sakshaug 2004, Stirling 1997). Nevertheless, little research has been undertaken on the phytoplankton dynamics of interior continental shelves due to logistical constraints, and this holds particularly true for the southeastern Beaufort Sea (Horner & Schrader 1982, Carmack et al. 2004). In the Beaufort Sea, the last study of phytoplankton on the Mackenzie shelf was conducted in the late 80's (Carmack et al. 2004), and very few direct measurements were taken in the Amundsen Gulf (Lee & Withledge 2005). Recent satellite-based surveys have revealed a strong interannual

variability of the sea ice cover and potentially of phytoplankton dynamics in the Amundsen Gulf, which contains a large recurrent polynya (Arrigo & Van Dijken 2004). In the current climate change context, the ice-free season, that is the phytoplankton productive season, is expected to lengthen (Sakshaug 2004); however, little is known about phytoplankton dynamics at the end of the growth season (Hegseth 1997), under decreasing temperature, sea ice formation, and reduced light availability. Conditions at the end of the productive season have been rarely studied in the Arctic (Heimdal 1983, Hegseth 1997), but numerical models predict that light limitation would terminate phytoplankton growth (Slagstad & Støle-Hansen 1991).

The spatio-temporal distribution of phytoplankton needs to be studied in order to understand ecosystems and biogeochemical cycles and to later model the impacts of climate change on the Arctic Ocean and its marginal seas (Carmack & Wassmann 2006). In the framework of the Canadian Arctic Shelf Exchange Study (CASES), the southeastern Beaufort Sea, comprising the Mackenzie continental shelf and the Amundsen Gulf, was studied in fall 2002 (mid-September to mid-October) and 2003 (end of September to end of November). This study focuses on the factors influencing phytoplankton production and biomass distribution, as well as interannual variability, and development at the end of the growth season in the southeastern Beaufort Sea.

MATERIALS AND METHODS

Study area

The Mackenzie shelf is shallow and bounded by the Amundsen Gulf to the east, and the Canada Basin to the north. The surface circulation in the Mackenzie shelf and its surrounding regions is mainly driven by wind forcing, the Mackenzie River discharge, and thermohaline convection during freeze-up (Carmack & Chapman 2003). The Mackenzie shelf is strongly influenced by the Mackenzie River, which has the highest sediment and organic carbon loads of all arctic rivers (Holmes et al. 2002). Over the sampling area, the water column is typically formed by the Polar Mixed Layer (0-50 m), overlying the Cold Halocline Layer (50-200 m), mainly formed by waters of Pacific origin, and the Atlantic Layer (>200 m) (Carmack et al. 1989, McLaughlin et al. 1996). Beyond the shelf-break, the surface circulation is dominated by the south branch of the anticyclonic Beaufort gyre that drives the pack ice and the surface waters westward (Carmack & Macdonald 2002), below 50-85 m, the eastward Beaufort counter-current carries waters of Pacific origin along the slope (Pickart 2004).

The area is characterized by three main features related to sea ice dynamics. On the shelf, the new sea ice typically forms in October; offshore, the mobile permanent pack ice comprises annual and multiyear sea ice and drifts following the Beaufort gyre, while the Cape Bathurst polynya is generally located at the entrance of the Amundsen Gulf (Barber & Hanesiak 2004).

Region definition

Stations were separated according to their locations relative to 128.35°W, which barely corresponds to the tip of the Cape Bathurst, as in Simpson et al. (2008). Stations east of 128.35°W with a depth >150 m were considered to be in the Amundsen Gulf region, and stations west of 128.35°W on the Mackenzie shelf and slope were considered as Mackenzie shelf stations (Fig. 1) (station CA13 in early fall 2003 was excluded from the shelf region owing to its closeness to the pack ice).

Sampling

Sampling took place, during the Canadian Arctic Shelf Exchange Study (CASES), in the southeastern Beaufort Sea (69-72°N, 120-140°W) over the Mackenzie shelf area and the Amundsen Gulf, during the preliminary cruise of fall 2002 (23 September – 14 October) on board the CCGS *Pierre Radisson*, and during early (30 September – 13 October) and late fall 2003 (16 October - 14 November) on board the CCGS *Amundsen*. We separated the sampling periods in early and late fall periods, according to the time elapsed between sampling of the shelf and gulf regions (one week or more) and also to the larger decrease in light availability from mid-October. Water samples were collected with a rosette sampler SBE-carousel (Seabird) fitted with twenty-four 12 l Niskin bottles (Ocean Test Equipment Inc.), a SBE-9plus CTD and a Seapoint chlorophyll fluorometer. All water samples were collected at fixed depth (surface, 5, 10, 15, 25 and 50 m) and at fluorescence maximum at all stations (n=73) (Table 1). At stations with primary production estimations (n=16), additional water samples were taken at six or five photic depths detailed below

(Table 1). The photic depths were established after calculating the light attenuation coefficient, K_d, using a Secchi disk (Parsons et al. 1984). Samples for phytoplankton were pre-filtered on a 333 μm mesh in order to remove large zooplankton.

The depth of the Surface Mixed Layer (SML) was calculated according to Thomson and Fine (2003) and the bottom of the Polar Mixed Layer (PML) is defined by the 31.6 isohaline (Carmack et al. 1989).

Inorganic nutrient concentrations (nitrate + nitrite, phosphate and silicic acid) were measured on board using standard colorimetric methods (Grasshoff 1999) as described in Schloss et al. (2008) for 2002 and in Simpson et al. (2008) for 2003.

In 2003, downwelling PAR irradiance was collected using a GUV-510 surface radiometer (Biospherical Instruments) from 30 September to 7 November. Data collection was stopped before the end of the cruise due to weather conditions (snow fall).

Table 1: Stations sampled for biomass, primary production and taxonomy during all cruises.

	2002	2003	
	Early fall 23 Sep – 14 Oct	Early fall 30 Sep – 13 Oct	Late fall 16 Oct – 14 Nov
Biomass	All stations (36)	All stations (11)	All stations (26)
Production	24, 49, 65, 66, 83, 101	718, CA07, CA10, CA15, CA18	718, 709, 506, 124, 112, 200
Taxonomy	24, 49, 65, 66, 83, 101	718, CA07, CA10, CA15, CA18	718, 715, 712, 709, 706, 703, 124, 112, 100, 206, 200, 400, 406, 409, 415, 312, 306, 300

24
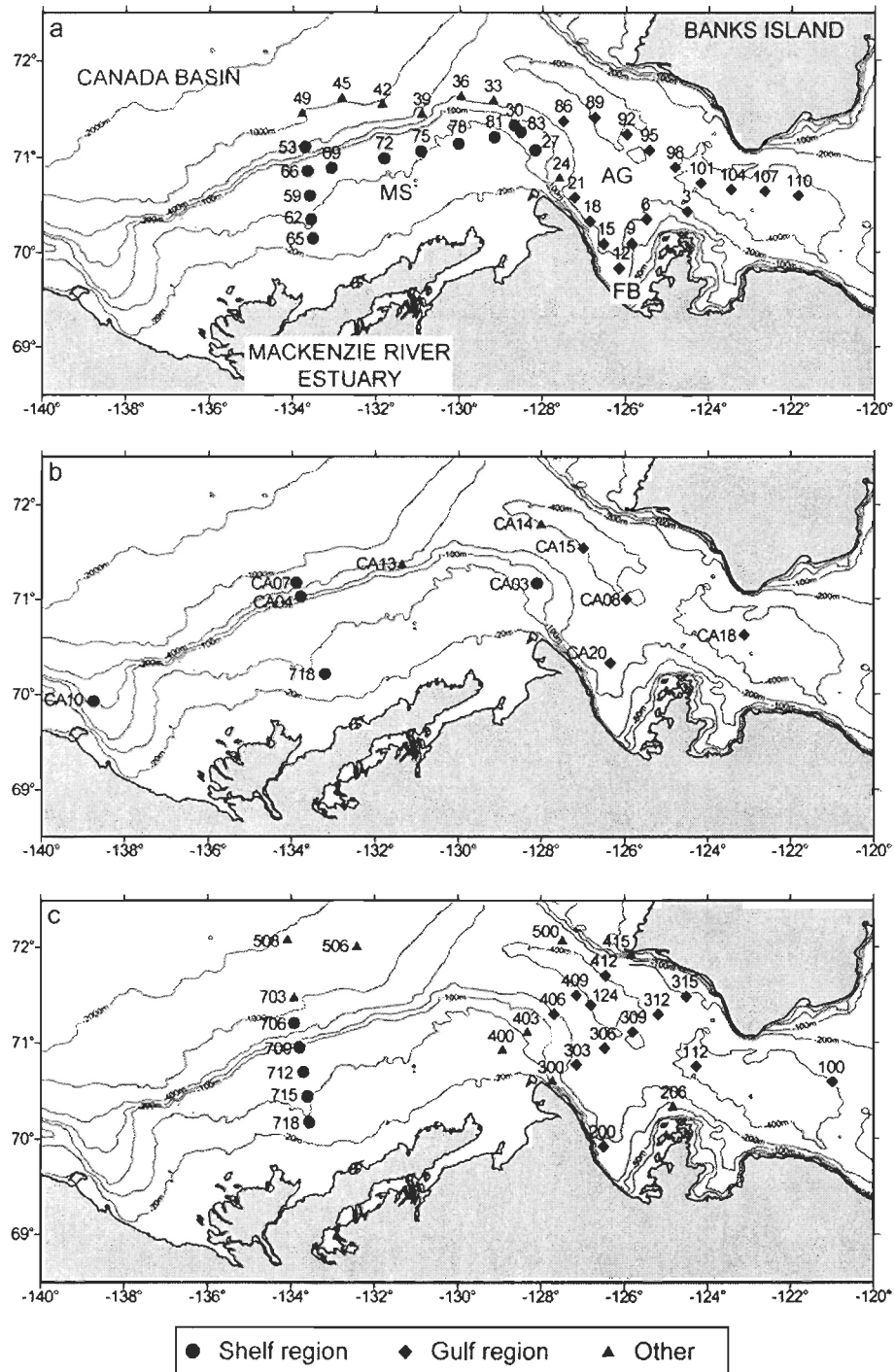
Figure 1: Location of stations sampled in (a) early fall 2002, (b) early fall 2003 and (c) late fall 2003 (AG: Amundsen Gulf; FB: Franklin Bay; MS: Mackenzie Shelf).

Chlorophyll *a* determination

For the determination of phytoplankton chlorophyll *a* (chl *a*) concentration, water sub-samples of 0.5 to 1 l were filtered onto glass fibre filters (poresize 0.7 μm, Whatman GF/F) (total biomass) and 5 μm polycarbonate filters (Poretics) (large cells biomass). Chl *a* concentrations were determined with a 10-AU Turner Designs fluorometer following 24 hr extraction in 90 % acetone at 5°C in the dark without grinding (Parsons et al. 1984). Concentrations of chl *a* were corrected for phaeopigments by acidification of the extract (Knap et al. 1996). All values were integrated over 50 m at all stations. At stations with primary production estimates, chl *a* concentrations were also integrated over the euphotic zone. As the euphotic zone was not measured at all stations, the depth of 50 m was chosen for integration of chl *a* concentration values in order to include the euphotic zone, the PML and the deep chl *a* maximum for most of the stations.

Phytoplankton production

Particulate primary production was estimated from six photic depths in 2002 (100, 40, 20, 10, 5 and 1 % of surface irradiance) and five photic depths in 2003 (100, 50, 25, 10 and 1 % of surface irradiance) using the ^{14}C uptake method (Knap et al. 1996). Samples were incubated in 500 ml polycarbonate bottles (two light and one dark with DCMU [3-(3,4-dichlorophenyl)-1, 1-dimethyl urea]), inoculated with 20 to 30 μCi of $NaH^{14}CO_3^-$, and placed under *in situ* simulated conditions in on-deck incubators, with running surface seawater and incident irradiances adjusted with neutral density filters. The total added activity was determined in triplicates by adding 250 μl of ethanolamine and 10 ml Ecolume

scintillation fluid (ICN) to a 250 µl inoculated water sub-sample. After 24 hours of incubation, water sub-samples (150 ml or more) were filtered onto glass fibre filters (poresize 0.7 µm, Whatman GF/F) (total particulate primary production) and 5 µm polycarbonate filters (Poretics) (large cell particulate primary production). Non-incorporated ^{14}C was removed by addition of 250 µl of 0.5N HCl. Upon complete evaporation of the acid, 10 ml of Ecolume scintillation cocktail were added. The activity was determined using a Beckman Liquid scintillation system 3801 Series in 2002 and a Packard Liquid Scintillation Analyzer Tri-Carb 2900 TR in 2003. Primary production rates were estimated with the actual DIC concentrations measured by coulometric titration (Johnson et al. 1993, DOE 1994). All counts were dark-corrected and daily primary production rates were integrated over the euphotic zone. Incubations were initiated early in the morning (minimal PAR) in order to reduce the variability in ^{14}C accumulation (Mingelbier et al. 1994). Water samples for primary production measurements were taken in ice-free waters in early fall 2002 and 2003, and at stations with no or undefined sea ice cover (i.e. partial presence of new ice) in late fall, therefore no correction for sea ice concentration was applied.

The *f*-ratio can be estimated from primary production rates following this equation: $f = 0.04 + 0.74 \ (P_L/P_T)$, $r^2 = 0.80$, where P_T corresponds to total particulate primary production in the euphotic zone and P_L to large cells production in the euphotic zone (Tremblay et al. 1997). The phytoplankton new production, which corresponds to the maximum potential export of particulate primary production from the euphotic zone, can be

further derived from the f-ratios (Dugdale & Goering 1967, Eppley & Peterson 1979):
$P_{ex} = P_T \times f$-ratio.

Taxonomic identification

Water sub-samples (250 ml) were collected at the fluorescence maximum for phytoplankton cell identification and enumeration (Table 1). The samples were fixed with acidic Lugol solution (4 % final concentration) and stored in the dark at 4°C until analysis. Water samples of 50 to 100 ml were settled in Zeiss-type settling chambers for at least 12 hr before cell enumeration with a Leitz Diavert inverted microscope with phase contrast optics at 250x and 400x. The main taxonomic references used to identify phytoplankton were Tomas (1997), Jensen and Møestrup (1998), Bérard-Therriault et al. (1999) and Throndsen et al. (2003). Some dinoflagellates and diatoms unidentified were grouped in size classes (5-10, 11-20, 21-50 and >50 µm), while chlorophytes, chrysophytes, dictyochophytes, cryptophytes, euglenophytes, prasinophytes and prymnesiophytes unidentified to species or genus level were also grouped according to their size classes (<5, 5-10, 11-20 and >20 µm), as well as unidentified flagellates.

Statistical analyses

In order to investigate differences in chl a biomass integrated over 50 m (total and large size fractions) between the different regions and cruises, the non-parametric pair comparison Mann-Whitney U test was applied, as the data did not meet normal distribution and homoscedasticity (Zar 1999). The small number of observations for primary production

rates and f-ratios precluded statistical analyses of regional differences. Association between pairs of surface values of variables was measured with the Pearson moment product correlation (r coefficient) for all variables, as there were no large deviations from normality (Zar 1999). We ran partial correlations to examine the interactions between three variables in order to remove spurious correlations. First-order partial correlation considers the relation between two variables, while holding constant the value of a third variable (Zar 1999), (coefficient $r_{x,y/z}$ represents the relationship between the variables x and y, while holding the variable z constant), significance tests for the first-order partial coefficients were made with Student's t-test with df = n − 3 (Myers & Well 2003). Regressions were performed on paired variables for which a significant correlation was found. All statistical tests were carried out with the Statistica 6.0 program (StatSoft).

Multivariate approaches were applied to the community analysis. Phytoplankton cell abundances data were ordinated by non-metric multi-dimensional scaling (MDS) (Clarke 1993). The input was a similarity matrix based on Bray-Curtis similarity of fourth-root transformed cell abundances, to put more weight on the species composition in the samples (Field et al. 1982). The relevant species, in supporting regional or temporal differences, were further determined by the SIMPER procedure. The multivariate analyses were performed with the program Primer version 5.0 (Plymouth Marine Laboratory).

RESULTS

Physico-chemical conditions

Information on the sea ice cover during the sampling periods was gathered from the Canadian Ice Service. In 2002, stations 18 to 33 and 49 to 65 were sampled in ice-free waters, whereas stations 36 to 45 were sampled at the edge of the arctic pack ice (see Fig. 1a for station location). Newly formed sea ice was present at stations 69 to 81, while the pack ice had moved south so as both old and grey drifting ice were present from stations 83 to 92. Stations in the middle part of the Amundsen Gulf were free of ice at time of sampling (stations 95 to 101), whereas stations sampled in the southern part of the gulf (stations 3 to 15, 104, 107 and 110) were partly covered by new and grey ice. In early fall 2003, old ice in strips was present at stations 718 and CA10 over the Mackenzie shelf. Stations CA04, CA07 and CA13 were sampled close to the pack ice (see Fig. 1b for station location). In the Amundsen Gulf, all stations were ice-free the second week of October 2003. In late fall 2003, newly formed sea ice was present over the Mackenzie shelf and the Amundsen Gulf, and started to consolidate the beginning of November.

The daylength decreased in 2002 from 14 hr on 23 September to 9 hr on 14 October. In 2003 the daylength decreased from 13 to 9 hr for the early fall period and from 8 hr on 19 October to 3 hr on 19 November for the late fall period. Daily solar incoming PAR irradiance measured in 2003 declined with time and ranged between 2321 and 7361 mmol photon $m^{-2} d^{-1}$ in early fall and between 336 and 1649 mmol photon $m^{-2} d^{-1}$ in late fall.

Salinity and temperature allowed us to identify the stations strongly influenced by the Mackenzie River outflow. The fall 2002 temperature and salinity fields throughout the sampling area have been described by Garneau et al. (2006). Sea surface temperature was generally below -0.5°C beyond the influence of the river, while river-influenced stations had warmer surface temperature and low salinity (i.e. stations 59, 62, 66, 69 and 75; see Fig. 1a for station location). However, the marine physical characteristics of the most inshore station 65 were attributed to upwelling of deeper water (Garneau et al. 2006). During early fall 2003, sea surface temperature was usually below -0.5°C and only station 718 (see Fig. 1b for station location) was influenced by the river plume. Later in fall along the transect off the Mackenzie River mouth, the freshwater influence was only detected at stations 718 and 715 (see Fig. 1c for station location). At that time, sea surface temperature was colder and below -1°C at most stations.

Both in 2002 and 2003, the surface mixed layer (SML) was generally thinner on the Mackenzie shelf, ranging typically from 5 m close to the river mouth to 12-15 m offshore. In the Amundsen Gulf, the average SML depth was usually larger than on the shelf ranging from 7 to 20 m. The SML was generally thicker during late fall than earlier in the year.

The concentrations of phosphate and silicic acid were always in excess in both 2002 and 2003 compared to dissolved inorganic nitrogen, which was the limiting element (Simpson et al. 2008). In 2002, nitrate+nitrite were generally depleted throughout the PML with concentrations well below 1 μM in the SML and below 3-4 μM at the bottom of the PML, and averaging 92 mmol m^{-2} over the first 50 m. The Amundsen Gulf area had slightly higher nitrate+nitrite concentrations than the shelf area. In early fall 2003, the

nitrate+nitrite distribution was the same with an average availability of 94 mmol m^{-2} over the first 50 m. Later in fall, despite a slight replenishment at the bottom of the PML, nitrate+nitrite concentrations remained low in the surface layer and averaged 120 mmol m^{-2} over the first 50 m.

Chlorophyll *a* concentrations

In fall 2002, chl *a* concentrations were generally low (< 1 mg m^{-3}) throughout the water column. The maximum concentration usually occurred at surface water, except for the stations north of the Mackenzie shelf close to the permanent pack ice edge (36 to 45), where a weak deep chlorophyll maximum was observed. The vertical distribution of the chl *a* concentrations was similar on the Mackenzie shelf and in the Amundsen Gulf: concentrations were maximal in the SML (the top 10 to 20 meters approximately), decreased slightly down to the bottom of the PML or to the sediments on the shallow shelf and reached very low values below 50 m (< 0.1 mg chl *a* m^{-3}). In early fall 2003, the vertical distribution followed almost the same pattern, but in the middle of the Amundsen Gulf, a deep chl *a* maximum > 1 mg chl *a* m^{-3} was observed at about 25 m, between the SML and the bottom of the PML. Later in the fall, chl *a* concentrations decreased with time from 0.80 to 0.15 mg m^{-3} at the surface. The vertical distribution in the shelf and in the gulf regions followed the same trend as the one observed in 2002.

Integrated chl *a* biomass (over 50 m), as well as the contribution of large phytoplankton cells to biomass, are presented in table 2 for both the shelf and gulf regions. In fall 2002, from the end of September to mid-October, chl *a* biomass varied considerably

throughout the sampling area, i.e. from 2.8 to 25.9 mg m^{-2} at stations 62 in the river plume and 12 in Franklin Bay respectively (Fig. 2). Both biomass and contribution of large cells to biomass in the Amundsen Gulf were significantly higher than over the Mackenzie shelf region (Mann-Whitney U test, p < 0.01) (Table 2). Along the pack ice edge (stations 36 to 45), the biomass and the size structure were highly variable. This high variability was also observed on the Mackenzie shelf, where biomasses were higher at stations strongly influenced by freshwater inputs (i.e. stations 59, 66, 69 and 75) (Fig. 2). The biomass was more homogeneously distributed in the Amundsen Gulf, though high biomasses and contributions of large cells to biomass were observed in Franklin Bay. For the same period in 2003, phytoplankton biomass reached comparable values (9.9 to 36.5 mg chl a m^{-2}) (Fig. 3). Indeed, on the Mackenzie shelf, there was no difference in biomass and size structure between the two years (Mann-Whitney U test, p > 0.05); whereas in the Amundsen Gulf, despite comparable biomasses for both year, the contribution of large cells to biomass was higher in 2003 (Mann-Whitney U test, p < 0.05) (Table 2), reaching a maximum of 61 % of the biomass at station CA15. In 2003, the difference between the regions could only be noted by the higher contribution of large cells to biomass in the Amundsen Gulf (Mann-Whitney U test, p < 0.05), probably resulting from the small number of observations (Fig. 3). Later in 2003, from mid-October to mid-November, integrated biomass decreased throughout this period from 15.5 to 6.3 mg chl a m^{-2}, which could at least partially explain the differences found between the Mackenzie shelf and the Amundsen Gulf, which was sampled later (Mann-Whitney U test, p < 0.05) (Fig. 4). However, the biomass size

structure was the same for both regions, and showed a strong dominance of cells smaller than 5 μm (Fig. 4), which contributed on average to 70 % of the biomass.

Table 2: Chl *a* biomass (integrated over the upper 50 m) and the relative contribution of large phytoplankton cells (>5 μm) to this biomass on the Mackenzie shelf and in the Amundsen Gulf during the different cruises, mean ± SD, the number of stations is in brackets.

		Chl *a* biomass $(mg\ m^{-2})$		Contribution of large cells (%)		
2002	Shelf	11 ± 4.9	(13)	25 ± 8		(13)
Early fall	Gulf	18 ± 4.3	(16)	31 ± 11		(16)
2003	Shelf	14 ± 2.8	(5)	26 ± 12		(5)
Early fall	Gulf	26 ± 10.5	(4)	50 ± 12		(4)
2003	Shelf	14 ± 1.7	(5)	34 ± 10		(5)
Late fall	Gulf	10 ± 2.9	(13)	30 ± 7		(13)
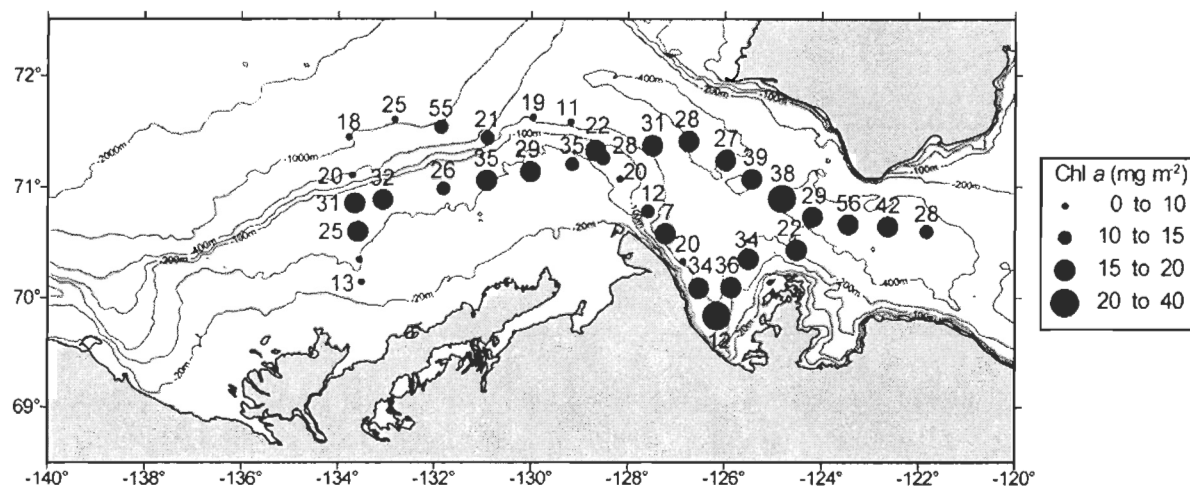
Figure 2: Spatial distribution of chl *a* biomass (integrated over 50 m) in mg chl *a* m^{-2} during early fall 2002, with the percent contribution of large phytoplankton cells (>5 μm) to biomass labelling each station.
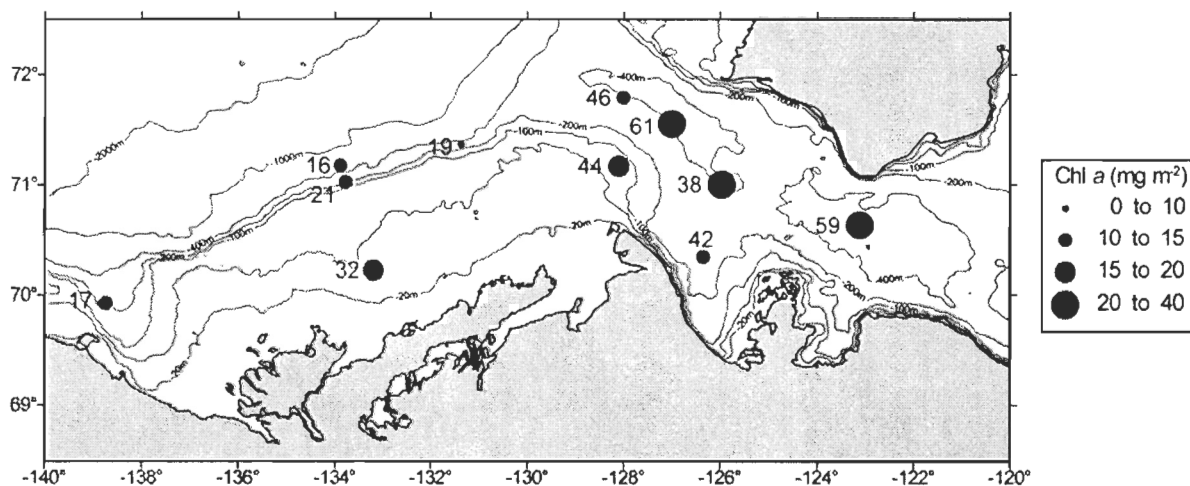
Figure 3: Spatial distribution of chl *a* biomass (integrated over 50 m) in mg chl *a* m^{-2} during early fall 2003, with the percent contribution of large phytoplankton cells (>5 μm) to biomass labelling each station.
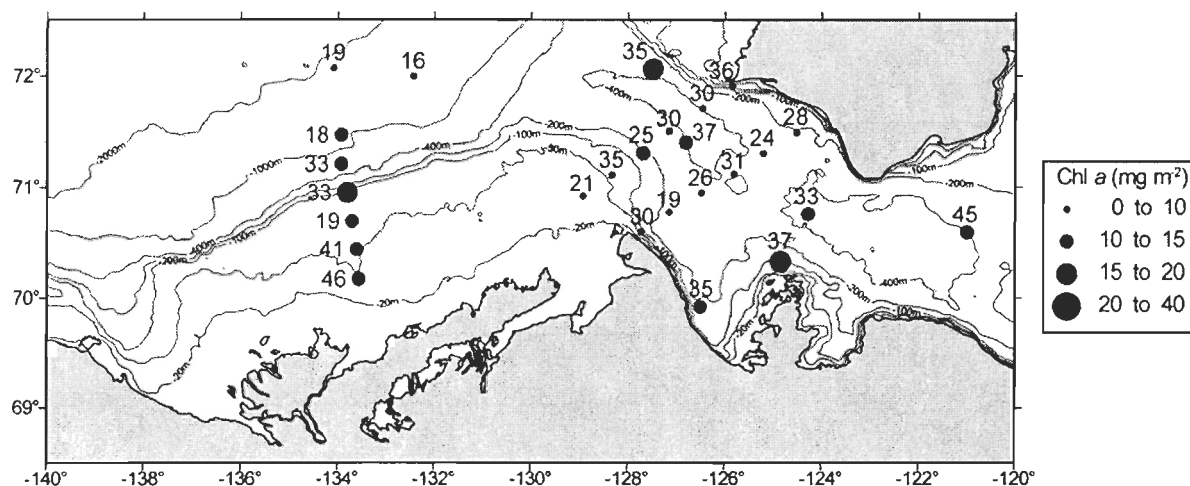
Figure 4: Spatial distribution of chl *a* biomass (integrated over 50 m) in mg chl *a* m^{-2} during late fall 2003, with the percent contribution of large phytoplankton cells (>5 μm) to biomass labelling each station.

Primary production

Maximum production rates were generally observed at the surface in both 2002 and 2003 sampling periods. The contribution of large phytoplankton cells to primary production was the same as that observed for the biomass for all the sampling periods (data not shown). Integrated particulate primary production rates, which were estimated from the end of September to the beginning of November, are presented in figure 5. From the end of September to mid-October 2002, integrated primary production rates averaged 73 ± 36 mg C m^{-2} d^{-1}, which was close to the average value of 78 ± 27 mg C m^{-2} d^{-1} for the same period in 2003. Later in 2003, production rates decreased strongly until 4 November, and averaged a third of the rates seen earlier in the season (23 ± 11 mg C m^{-2} d^{-1}).

In 2002, *f*-ratios were about 0.17 for the whole sampling area. In 2003 for the same period, *f*-ratios were about the same on the Mackenzie shelf area (0.18), whereas higher

values above 0.30 were recorded in the Amundsen Gulf. During the second half of October, f-ratios remained about the same level as in 2002 or earlier in the season in 2003 on the Mackenzie shelf and averaged 0.17.

The potential export of primary production (P_{ex}) from the euphotic zone was estimated on the basis of the f-ratio calculations. P_{ex} estimates were variable throughout the sampling area and the seasons (Fig. 5). In 2002, P_{ex} averaged 14 ± 10 mg C m^{-2} d^{-1} and never exceeded 25 % of the primary production. One year later, P_{ex} rates were almost the same, averaging 25 ± 22 mg C m^{-2} d^{-1}, but they accounted for up to 60 % of the primary production in the Amundsen Gulf. Later in the season, P_{ex} decreased like the primary production rates to low levels of 4 ± 2 mg C m^{-2} d^{-1} on average.
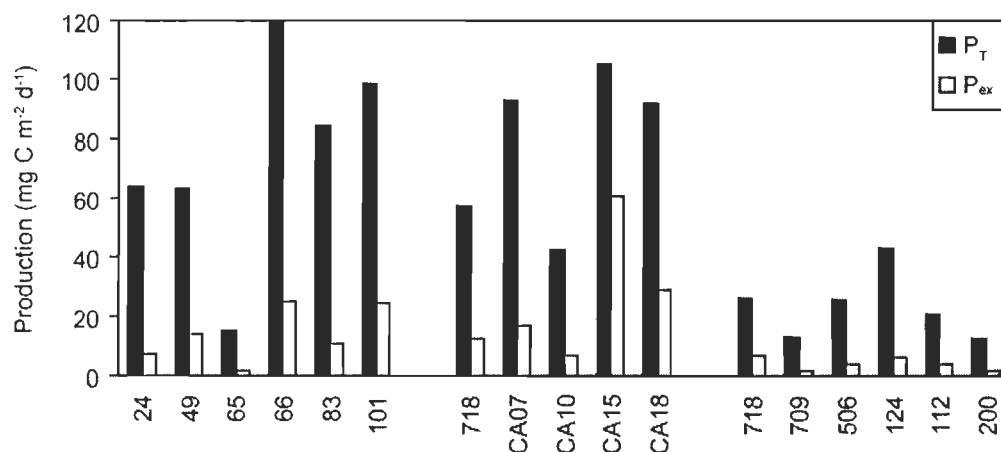
Figure 5: Rates of total particulate primary production (P_T) and estimates of maximum potential export of this particulate primary production (P_{ex}) (in mg C m^{-2} d^{-1}), during the three cruises: early fall 2002 (stations 24, 49, 65, 66 and 101) and 2003 (stations 718, CA07, CA10, CA15 and CA18) and late fall 2003 (stations 718, 709, 506, 124, 112 and 200).

Cell abundance and taxonomic composition

The phytoplankton communities of the Mackenzie shelf and Amundsen Gulf regions were composed of 229 taxa, including 53 diatom, 64 dinoflagellate and 45 flagellate species. In early fall, phytoplankton cell abundances were comparable for 2002 and 2003, ranging from 14×10^4 to 82×10^4 cells l^{-1} and from 17×10^4 to 73×10^4 cells l^{-1}, respectively; while decreasing in late fall 2003, with abundances ranging from 15×10^4 to 46×10^4 cells l^{-1}. The phytoplanktonic community was mainly composed of phytoflagellates, which accounted for 58 to 82 % of the cell abundance during all the sampling periods, except in early fall 2003 in the Amundsen Gulf, where the community was dominated by diatoms (49 % of the cell abundance on average). During both sampling periods in 2002 and 2003, no cyanobacteria were observed in samples from the Mackenzie shelf and the Amundsen Gulf. Some regional differences based on the main algal classes were observed during all sampling periods (Table 3). Chlorophytes were only present on the Mackenzie shelf even at very low abundances (1106 to 2212 cells l^{-1}). In the Amundsen Gulf, dinoflagellates were mostly represented by athecate species (*Gymondinium* spp. or *Gyrodinium* spp.), whereas in the shelf area thecate species (*Heterocapsa rotundata* (Lohmann) Hansen) were more abundant. Finally, the Mackenzie shelf area also showed higher abundances of prasinophytes (*Pyramimonas* spp.) and lower abundances of diatoms than the Amundsen Gulf. We further examined phytoplankton communities using MDS analysis (Fig. 6). In 2003, samples from the Mackenzie shelf and the Amundsen Gulf were well separated, whereas this regional difference was less pronounced in 2002. Early fall 2003 samples from the Amundsen Gulf were also distinct from those of the late fall period.

On the Mackenzie shelf, the same species or genera were responsible for the similarity within and between the sampling season, i.e. *Chrysochromulina spinifera* (Fournier) Pienaar *et* Norris, *Heterocapsa rotundata* , *Pyramimonas* spp., *Gymnodinium* spp (11-20 µm) and <5 µm unidentified flagellates. In the shelf region in 2003, the community composition of the two sampling periods, i.e. early and late fall, had a similarity higher than 50 % preventing them to separate out on the MDS plot. The outlier from the 'shelf 2002' group (upper right hand corner of Fig. 6) was station 65; there pennate diatoms were unusually abundant (2×10^4 cells l^{-1}), whereas dinoflagellates, chrysophytes, cryptophytes and prasinophytes had very low cell abundances, and chlorophytes and choanoflagellates were completely absent. In the Amundsen Gulf, the dissimilarity between early and late fall 2003 was mostly due to the following centric diatoms taxa which dominated in early fall, *Chaetoceros contortus* Schütt, *C. socialis* Lauder, *C. diadema* (Ehrenberg) Gran, *C. constrictus* Gran, *C. ingolfianus* Ostenfeld, spores of *Chaetoceros* spp., *Leptocylindrus danicus* Cleve and *Attheya septentrionalis* (Østrup) Crawford. On the contrary in late fall 2003, the phytoplankton community was characterized by the dominance of <10 µm unidentified flagellates, *Chrysochromulina spinifera*, *Chrysochromulina* spp., *Gymnodinium* spp., *Amphidinium* cf. *kesslitzii* Schiller, *Pseudopedinella pyriforme* Carter and *Thalassionema nitzschioides* (Grunow) Mereschkowsky.
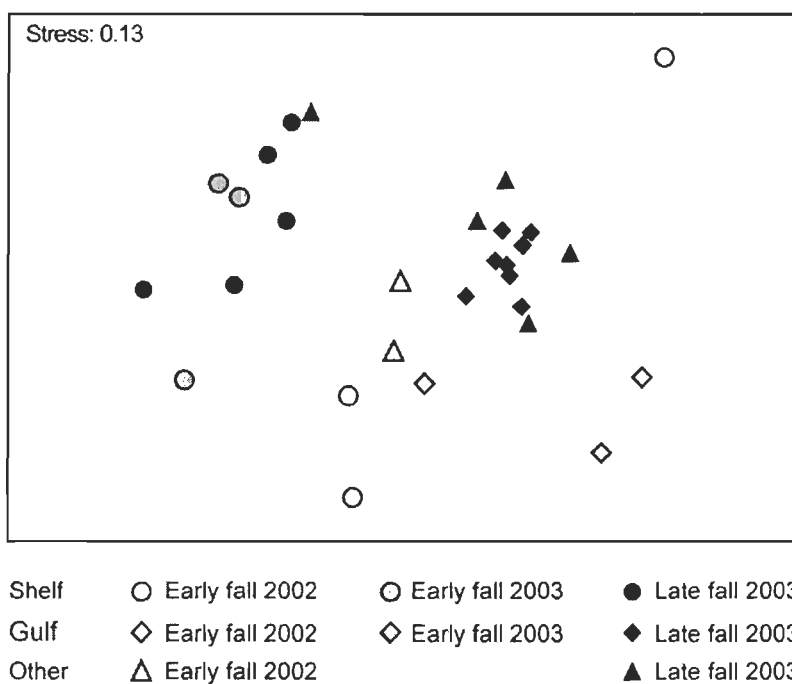
Figure 6: Multidimensional scaling ordination plot of phytoplankton community composition (based on species abundances) (open symbols: early fall 2002, grey symbols: early fall 2003, black symbols: late fall 2003; circles: Mackenzie shelf stations, diamonds: Amundsen Gulf stations and triangles: stations out of Mackenzie shelf and Amundsen Gulf regions).

Table 3: Average percent contribution of the major algal groups to the phytoplankton cell abundances on the Mackenzie shelf and in the Amundsen Gulf for the two sampling years (in early fall 2002, station 65 was not included in the average calculation of the shelf region).

| | 2002 | | 2003 | | | |
| | Early fall | | Early fall | | Late fall | |
	Shelf	Gulf	Shelf	Gulf	Shelf	Gulf
Diatoms	1.1	6.5	4.9	48.7	3.4	4.2
Centrics	0.7	4.1	3.6	45.0	2.9	2.7
Pennates	0.4	2.5	1.3	3.7	0.5	1.5
Dinoflagellates	9.7	11.6	20.8	8.9	14.2	9.7
Athecate	4.7	9.7	10.0	8.0	8.1	9.4
Thecate	5.0	1.9	10.8	0.9	6.1	0.3
Chlorophytes	0.3	0.0	0.5	0.0	0.8	0.0
Chrysophytes	1.4	0.5	0.8	0.6	0.6	0.0
Dictyochophyceae	2.1	2.8	1.2	0.4	2.3	1.4
Cryptophytes	7.2	5.7	6.1	1.5	2.0	1.2
Prasinophytes	26.2	4.3	17.0	0.5	15.3	1.8
Prymnesiophytes	5.9	21.3	14.7	4.9	25.0	23.9
Unidentified flagellates	36.4	40.2	17.1	30.3	25.6	53.0

DISCUSSION

Estimates of phytoplankton biomass in the Beaufort Sea are very scarce and were until now absent for the end of the productive period, i.e. the fall (Horner & Schrader 1982, Carmack et al. 2004). However, the low biomass (< 1 mg chl a m^{-3}) we observed during two consecutive autumns are consistent with concentrations measured at the end of September in waters northwest of Spitsbergen (Heimdal 1983). Integrated biomasses for the whole Beaufort Sea were on average 15.8 and 10.5 mg chl a m^{-2} for early and late fall, respectively, consistent with the range of 9.6 to 24.0 mg chl a m^{-2} measured in early October in the Barents Sea (Hegseth 1997). Our biomass estimates were also within the range of 7.1 to 28 mg chl a m^{-2} recorded in the Weddell Sea during austral fall, in April (Dower et al. 1996) but twice higher than the range of 4.1 to 2.4 mg chl a m^{-2} measured in the Ross Sea in April (Smith et al. 2000). During the two fall seasons and throughout the study area, the phytoplankton biomass was generally dominated by small phytoplankton cells (<5 μm), which contributed to about 70 % of the biomass, except in early fall 2003 in the Amundsen Gulf. The dominance of small cells has been previously reported in the Beaufort Sea in fall 2002 (Garneau et al. 2006, Schloss et al. 2008) and in the Greenland Sea in October (Gradinger & Ikävalko 1998), as well as in summer in the central Arctic (Gosselin et al. 1997) and the Barents Sea (Not et al. 2005).

During our study, the strong stratification constrained the vertical distribution of the phytoplanktonic biomass in the shallow SML and the PML. In ice-covered regions, concentration of phytoplankton biomass in upper waters is typical, owing to the

stratification due to ice melt in summer (Borstadt & Gower 1984). Consistent with previous studies of the Beaufort Sea (Macdonald et al. 1987, Carmack et al. 2004), nitrogen was the potential limiting element for phytoplankton growth, as indicated by N/P ratios always < 6 in the upper 50 m. The strong episodic winds blowing during 2002 and 2003 sampling periods (Environment Canada 2002, 2003) were unable to allow a significant replenishment of the surface water layers in nitrogen, because of the strong stratification. In fall 2003, Simpson et al. (2008) reported high ammonium concentrations of 17.4 mmol m^{-2} in the PML, which accounted for about 20 % of the total inorganic nitrogen sources. Those high ammonium concentrations suggest an active nitrogen recycling in the upper water column, supporting the general dominance of small phytoplanktonic cells on biomass observed in 2003 (except in the Amundsen Gulf in early fall).

Spatial distribution

Despite different sampling coverage during the two years, some regional differences in the phytoplankton community between the Mackenzie shelf and the Amundsen Gulf regions persisted, and some general trends can characterized both regions, apart from the early fall period in the Amundsen Gulf. The spatial differences were solely based on integrated phytoplankton biomass levels and biomass size structure on the 5 μm threshold, and further confirmed by taxonomic identifications. In the early fall periods of 2002 and 2003, the Amundsen Gulf was characterized by higher biomasses and a higher contribution of large phytoplankton cells to biomass compared to the Mackenzie shelf region (Table 2). The stronger stratification on the Mackenzie shelf, likely due to freshwater inflow, could

maintain less favourable conditions for phytoplankton growth in surface waters, with a severe light attenuation by particle load, and nitrogen deficiency as the Mackenzie River is only a weak source of this element (Carmack et al. 2004, Simpson et al. 2008).

Prasinophytes were an important group of the Mackenzie shelf phytoplankton community accounting for up to 31 % of the total phytoplankton cell abundance (Table 3), which is consistent with pigment analyses performed by Lovejoy et al. (2007), showing that prasinophytes made up 38 % of chl *a* concentrations in fall 2002. The taxonomic composition of dinoflagellates also showed some marked differences between the Mackenzie shelf and the Amundsen Gulf region (Table 3), with almost comparable cell abundances of thecate and athecate species in the shelf region as opposed to a much greater cell number of athecate over the thecate species in the gulf region. Thecate dinoflagellates were mainly represented by a single species *Heterocapsa rotundata*, which is known as autotrophic (Olli 1999), while athecate dinoflagellates were mostly composed of species from the genera *Gymnodinium* and *Gyrodinium*, known as being capable of heterotrophy (Levinsen et al. 1999, Jensen & Hansen 2000, Levinsen & Nielsen 2002, Rat'kova & Wassmann 2002). Thecate dinoflagellates dominated autotrophic phytoplankton cells larger than 10 μm on the Mackenzie shelf, while diatoms were paramount for this group in the Amundsen Gulf for all the sampling periods. The high contribution to cell abundance of potentially heterotrophic athecate dinoflagellates, among cells larger than 10 μm, suggests the importance of the microbial food web in the southeastern Beaufort Sea during the autumnal season, which has been previously highlighted by some authors (Parsons et al. 1989, Garneau et al. 2006, Simpson et al. 2008). Chlorophytes were only observed on the

Mackenzie shelf, and during late fall 2003 their abundance decreased with the distance offshore, which implied a dilution of the freshwater species cells as the river waters spread over the shelf; a similar feature was reported for the coastal Laptev Sea (Tuschling et al. 2000).

In 2002, the more intensive sampling over the Mackenzie shelf highlighted the high spatial variability and the importance of the freshwater input over this region. In front of the Mackenzie River estuary, stations close to the river mouth (i.e., stations 65 and 62) had lower biomasses and contribution of large cells to biomass compared to the group of stations offshore (i.e., stations 59, 66 and 69) (Fig. 2). In 2002, the Mackenzie River plume was deflected to the west before curving back to the east further offshore (Garneau et al. 2006), which may explain the higher biomasses recorded at the group of stations with low surface salinities (i.e., stations 59, 66 and 69). This group of stations was isolated from the river mouth by wind-driven upwelling of higher-salinity deep waters (Garneau et al. 2006), which were observed at station 65. At this station, despite low biomass, maximum fluorescence occurred near the bottom at 31 m. The phytoplankton community was characterized by low abundance of flagellate groups and high number of pennate diatoms, including numerous empty frustules, and by a low phaeopigments concentration compared to total chloropyllous pigments. Thus upwelling likely led to the development of a deep maximum of actively growing phytoplankton cells 20 meters above the bottom. Another location of interest is the Franklin Bay, in the southwest of the Amundsen Gulf region (Fig. 2). There, high phytoplankton biomasses were observed in 2002, with a high contribution of large cells, which probably transfer the food energy required to sustain the high

zooplankton biomass (Darnis et al. 2007) and high benthic meiofauna biomass (Bessière et al. 2007).

During the study period, the phytoplanktonic biomass and its size structure were more variable over the Mackenzie shelf area. Multiyear ice often drifted over this region in early fall and the resulting intermittent shading of the water column could have been partly responsible for the variability in phytoplankton standing stock over the Mackenzie shelf region.

Interannual variability

In the Amundsen Gulf, the phytoplanktonic community was different between the two years, even if the sampling was performed the second week of October in both cases. In 2002, the community was typical of post-bloom conditions under limited nitrogen availability, with low biomass concentrated in the surface layer and contribution of large cells around 30 %, which seems to be a baseline value for the fall in the Amundsen Gulf (Table 2). In 2003, at stations in the middle of the Amundsen Gulf, phytoplankton biomass was still reaching high values, with a deep chl *a* maximum, and the biomass was dominated by large cells (50 %) and centric diatoms. However, the low nitrate concentration and the high abundance of centric diatom spores (up to 13 % of centric diatom cell number) at the deep chl *a* maximum of stations CA15 and CA18 suggest that the phytoplanktonic community was at the end of a bloom period the second week of October 2003. Arrigo and van Dijken (2004) highlighted seasonal trends based on SeaWiFS-derived chlorophyll concentrations from 1998 to 2002 in the Amundsen Gulf. Despite a high interannual

variability, an autumnal bloom seemed to be a recurrent feature, even if the timing, importance and duration of these blooms differed widely over these five years. In 2002 the autumnal bloom started at the end of August and was already over by October when we conducted our sampling in the region. The latest autumnal bloom was observed at the end of September 2000 and was of low amplitude. Following the pattern of Arrigo and van Dijken (2004), the phytoplanktonic community structure, we observed during the second week of October 2003, could imply that the bloom had started the last week of September.

On the Mackenzie shelf, the few stations sampled in early fall 2003 do not allow us to comment on the interannual variability in that area.

Temporal changes

In the Beaufort Sea, the temporal evolution during fall 2003 was characterized by a decrease in biomass and taxonomic diversity from the end of September to mid-November, and this trend was even more pronounced in the Amundsen Gulf since a bloom ended during the early fall period. As the season progressed, the light availability and the daylength sharply decreased, surface temperature dropped, and new ice formed, which further limited light penetration in the water column. As the Mackenzie River water inflow strongly influences the surface temperature over the Mackenzie shelf, the effect of the temperature decrease was examined only for the Amundsen Gulf. Temperature did not directly influence phytoplankton growth, since there was no significant correlation between surface chl a concentration and temperature (t-test, $p > 0.05$). However, surface chl a concentrations were strongly correlated with the daylength ($r_{chl\ a,\ daylength/temperature} = 0.69$, t-

test p < 0.05). During fall 2003, integrated phytoplankton biomass decreased exponentially when daylength was shorter than 8 hr (Fig. 7). Light availability was therefore likely the most important factor constraining phytoplankton production in late fall. At the end of October, strong southeast winds blew in the Amundsen Gulf region (Environment Canada 2003), and were likely responsible for the slight replenishment of nutrients at the bottom of the PML. However, phytoplankton could not take advantage of the nutrient availability since light was the main limiting factor. Even if the influence of sea ice formation on phytoplankton could not be assessed, owing to the nature of the data available, the ice cover probably shaded the water column, thus the relationship observed between the daylength and the phytoplankton biomass likely includes the effect of the ice cover. However, in the context of climate change, which would lengthen the ice-free season at high latitude, the phytoplankton production season would probably not be expanded in fall, since light availability, i.e. solar incoming irradiance and daylength, would remain the main factor constraining phytoplankton growth.
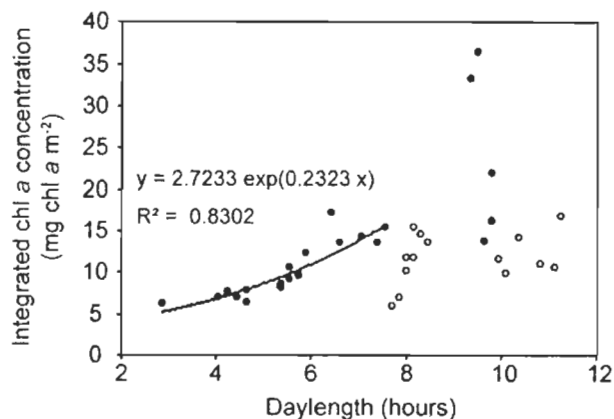
Figure 7: Relationship between daylength and chl *a* biomass (integrated over 50 m) in early and late fall 2003 (closed symbols: stations from the Amundsen Gulf, open symbols: stations out of the Amundsen Gulf).

Phytoplankton production

Primary production rates, for early fall on the Mackenzie shelf, ranged from 15 to 119 mg C m^{-2} d^{-1} (Fig. 5), falling in the same range (40-100 mg C m^{-2} d^{-1}) reported in August by Carmack et al. (2004), but lower than summer primary production rates (100 to 1190 mg C m^{-2} d^{-1}) recorded by Hsiao et al. (1977). The Mackenzie shelf production was also comparable to the 50 to 170 mg C m^{-2} d^{-1} reported for the Laptev Sea/Lena River system in September (Sorokin & Sorokin 1996). In early October, primary production ranged from 92 to 105 mg C m^{-2} d^{-1} in the Amundsen Gulf, while two months before our 2002 sampling, Lee and Whitledge (2005) found similar rates ranging from 79 to 145 mg C m^{-2} d^{-1} in the Amundsen Gulf and Canada Basin. The latest fall primary production estimates made to date in the Arctic Ocean showed also similar rates from 72 to 148

mg C m^{-2} d^{-1} at the end of September and beginning of October northwest off Spitsbergen (Heimdal 1983). Primary production rates decreased to low levels of 12-43 mg C m^{-2} d^{-1} until the beginning of November, and were close to austral fall estimates (April) of 22 to 27 mg C m^{-2} d^{-1} in the Weddell Sea (Dower et al. 1996) and 13 to 18 mg C m^{-2} d^{-1} in the Ross Sea (Smith et al. 2000).

The persistent nitrate depletion observed during our study, together with the high integrated primary production-to-biomass ratios (usually > 5) measured in early fall, suggests that active phytoplankton grazing prevented the accumulation of phytoplankton biomass and also that recycling was efficient; such highly dynamic food webs have previously been reported in the Arctic Ocean by Wheeler et al. (1996). The f-ratios estimated from the size structure of the phytoplankton community were low and close to f-ratios measured in August in the Canada Basin and the Amundsen Gulf (0.25 ± 0.13, Lee & Whitledge 2005) and in the Chuckchi Sea (0.05-0.38, Cota et al. 1996), where phytoplankton production was dependent upon ammonium. Thus, the f-ratio estimates further support the high recycling efficiency prevailing in the southeastern Beaufort Sea during fall.

The potential phytoplankton production that could be exported out of the euphotic zone was only about 17 % for the whole study. In the Amundsen Gulf, we estimated a high potential carbon export out of the euphotic zone at 40 % of the primary production in October 2003, probably resulting from the declining bloom situation. However, the potential primary production exported out of the upper halocline would probably be even lower, which is consistent with the marine particulate organic carbon flux accounting for

22 % of the primary production measured at 200 m north of Franklin Bay for the same period (Forest et al. 2008).

The new production estimates (from f-ratios), derived from the size structure of the phytoplankton community, were in good agreement with the new production based on N^{15} uptakes experiments conducted during the CASES program (Simpson 2008). Moreover, various estimation methods of potential carbon production export were compared by Garneau et al. (2007) for the North Water polynya, and they concluded that the method of Tremblay et al. (1997) gave good estimates of new production in arctic seas; our results thus further support this statement.

In the Arctic, most annual phytoplankton production calculations, based on direct primary production measurements, are estimated over a 120 or 150 days period, usually starting in May or June and ending in September. However, blooms can occur even as late as October (Hegseth 1997, Arrigo & van Dijken 2004), and primary production is still detectable in November (Richardson et al. 2005). Carmack et al. (2004) estimated an annual production of 12-16 g C m^{-2} y^{-1} from early April to early September in the Beaufort Sea. Based on our measurements, from mid-September to the end of October, primary production would be around 3.3 and 2.3 g C m^{-2}, in the Amundsen Gulf and on the Mackenzie shelf, respectively; thus the annual primary production estimate of Carmack et al. (2004) would be increased by 14 to 19 %. Autumnal primary production is rarely measured, owing to logistical problems to access arctic regions, but in the Beaufort Sea, the autumnal production, from mid-September to the end of October (roughly 45 days) accounted for at least 15 % of the total annual production. Thus, the autumnal

phytoplankton production can significantly contribute to the annual production in arctic systems, at least at latitudes similar to that of the Beaufort Sea (e.g. Chukchi Sea, East Siberian Sea), and the 'productivity period' should be extended by at least one month for such arctic systems.

CHAPITRE II

PHYTOPLANKTON DYNAMICS IN SPRING AND SUMMER IN THE

SOUTHEASTERN BEAUFORT SEA

RESUME

La dynamique du phytoplancton a été étudiée dans le sud-est de la mer de Beaufort au printemps et en été 2004. En juin, la communauté phytoplanctonique était dans une situation de pré-bloom dans le sud du golfe d'Amundsen, et en situation de post-bloom au centre du golfe, en raison de l'ouverture précoce de la polynie du Cap Bathurst. En juillet et en août, le phytoplancton formait un maximum de chlorophylle profond à la base de l'halocline, qui correspondait également à la nitracline. Dans le golfe d'Amundsen, la biomasse chlorophyllienne, ainsi que la contribution des cellules de grande taille (>5 μm), restaient faibles du printemps à l'été. Sur le plateau continental du Mackenzie, les phénomènes d'upwelling liés au vent et l'extension du panache des eaux du fleuve Mackenzie favorisaient la production phytoplanctonique, en augmentant la biomasse chlorophyllienne due aux cellules de grande taille (>20 μm) et l'export potentiel de production primaire en profondeur. En mer de Beaufort, le phytoplancton présentait des caractéristiques photosynthétiques d'adaptation aux faibles intensités lumineuses du printemps à l'été, et ce, même en surface, où une limitation en éléments nutritifs aurait pu contraindre l'adaptation à des intensités lumineuses élevées. En général, les proportions élevées de production primaire par rapport à la biomasse, ainsi que l'absence d'accumulation de cellules de grande taille (>5 μm) dans le golfe d'Amundsen, suggèrent une forte pression de broutage sur le phytoplancton et un recyclage actif en mer de Beaufort. Dans le golfe d'Amundsen, la production primaire annuelle a été estimée à 21 g C m^{-2} a^{-1}. Cette faible valeur résulte probablement d'une sous-estimation liée à l'extrapolation, mais également du faible niveau hivernal de nitrates, qui pré-conditionnait vraisemblablement la faible production phytoplanctonique annuelle.

ABSTRACT

Phytoplankton dynamics was investigated in the southeastern Beaufort Sea in spring and summer 2004. In June, the phytoplankton community experienced pre-bloom conditions in the southern part of the Amundsen Gulf, and post-bloom conditions in the middle of the gulf, owing to the earlier opening of the Cape Bathurst polynya. In July-August, phytoplankton formed a typical deep chlorophyll maximum at the bottom of the Polar Mixed Layer, which corresponded to the nitracline. In the Amundsen Gulf, the chlorophyll a biomass, as well as the contribution of large cells (>5 μm), remained low from spring to summer. Meanwhile, over the Mackenzie shelf, wind-driven upwelling and the Mackenzie River plume spreading enhanced phytoplankton production, increasing the chlorophyll a biomass due to large cells (>20 μm) and the primary production potential export to the bottom. Over all the southeastern Beaufort Sea, phytoplankton presented photosynthetic characteristics of shade-adaptation throughout spring and summer, even at surface where nutrient limitation might limit adaptation to high light intensities. Overall high primary production-to-biomass ratios, as well as the lack of large cells (>5 μm) accumulation in the Amundsen Gulf, suggests a high grazing pressure on phytoplankton and an active recycling in the Beaufort Sea. In the Amundsen Gulf, the annual primary production was estimated to 21 $g\,C\,m^{-2}\,y^{-1}$. This low value resulted probably from underestimation linked to uncertainties in the calculation, but also from the low pre-conditioning winter nitrate inventory, which probably set a low limit to the annual phytoplankton production.

INTRODUCTION

The Arctic Ocean is strongly impacted by the ongoing global trend towards warming (ACIA 2005, IPCC 2007). Over the 1978-2003 period, the arctic sea ice minimum extent has decreased by $8x10^5$ km^2 (Johanessen et al. 2004). Moreover, the Arctic Ocean has experienced minimal sea-ice extent records since 2002, with a new maximum in summer open water in September 2007 (NSIDC 2007, Comiso et al. 2008), suggesting the acceleration of sea-ice cover shrinking. The Arctic Ocean is expected to be free of ice in summer by the end of the 21st century (Serreze et al. 2007) or as early as 2040 (Holland et al. 2006), as predicted by numerical simulations. In addition, the Arctic Ocean receives large river inflows (Macdonald et al. 2004a) and the predicted rise in freshwater discharge (Peterson et al. 2002) would make its marginal seas even more sensitive to climatic change (ACIA 2005). Arctic ecosystems are expected to be affected by climatic changes, though the impacts on food web structure and carbon cycling pathways are unclear (Wassmann 2004). The identification and analysis of climate change impacts, as well as model validation, requires field measurements; but such data are still lacking in some biologically active regions of the Arctic Ocean (Carmack & Wassmann 2006).

Large variations in sea ice cover and solar radiations usually constrain pelagic phytoplankton production between spring sea ice melt and fall freeze-up, with high phytoplankton production and standing stocks restricted to relatively short periods of the ice-free season (Sakshaug 2004). In spring, phytoplankton blooms are generally set up by sea ice retreat and often terminated by nutrient limitation (Sakshaug & Skjoldal 1989,

Carmack et al. 2006, Tremblay et al. 2006). Late blooms can also occur in late summer or in fall, as wind mixing reintroduces nutrients in surface layers (Arrigo & van Dijken 2004, Carmack et al. 2006). The production of large phytoplankton cells favors carbon export and transfer to higher trophic levels (Chisholm 1992); however, large microphytoplankton cells are often constrained to bloom periods of a couple of weeks, while smaller cells, i.e. nano- and picophytoplankton, often dominate outside these periods (Not et al. 2005).

Arctic continental shelves and polynyas are the most productive regions of the Arctic Ocean (Sakshaug 2004, Stirling 1997). Polynyas are generally highly productive regions due to their physical characteristics such as early sea ice cover retreat in spring and the physical forcing allowing nutrient replenishment (Smith 1995, Klein et al. 2002, Tremblay & Smith 2007). These aspects make polynyas ideal regions to study climatic change impacts because of their reduced sea ice cover (Tremblay et al. 2006). Among arctic shelves, interior continental shelves, which are strongly influenced by river discharge, have been poorly studied in terms of phytoplankton dynamics (Carmack & Wassmann 2006). In the Beaufort Sea, phytoplankton was only studied in the 70 and 80's over the Mackenzie shelf (Hsiao et al. 1977, Horner & Schrader 1982, Carmack et al. 2004), and almost not in the Amundsen Gulf (Lee & Withledge 2005). The Cape Bathurst polynya, which is located in the Amundsen Gulf, has been suggested to be a highly productive region by satellite surveys (Arrigo & Van Dijken 2004), nevertheless it has never been confirmed by field measurements. In order to make predictions about how phytoplankton dynamics might change in the Arctic as a whole, it is essential to investigate polynyas such as the Cape Bathurst polynya. Therefore, in the context of climatic change, the acquisition of time

series of phytoplankton biomass is essential to understand its dynamics in the Beaufort Sea. The spatial and temporal variability in phytoplankton biomass and production was thus investigated in the southeastern Beaufort Sea in spring and summer 2004. This study addresses the spring to summer seasonal phytoplankton dynamics, the physical factors driving phytoplankton spatial distribution and production, and the phytoplankton standing stocks and primary production.

MATERIALS AND METHODS

Study area

The Mackenzie shelf is shallow and bounded by the Amundsen Gulf to the east, and the Canada Basin to the north (Fig. 1), and it is crossed by the Mackenzie and Kugmallit canyons, which are sites known to favour upwelling (Macdonald et al. 1987, Williams et al. 2006, 2008). The surface circulation in the Mackenzie shelf and its surrounding regions is mainly driven by wind forcing, the Mackenzie River discharge, and thermohaline convection (Carmack & Chapman 2003). The Mackenzie River strongly influences the Mackenzie shelf and its maximum discharge usually occurs at the end of June (Carmack & Macdonald 2002). Over the sampling area, the water column is typically formed by the Polar Mixed Layer (0-50 m), overlying the Cold Halocline Layer (50-200 m), mainly formed by waters of Pacific origin, and the Atlantic Layer (>200 m) (Carmack et al. 1989, MacLaughlin et al. 1996, Simpson et al. 2008). Beyond the shelf-break, the surface circulation is dominated by the south branch of the anticyclonic Beaufort gyre that drives the mobile permanent pack ice and the surface waters westward (Carmack & Macdonald 2002), below 50-85 m, the eastward Beaufort counter-current carries waters of Pacific origin along the slope (Pickart 2004).

The Cape Bathurst polynya, a large recurrent polynya lies within the Amundsen Gulf (Smith et al. 1990), where high interannual variability results in sea ice retreat occurring as early as April or as late as late June (Arrigo & van Dijken 2004).
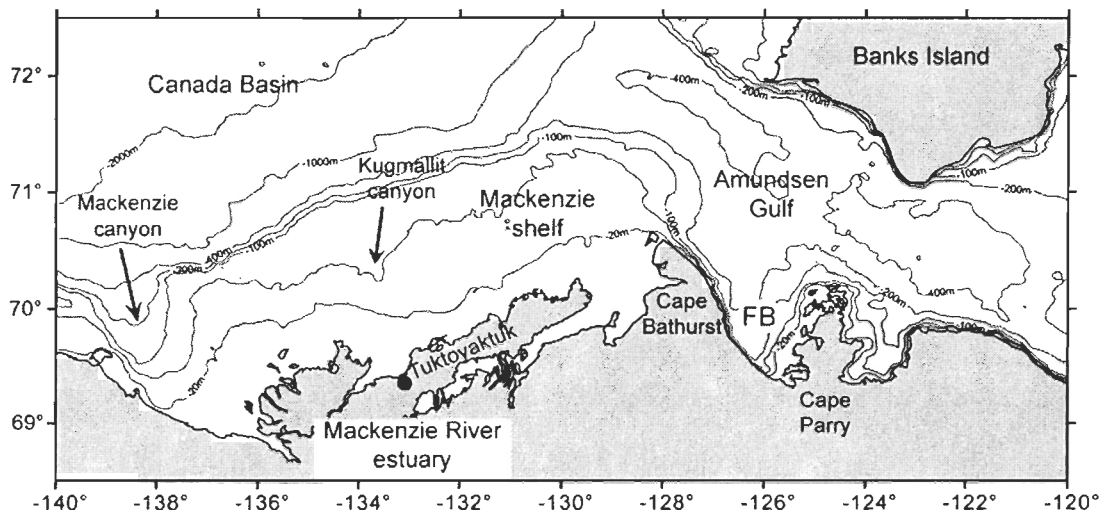
Figure 1: Study area in the southeastern Beaufort Sea (FB: Franklin Bay).

Sampling

Sampling took place in the southeastern Beaufort Sea (69-72°N, 120-140°W) during spring (4 – 21 June) and summer 2004 (26 June - 10 August) on board the CCGS *Amundsen*, in the framework of the Canadian Arctic Shelf Exchange Study (CASES) program. The Amundsen Gulf region was sampled in spring and summer (16 July – 10 August) 2004, whereas the Mackenzie shelf area was only sampled in summer (26 June – 27 July). Water samples were collected with a rosette sampler SBE-carousel (Seabird) fitted with twenty-four 12 l Niskin bottles (Ocean Test Equipment Inc.), a SBE-9plus CTD, a Seapoint chlorophyll fluorometer and a QCP2300 Biospherical PAR (Photosynthetically Available Radiation) sensor. All water samples were collected at fixed depth (surface, 5, 10, 15, 25 and 50 m) and at fluorescence peaks at all stations (n=55) (Table 1). At stations with primary production estimations (n=17), additional water samples were taken at five

photic depths detailed below (Table 1). The photic depths were established after calculating the light attenuation coefficient, K_d, using a Secchi disk (Parsons et al. 1984). Samples for phytoplankton were pre-filtered on a 333 μm mesh in order to remove large zooplankton.

The depth of the Surface Mixed Layer (SML) was calculated according to Thomson and Fine (2003). The 31.6 isohaline defines the bottom of the Polar Mixed Layer (PML), and the isohaline 32.4 is characteristic of waters of Pacific origin (Carmack et al. 1989).

Dissolved inorganic carbon (DIC) concentrations used in phytoplankton production calculation were measured by coulometric titration (Johnson et al. 1993, DOE 1994).

Inorganic nutrient concentrations (nitrate + nitrite, phosphate and silicic acid) were measured on board using standard colorimetric methods (Grasshoff 1999) as described in Simpson et al. (2008).

Downwelling PAR (400–700 nm) irradiance was acquired using a GUV-510 surface radiometer (Biospherical Instruments). Underwater downwelling PAR profiles were collected at some stations using a PUV-500 radiometer (Biospherical Instruments) around noon. Irradiance profiles were recorded from the surface down to 60-75 m (or to the bottom at shallow stations). Underwater irradiance measurements were corrected for dark current measured in the field using light-tight neoprene caps. The depth of the euphotic zone (1 % isolume) was further estimated by linear regression of the natural logarithm of underwater downwelling irradiance versus depth. PAR irradiance at sampling depth was obtained from the CTD PAR sensor.

Wind speed and direction at Tuktoyaktuk and Cape Parry (Fig. 1) were obtained from the Weather Archive of Environment Canada (http://climate.weatheroffice.ec.gc.ca).

Table 1: Stations sampled for the different measurements during spring and summer 2004.

Season	Date		Station	Sampling	Season	Date		Station	Sampling
Spring	June	4	206	Biomass, Taxo, PP, PE	Summer	July	12	606	Biomass, Taxo
		5	256	Biomass			13	650	Biomass, Taxo, PP
		7	108	Biomass, Taxo, PP, PE			16	200	Biomass, Taxo, PP, PE
		8	112	Biomass, Taxo			18	118	Biomass, Taxo
		9	115	Biomass, Taxo			19	309	Biomass, Taxo, PP, PE
		10	117	Biomass, Taxo, PP, PE			19	312	Biomass, Taxo
		11	124	Biomass, Taxo			20	315	Biomass
		12	414	Biomass, Taxo			21	415	Biomass, Taxo, PP, PE
		14	409	Biomass, Taxo			21	412	Biomass
		15	406	Biomass, Taxo, PE			23	409	Biomass, Taxo, PP, PE
		17	403	Biomass, Taxo			24	406	Biomass, Taxo
		17	400	Biomass, Taxo			24	403	Biomass, Taxo
		19	303	Biomass, Taxo, PP, PE			25	400	Biomass, Taxo
		21	300	Biomass, Taxo			27	721	Biomass, Taxo
		21	CA20	Biomass, Taxo			28	124	Biomass, Taxo
Summer	June	26	600	Biomass			29	115	Biomass, Taxo
		27	609	Biomass, Taxo			30	109	Biomass, Taxo
		28	703	Biomass, Taxo			30	215	Biomass, Taxo
		30	709	Biomass, Taxo, PP			31	212	Biomass
	July	4	906	Biomass, Taxo, PP, PE			31	209	Biomass, Taxo
		5	909	Biomass, Taxo		August	1	206	Biomass, Taxo, PP, PE
		6	912	Biomass, Taxo, PP, PE			1	203	Biomass, Taxo
		7	809	Biomass, Taxo			6	200b	Biomass, Taxo, PP, PE
		8	803	Biomass, Taxo, PP, PE			7	124b	Biomass
		9	706	Biomass, Taxo			8	118b	Biomass
		10	712	Biomass, Taxo			9	112	Biomass, Taxo
		10	715	Biomass, Taxo			10	106	Biomass, Taxo, PP, PE
		11	718	Biomass, Taxo, PP, PE					

Biomass: total and fractionated chl *a* measurements; Taxo: phytoplankton taxonomic identifications; PP: primary production measurements and PE: photosynthetic parameters estimation.

Region definition

Stations of the summer sampling period were separated according to their locations relative to 128.35°W, which roughly corresponds to the tip of the Cape Bathurst. Stations west of 128.35°W on the Mackenzie shelf and slope (depth < 400 m) were considered as Mackenzie shelf stations, and stations east of 128.35°W were considered to be in the Amundsen Gulf region. However, the coastal station 415 was not considered in the Amundsen Gulf region.

Chlorophyll *a* determination

For the determination of phytoplankton chlorophyll *a* (chl *a*) concentration, water sub-samples of 0.5 to 1 l were filtered onto glass fibre filters (poresize 0.7 μm, Whatman GF/F) (total biomass), 5 μm polycarbonate filters (Poretics) (large cells biomass) and 20 μm Nitex filters. Chl *a* concentrations were determined with a 10-AU Turner Designs fluorometer following 24 hr extraction in 90 % acetone at 5°C in the dark without grinding (Parsons et al. 1984). Concentrations of chl *a* were corrected for phaeopigments by acidification of the extract (Knap et al. 1996). All values were integrated over 50 m at all stations. At stations with primary production estimates, chl *a* concentrations were also integrated over the euphotic zone. As the euphotic zone was not measured at all stations, the depth of 50 m was chosen for integration of chl *a* concentration values in order to include the euphotic zone, the PML and the deepest chl *a* peak for most of the stations.

Taxonomic identification

Water sub-samples (250 ml), for phytoplankton cell identification and enumeration, were collected at the fluorescence peaks at all stations, and additionally at surface and the 1 % isolume depth for stations with primary production estimates (Table 1). The samples were fixed with acidic Lugol solution (4 % final concentration) and stored in the dark at 4°C until analysis. Water samples of 10 to 100 ml were settled in Zeiss-type settling chambers for at least 12 hr before cell enumeration with a Leitz Diavert inverted microscope with phase contrast optics at 250x and 400x. The main taxonomic references used to identify phytoplankton were Tomas (1997), Jensen and Møestrup (1998), Bérard-Therriault et al. (1999) and Throndsen et al. (2003). Some dinoflagellates and diatoms unidentified were grouped in size classes (5-10, 11-20, 21-50 and >50 μm), while chlorophytes, chrysophytes, dictyochophytes, cryptophytes, euglenophytes, prasinophytes and prymnesiophytes unidentified to species or genus level were also grouped according to their size classes (<5, 5-10, 11-20 and >20 μm), as well as unidentified flagellates.

Photosynthetis/irradiance relationships

Photosynthesis/irradiance relationships were measured by ^{14}C uptake using a small-volume, short-incubation time method adapted from Lewis & Smith (1983). Stations were sampled at two or three depths : surface, chlorophyll maximum and 1 % isolume (Table 1). Under dim light, one 100 ml water sub-sample was poured into a flask where 160 μCi of $NaH^{14}CO_3^-$ were added. After a gentle homogenisation, 3 ml aliquots were dispensed into 23 clean 20 ml borosilicate scintillation vials. The vials were then placed under an artificial

light gradient, and maintained at low temperature (*in situ* temperature ± 2°C) using a circulating water bath. The range of light intensities was created by the use of neutral density screens. Light intensities from 10 to 1500 µmol m^{-2} s^{-1} (PAR) within the incubator were measured with a scalar irradiance meter (QSL-100 Biospherical Instruments). Three scintillation vials were incubated in the dark. The total added activity was determined (triplicates) by adding 250 µl of the inoculated water sub-sample into 10 ml Ecolume scintillation fluid (ICN) containing 250 µl ethanolamine. After 1 hour of incubation, non-incorporated ^{14}C was removed by adding 500 µl of 6N HCl. After 24 hours, 500 µl of 6N NaOH were added to the samples to avoid pH changes, then 15 ml of scintillation cocktail were added and the samples were counted using a Packard Liquid Scintillation Analyzer Tri-Carb® 2900 TR scintillation counter. Counts were transformed into carbon fixation rates using actual DIC concentrations and dark-corrected.

Carbon fixation data were normalised to chl *a* and fitted to the equation of Platt et al. (1980) using an iterative non-linear regression (Statistica 7):

$$P^B = P_s^B \times [1 - \exp(-\alpha E / P_s^B)] \times [\exp(-\beta E / P_s^B)] \quad (1)$$

where P^B is the photosynthesis normalized to chl *a* concentration (mg C (mg chl *a*)$^{-1}$ h^{-1}); P_s^B is the theoritical maximum for photosynthesis in the absence of phototinhibition (mg C (mg chl *a*)$^{-1}$ h^{-1}); α is the initial rate of photosynthesis (mg C (mg chl *a*)$^{-1}$ h^{-1} (µmol m^{-2} s^{-1})$^{-1}$); β is a measure of photoinhibition (mg C (mg chl *a*)$^{-1}$ h^{-1} (µmol m^{-2} s^{-1})$^{-1}$). The actual maximal photosynthetic rate P_{max}^B (mg C (mg chl *a*)$^{-1}$ h^{-1}) and the optimal irradiance for photosynthesis E_k (µmol m^{-2} s^{-1}) were calculated as follows:

$$P_{\max}^{B} = P_{s}^{B} \times [\alpha/(\alpha + \beta)] \times [\beta/(\alpha + \beta)]^{\beta/\alpha} \qquad (2)$$

$$E_{k} = P_{\max}^{B}/\alpha \qquad (3)$$

Phytoplankton production

Particulate primary production was estimated from five photic depths (100, 50, 25, 10 and 1 % of surface irradiance) using the ^{14}C uptake method (Knap et al. 1996). Samples were incubated in 500 ml polycarbonate bottles (two light and one dark with DCMU [3-(3,4-dichlorophenyl)-1, 1-dimethyl urea]) with 20 to 30 µCi of NaH^{14}CO$_3^-$, and placed under *in situ* simulated conditions in on-deck incubators, with running surface seawater and incident irradiances adjusted with neutral density filters. The total added activity was determined in triplicates by adding 250 µl of ethanolamine and 10 ml Ecolume scintillation fluid (ICN) to a 250 µl inoculated water sub-sample. After 24 hours of incubation, water sub-samples (150 ml or more) were filtered onto glass fibre filters (poresize 0.7 µm, Whatman GF/F) (total particulate primary production) and 5 µm polycarbonate filters (Poretics) (large cell particulate primary production). Non-incorporated ^{14}C was removed by addition of 250 µl of 0.5N HCl. Upon complete evaporation of the acid, 10 ml of Ecolume scintillation cocktail were added. The activity was determined using a Packard Liquid Scintillation Analyzer Tri-Carb 2900 TR. Primary production rates were estimated with the actual DIC concentrations. All counts were dark-corrected and daily primary production rates were integrated over the euphotic zone. Incubations were initiated early in the morning (minimal PAR) in order to reduce the variability in ^{14}C accumulation (Mingelbier et al. 1994).

The f-ratio can be estimated from primary production rates following this equation: $f = 0.04 + 0.74$ (P_L/P_T), $r^2 = 0.80$, where P_T corresponds to total particulate primary production in the euphotic zone and P_L to large cells production in the euphotic zone (Tremblay et al. 1997). The phytoplankton new production, which corresponds to the maximum potential export of particulate primary production from the euphotic zone, can be further derived from the f-ratios (Dugdale & Goering 1967, Eppley & Peterson 1979): $P_{ex} = P_T \times f$-ratio.

Statistical analyses

In order to investigate differences in chl a biomass integrated over 50 m (total, >5 µm and >20 µm size fractions) between the different regions or seasons, the non-parametric pair comparison Mann-Whitney U test was applied, as the data did not meet normal distribution and homoscedasticity (Zar 1999). The small number of observations for primary production rates and f-ratios precluded statistical analyses of regional differences. Association between pair variables was estimated with the Spearman rank correlations (r coefficient), as data did not follow a normal distribution (Zar 1999). All statistical tests were carried out with the Statistica 7.0 program (StatSoft).

Multivariate approaches were applied to the community analysis. Phytoplankton cell abundances data were ordinated by non-metric multi-dimensional scaling (MDS) (Clarke 1993). The input was a similarity matrix based on Bray-Curtis similarity of fourth-root transformed and standardised cell abundances, to put more weight on the species

composition in the samples (Field et al. 1982). Those analyses were performed with the program Primer version 5.0 (Plymouth Marine Laboratory).

RESULTS

Physico-chemical conditions

During spring and summer, all stations were free of ice at sampling time. However, in spring stations 206, 256 and 108, in the south of the Amundsen Gulf, were sampled short after seasonal sea ice started to retreat (ca. 15 days), whereas station CA20 was sampled longer after sea ice retreated (ca. 30 days) (see Fig. 2a for stations location). North of the Amundsen Gulf, sea ice retreated earlier, though mobile sea ice could be present in the middle of the Amundsen Gulf in spring and summer. Sea ice was also present at stations north of the shelf slope (703, 706, 650 and 600) prior to sampling (see Fig. 3a for stations location).

Daily downwelling PAR irradiance decreased from spring to summer, ranging respectively from 22.6 to 63.3 and 14.7 to 57.2 mol photon $m^{-2} d^{-1}$. In spring, daily minimum irradiance ranged from 15 to 110 μmol photon $m^{-2} s^{-1}$ and daily maximum from 620 to 1480 μmol photon $m^{-2} s^{-1}$. In summer, daily minimum irradiance varied from 1 to 120 μmol photon $m^{-2} s^{-1}$ and maximum from 315 to 1360 μmol photon $m^{-2} s^{-1}$.

In spring, stations south of the Amundsen Gulf were characterised by low sea surface temperature (-1.3 to -1.1°C), relatively high surface salinity (ca. 30.1) and thin SML (6 to 15 m) and PML (16 to 26), consistent with a recent ice retreat. In the middle of the Amundsen Gulf, sea surface temperature and salinity were higher (-0.7 to -0.2°C and 30.2 to 30.5, respectively) and both SML and PML were thicker (11 to 55 m and 36 to 63 m, respectively). Station CA20 presented the same characteristics than stations in the

middle of the Amundsen Gulf, but its surface temperature was higher. In the area around the northeast corner of the Mackenzie shelf, physical characteristics were markedly different, sea surface temperature and salinity were high (0.6 to 1.8°C and 30.5 to 32.1, respectively) and the SML became thicker as the PML thinned. At station 400, waters of Pacific origin were present at 11 m, as shown by the 32.4 salinity threshold. This could indicate the occurrence of upwelling, consistent with strong easterlies winds blowing in the area during the two weeks prior to sampling.

In the Amundsen Gulf, sea surface temperature was generally higher in summer (-0.7 to 7.1°C) than in spring and surface salinity lower owing to sea ice melt (19.6 to 30.3). In general, lower surface temperature and salinity resulted probably from mobile sea ice moving over the Amundsen Gulf (stations 109, 215, 212, 106 and 112). The SML was usually thin (ca. 4 to 11 m), whereas the PML laid above 30 to 60 m.

Over the Mackenzie shelf and slope, offshore stations showed low sea surface temperature and high surface salinity, whereas warm surface temperature and low salinity were found close to the coast associated to the Mackenzie River plume. At time of sampling, the Mackenzie River flow was still high, about 14500 m^{-3} s^{-1} (Water survey of Canada, Environment Canada, www.wsc.ec.gc.ca). The Mackenzie River waters formed a warm brackish layer of 5 to 10 m over the shelf, which was present at stations 912, 909, 906, 809, 803, 718, 715 and 712 (surface temperature from 4.6 to 9.3°C and surface salinity from 15.0 to 23.9). The SML corresponded to this brackish layer (see Fig. 3 for stations location). The PML was thinner inshore and thicker offshore. Waters of Pacific origin were

also present at shallow depths at stations 609 and 912, suggesting upwelling of deep water masses over the shelf at the end of June and early July.

In the Amundsen Gulf, the depth of the euphotic zone (1 % isolume) was comparable in spring and summer, and roughly corresponded to the bottom of the PML around 40 to 60 m. Over the Mackenzie shelf, the euphotic zone was deep offshore (40 to 55m) and shallower close to the river mouth (3 to 20 m), with the thinnest euphotic zone at stations 912 to 909.

Over all sampling seasons and regions, nitrate was likely the limiting nutrient in the upper 50 m (N/P < 6) (Simpson et al. 2008), but was still at moderate concentrations at the bottom of the PML (> 1 μM). In spring, stations south of the Amundsen Gulf showed relatively high nitrate inventories in the upper 50m (223 to 242 mmol m^{-2}), which were not depleted at surface. Nitrate were depleted at surface (< 1 μM) at all other stations, which had low nitrate inventories (averaging 107 mmol m^{-2}), except station 400, exhibiting the highest nitrate inventory (404 mmol m^{-2}). In summer, nitrate inventories were also low in the gulf (averaging 91 mmol m^{-2} over 50 m) and depleted at surface. Over the Mackenzie shelf, nitrate were also generally depleted at surface and presented low inventories (141 mmol m^{-2} on average), however nitrates were still abundant at the surface of some inshore stations with high inventories (206 to 440 mmol m^{-2}).

Chlorophyll *a* concentrations

In spring, there was almost no chl *a* maximum at stations in the middle of the Amundsen Gulf and stations recently ice free, and phytoplankton biomass was concentrated

above the PML, where chl a concentrations ranged from 0.01 to 0.67 mg m^{-3}. Chl a maxima were present at stations 406, 303 and CA20, reaching the highest concentration of 22.4 mg m^{-3} at 35 m of station 303. At stations over the eastern part of the Mackenzie shelf, chl a concentrations were high from the surface to the chl a maximum (1.2 to 16.5 mg m^{-3}). Both fractionated chl a concentrations (>5 μm and >20 μm) were positively correlated to total chl a concentrations (p < 0.05). Based on integrated chl a biomass and its size structure, two groups of stations could be discriminated (Fig. 2). Group 1 included the stations in the middle of the Amundsen Gulf and stations recently ice free (206, 256, 108, 112, 115, 117, 124, 414 and 409), whereas group 2 comprised stations west of the gulf (406, 403, 400, 300, 303 and CA20). Group 1 stations presented significantly lower biomass and significantly lower contribution of cells >5 μm and >20 μm than stations from group 2 (Mann-Whitney U test, p < 0.05) (Table 2). At group 1 stations, the biomass varied from 1.7 to 33.7 mg chl a m^{-2} with a low average contribution of cells >5 μm (24 %) and cells >20 μm (10 %), whereas in group 2 the biomass ranged from 56 to 439 mg chl a m^{-2} with high average contribution of cells >5 μm (85 %) and cells >20 μm (59 %).

In summer, phytoplankton biomass formed a deep chl a maximum in the Amundsen Gulf, which generally laid at the bottom of the PML and the euphotic zone. Deep chl a peaks averaged 0.82 mg m^{-3} and reached 3.92 mg m^{-3} at station 312. Phytoplankton biomass and its size structure did not show any spatial pattern, and were rather homogeneously distributed in the Amundsen Gulf (Fig. 3). As in spring, fractionated (>5 μm and >20 μm) and total chl a concentrations were also positively correlated (p < 0.05). Phytoplankton biomass in summer was not significantly different from the spring group 1

(Mann-Whitney U test, p > 0.05), and varied from 8.0 to 50.6 mg chl a m^{-2}. Although in summer, >5 µm cells contribution to biomass was slightly higher than in spring (Mann-Whitney U test, p < 0.05), small cells (<5 µm) dominated the phytoplankton biomass (Table 2).

Table 2: Chl *a* biomass (integrated over the upper 50 m) and the relative contribution of large phytoplankton cells >5 μm and >20 μm to this biomass in spring, for groups 1 and 2, and in summer in the Amundsen Gulf and on the Mackenzie shelf, mean ± SD, the number of stations is in brackets.

		Chl *a* biomass (mg m^{-2})	Contribution of cells >5 μm (%)	Contribution of cells >20 μm (%)
Spring	Group 1	13.2 ± 10.4 (9)	24 ± 21 (9)	10 ± 16 (9)
	Group 2	204.2 ± 155.9 (6)	85 ± 11 (6)	59 ± 12 (6)
Summer	Gulf	18.8 ± 8.9 (21)	32 ± 16 (21)	6 ± 8 (21)
	Shelf	94.6 ± 121.9 (15)	66 ± 28 (11)	55 ± 27 (11)
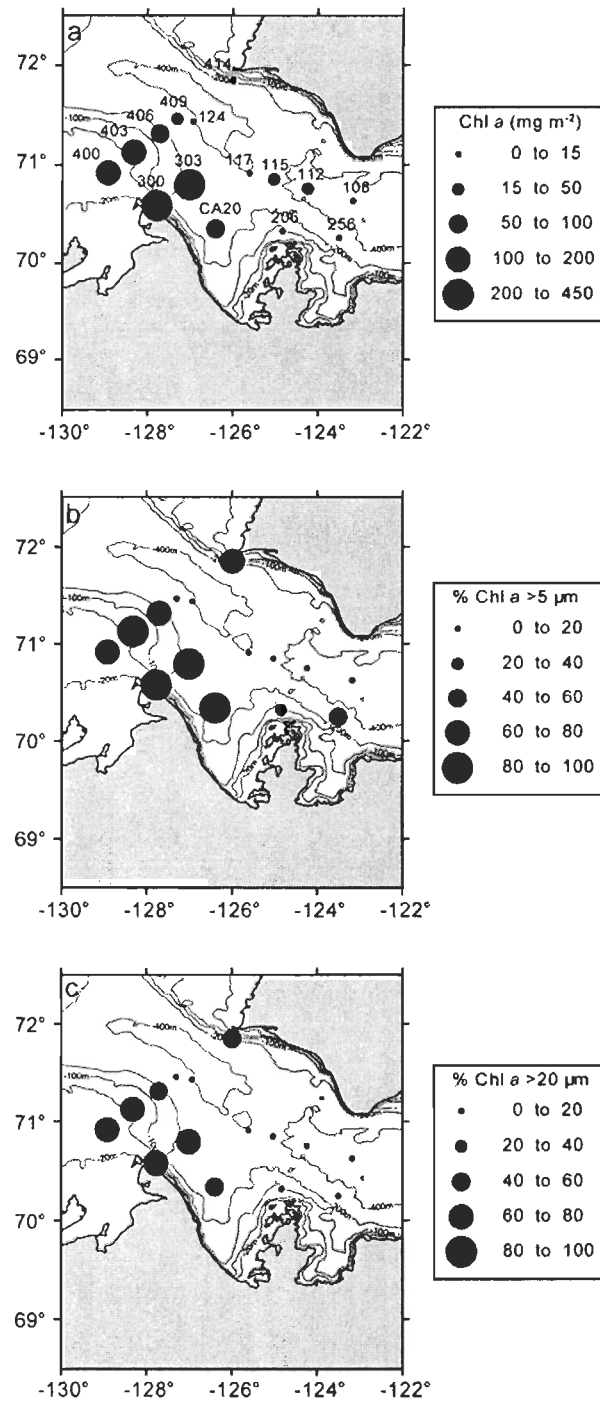
Figure 2: Spatial distribution of (a) chl *a* biomass (integrated over 50 m) in mg chl *a* m^{-2}, (b) percent contribution of cells >5 μm and (c) cells >20 μm to biomass, during spring 2004.
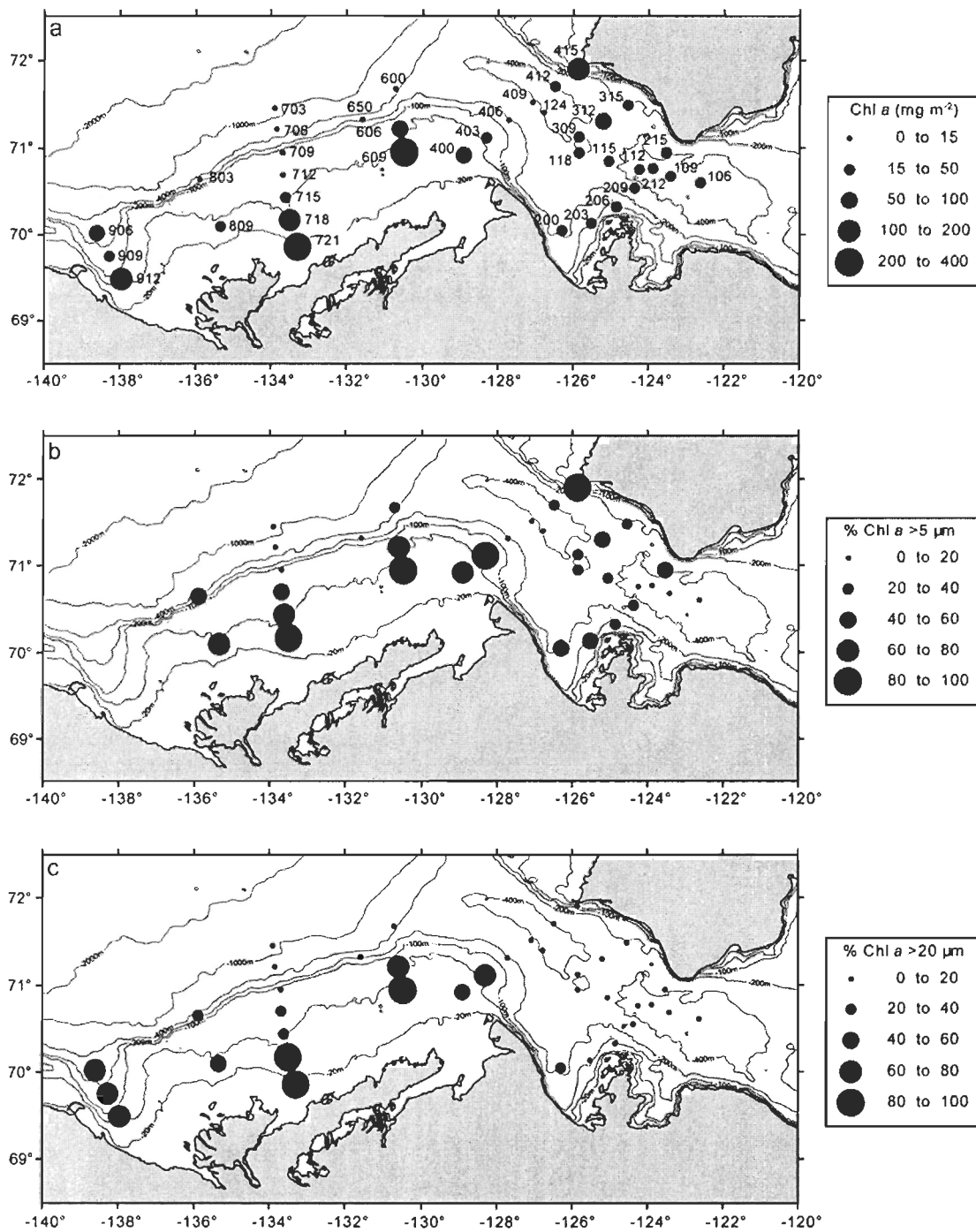
Figure 3: Spatial distribution of (a) chl *a* biomass (integrated over 50 m) in mg chl *a* m^{-2}, (b) percent contribution of cells >5 μm and (c) cells >20 μm to biomass, during summer 2004.

In summer, the vertical distribution of chl a at stations over the continental slope or north of the Mackenzie shelf was similar to that in the gulf, with a weak maximum (0.4 mg m^{-3} on average) at the bottom of the PML. Over the Mackenzie shelf, two chl a peaks were usually observed, the first in the top few meters, in the river plume, (0.3 to 7.2 mg m^{-3}) and the second at the bottom of the PML (0.3 to 26 mg m^{-3}). At stations over the Mackenzie and Kugmallit canyons, the PML was thinner close to the shore, and pacific waters were even present at 22 m of stations 912, however the chl a peaks associated to this water masses were below the euphotic zone (Fig. 4). Phaeopigments were at low concentration compared to total chloropyllous pigments and never exceeded 10 % at both chl a peak depths. Phytoplankton biomass and size structure were highly variable over the shelf (Fig. 3). Fractionated (>5 μm and >20 μm) and total chl a concentrations were again positively correlated (p < 0.05) and significantly higher over the shelf than in the Amundsen Gulf in summer (Mann-Whitney U test, p < 0.05) (Table 2). Phytoplankton biomass was high at stations influenced by the river plume (12 to 350 mg chl a m^{-2}) and dominated by large phytoplankton cells (42 to 78 % due to cells >5 μm and 26 to 86 % to cells >20 μm) (Table 2). This was also true at stations on the eastern part of the shelf, where biomass reached a maximum of 400 mg chl a m^{-2} at station 609, with maximal contribution of cells >5 μm and >20 μm of 94 and 83 % respectively.
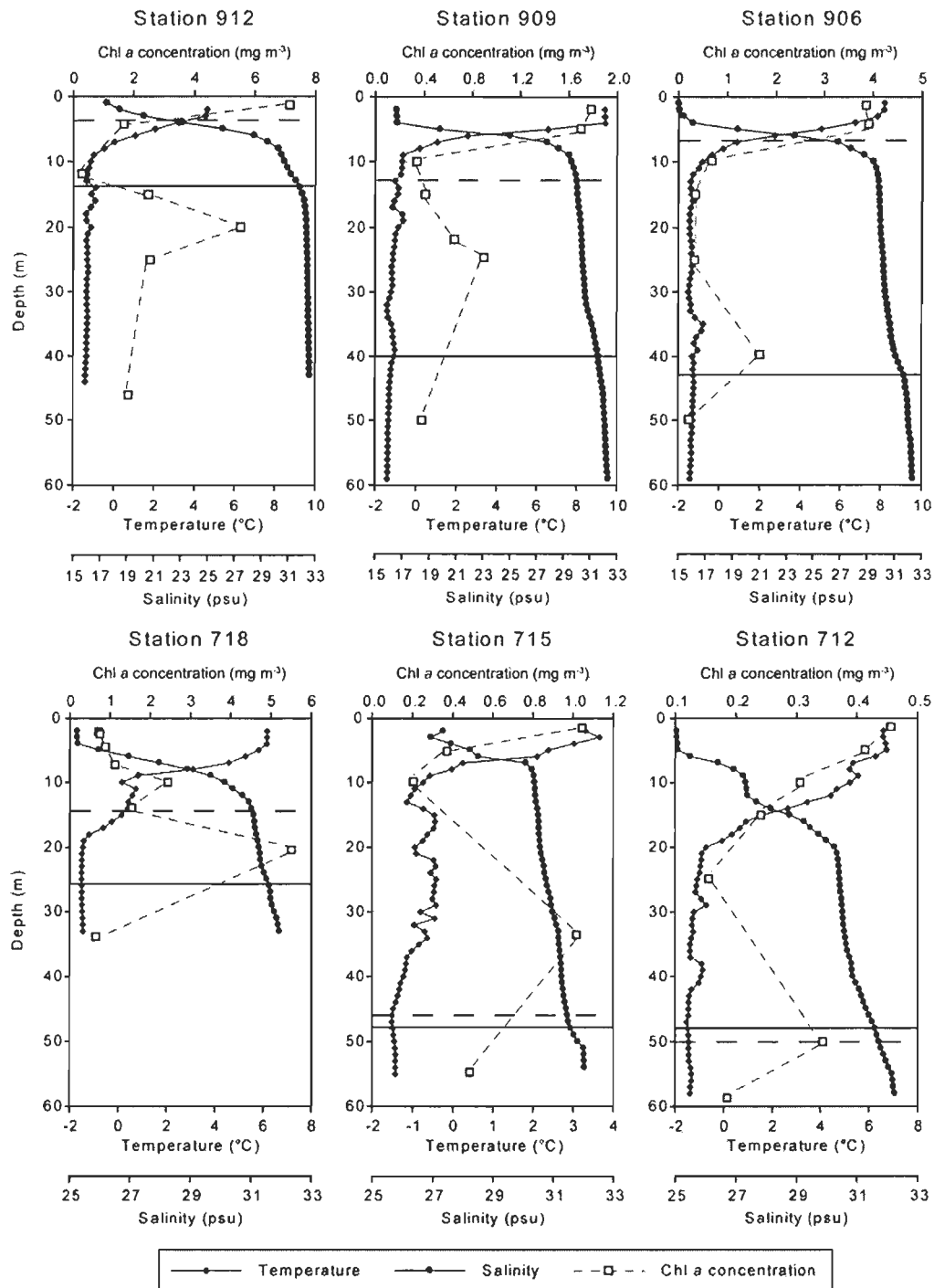
Figure 4: Vertical profiles of chl *a* (mg chl *a* m^{-3}), temperature (°C) and salinity (psu) at stations beyond the Mackenzie River plume influence. The dark line corresponds to the bottom of the PML and the dotted line to 1 % isolume.

Cell abundance and taxonomic composition

The phytoplankton communities of the Mackenzie shelf and Amundsen Gulf regions were composed of 273 taxa, including 84 diatom, 78 dinoflagellate and 66 flagellate species. During spring and summer, no cyanobacteria were observed in samples from the Amundsen Gulf and the Mackenzie shelf, despite the river plume influence. Phytoplankton cell abundances followed generally the seasonal and spatial pattern of biomass. In spring, phytoplankton cell abundance was higher at group 2 (54×10^4 to 450×10^4 cells l^{-1}) than group 1 stations (26×10^4 to 88×10^4 cells l^{-1}). Moreover, shelf stations had higher cell abundances in summer (11×10^4 to 666×10^4 cells l^{-1}) than gulf stations (21×10^4 to 170×10^4 cells l^{-1}).

In spring, the two groups defined by the biomass structure were also separated on the MDS ordination plot (Fig. 5a). Unidentified flagellates and prymnesiophytes (*Chrysochromulina* spp., *Chrysochromulina spinifera* (Fournier) Pienaar and Norris) dominated the phytoplankton community of group 1 stations; whereas at group 2 stations diatoms dominated and pennate and centric species were equally present (Table 3). Centric diatoms were represented by *Thalassiosira hyalina* (Grunow) Gran, *T. antarctica* Comber, *T. nordenskioeldii* Cleve, *Chaetoceros socialis* Lauder, *C. wighamii* Brightwell, and pennates diatoms by species commonly growing in sea ice *Fragilariopsis* spp., *Fragilariopsis cylindrus* (Grunow) Krieger, *F. oceanica* (Cleve) Hasle, *Navicula pelagica* Cleve, *Fossula arctica* Hasle Syvertsen and von Quillfeldt, and *Pseudo-nitzschia delicatissima* (Cleve) Kuntze. In summer, samples from the Amundsen Gulf were more similar than samples from the Mackenzie shelf (Fig. 5b). In the gulf, the community was

mainly composed of unidentified flagellates and centric diatoms (*C. socialis*, *Chaetoceros* cf. *minimus* (Levander) Marino, Giuffré, Montresor and Zingone, and *C. tenuissimus* Meunier) (Table 3). The summer phytoplankton communities of the Amundsen Gulf were more similar to the spring communities of group 1 stations than group 2 stations (Fig. 5c). In summer, Mackenzie shelf phytoplankton communities were generally dominated by diatoms, mostly centric (*C. socialis*, *C. wighamii* and *T. nordenskioeldii*), and unidentified flagellates (Table 3). In the area strongly influenced by the river plume, surface and deep samples were well discriminated (Fig. 5d). The surface communities consisted of centric diatoms (*C. wighamii*, *C. socialis*, spores of *C. holsaticus* Schütt, *T. nordenskioeldii* and spores of *Melosira arctica* (Ehrenberg) Ralfs) and unidentified flagellates (Table 3). Deeper communities were also dominated by centric diatoms (*C. socialis*, *C. wighamii*, *T. nordenskioeldii*, spores of *C. socialis* cf. *socialis* and spores of *C. holsaticus*) and unidentified flagellates, but showed a high proportion of pennate diatoms (*F. cylindrus*, *Achnanthes taeniata* (Grunow) Round and Basson, *F. oceanica*, *Pseudo-nitzschia* cf. *pseudodelicatissima* (Hasle) Hasle) and prymnesiophytes (*C. spinifera* and *Phaeocystis pouchetii* (Hariot) Lagerheim) (Table 3).
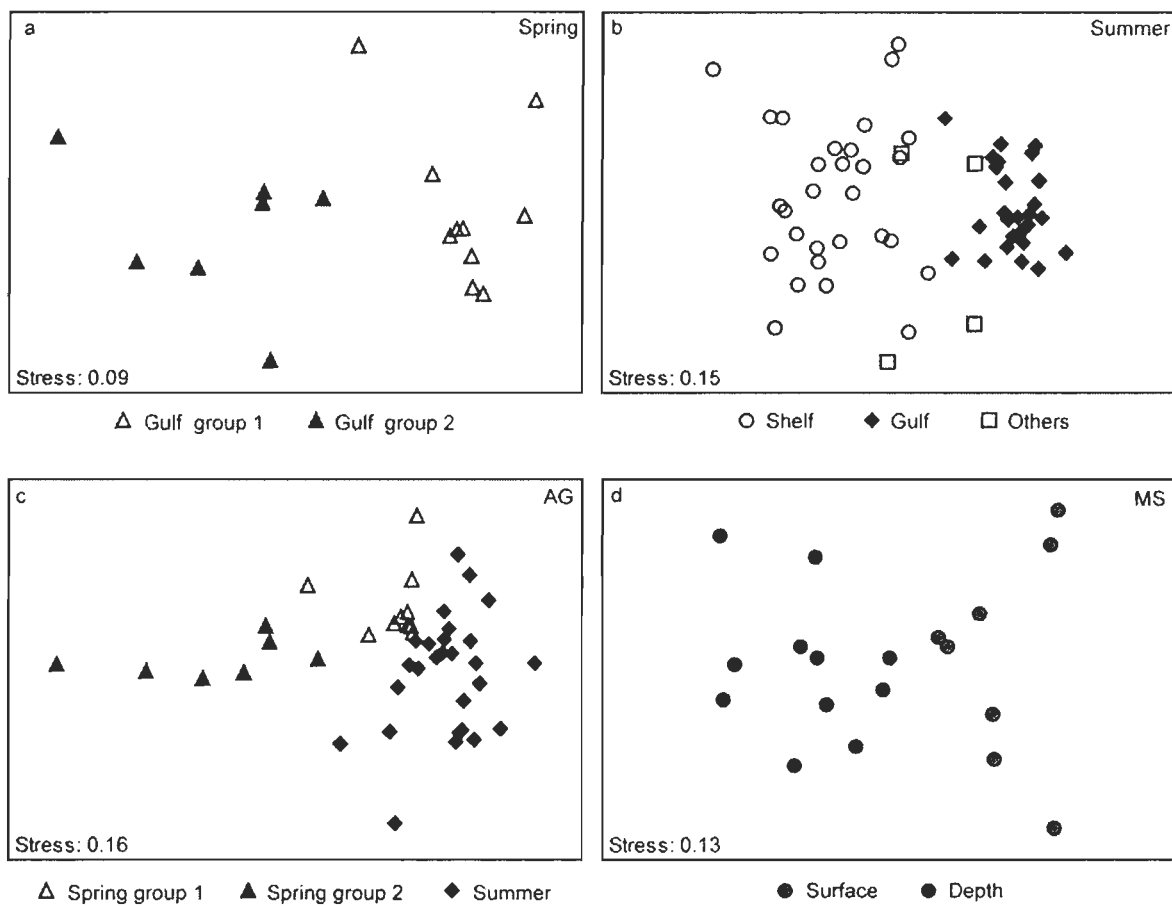
Figure 5: Multidimensional scaling ordination plot of species abundances (a) in spring 2004, (b) in summer 2004, (c) in the Amundsen Gulf (AG) in spring and summer 2004, and (d) over the Mackenzie shelf (MS).

Table 3: Average percent contribution of the major algal groups to the phytoplankton cell abundances in spring, for groups 1 and 2, and in summer in the Amundsen Gulf and on the Mackenzie shelf, in surface and deep waters.

	Spring		Summer			
	Group 1	Group 2	Gulf	Shelf	Surface	Deep
Diatoms	9.3	70.3	21.2	46.3	40.1	56.0
Centric	5.7	34.0	16.5	35.1	34.0	38.2
Pennate	3.6	36.3	4.7	11.2	6.1	17.8
Dinoflagellates	8.6	3.3	8.8	5.6	4.9	6.3
Athecate	7.7	2.6	8.2	4.9	3.9	5.7
Thecate	0.9	0.6	0.5	0.7	1.1	0.6
Chlorophytes	0.0	0.2	0.1	0.2	0.3	0.1
Chrysophytes	0.1	0.1	5.6	4.7	13.3	0.6
Dictyochophytes	3.4	1.7	2.0	1.7	2.6	0.5
Cryptophytes	2.9	1.7	2.0	1.0	1.4	0.8
Prasinophytes	2.1	0.4	3.2	3.1	4.2	1.5
Prymnesiophytes	22.5	8.0	9.9	7.9	0.3	8.9
Unidentified flagellates	40.7	7.9	42.0	23.4	30.7	19.9
Choanoflagellates	7.4	5.5	2.7	5.1	1.1	4.8

Photosynthetis/irradiance relationships

Photosynthesis exhibited a saturation response as a function of irradiance at all stations. The mean α value was 0.054 mg C (mg chl a)$^{-1}$ h^{-1} (μmol m^{-2} s^{-1})$^{-1}$, ranging from 0.003 to 0.113 mg C (mg chl a)$^{-1}$ h^{-1} (μmol m^{-2} s^{-1})$^{-1}$. The mean P^B_{max} value was 2.77 mg C (mg chl a)$^{-1}$ h^{-1} [range 0.01 to 38.38 mg C (mg chl a)$^{-1}$ h^{-1})], and the average E_k value was 69 μmol m^{-2} s^{-1}. The photoinhibition parameter β averaged 0.012 mg C (mg chl a)$^{-1}$ h^{-1} (μmol m^{-2} s^{-1})$^{-1}$. There was no clear difference between the regions and seasons (Table 4). However, there was a slight trend of decreasing α and increasing E_k from spring to summer. In surface samples, α and P^B_{max} were usually higher than at depth, while E_k was generally lower at surface. Surface E_k was usually close, or lower, than PAR irradiance available at sampling depth during the day. In the Mackenzie river plume waters, stations 912, 906 and 718 exhibited high α and P^B_{max} and low E_k, while at station 803, α and P^B_{max} were low, and lower than deeper at that station with the opposite trend for E_k (Table 5). The P/E parameters did not show any correlation with phytoplankton assemblage compostion, neither to physico-chemical variables.

Table 4: Photosynthetic parameters measured in spring and summer from surface and deeper waters.

		α	β	$P_{\max}^{B}$	E_k
Spring	Surface	0.039 ± 0.048	0.0011 ± 0.0008	1.5 ± 1.8	48 ± 28
		(5)	(5)	(5)	(5)
	Deep	0.219 ± 0.222	0.0677 ± 0.1522	11.2 ± 14.1	43 ± 30
		(7)	(7)	(7)	(7)
Summer	Surface	0.027 ± 0.020	0.0013 ± 0.0018	1.2 ± 0.8	49 ± 18
		(11)	(11)	(11)	(11)
	Deep	0.010 ± 0.008	0.0009 ± 0.0023	0.8 ± 0.4	97 ± 42
		(18)	(18)	(18)	(18)

Mean $\pm$ SD, the number of samples is between brackets.

Initial slope α [(mg C) (mg chl a)$^{-1}$ h^{-1} (μmol m^{-2} s^{-1})$^{-1}$], photoinhibition parameter β [(mg C) (mg chl a)$^{-1}$ h^{-1} (μmol m^{-2} s^{-1})$^{-1}$], actual maximal photosynthetic rate $P_{\max}^{B}$ [mg C (mg chl a)$^{-1}$ h^{-1}], optimal irradiance for photosynthesis E_k (μmol m^{-2} s^{-1}).

Table 5: Photosynthetic parameters measured from surface and deeper waters of stations influenced by the Mackenzie River plume.

Station	Depth	α	P_{max}^{B}	E_k
912	Surface	0.025	1.30	52
	1 % isolume	0.002	0.21	93
906	Surface	0.031	0.89	30
	1 % isolume	0.006	0.60	100
718	Surface	0.026	0.83	31
	1 % isolume	0.008	0.68	88
803	Surface	0.008	0.40	52
	1 % isolume	0.035	0.55	15

Initial slope α [(mg C) (mg chl a)$^{-1}$ h^{-1} (μmol m^{-2} s^{-1})$^{-1}$], actual maximal photosynthetic rate P_{max}^{B} [mg C (mg chl a)$^{-1}$ h^{-1}], optimal irradiance for photosynthesis E_k (μmol m^{-2} s^{-1}).

Primary production

In spring, integrated primary production rates were variable and averaged 254±182 mg C m^{-2} d^{-1} in the Amundsen Gulf, while later in summer primary production rates were lower and less variable about 105±26 mg C m^{-2} d^{-1}, except at station 415 characterised by maximum rate of 812 mg C m^{-2} d^{-1} (Fig. 6). Over the Mackenzie shelf, the highest production rates were measured at station beyond the river plume and the lowest offshore. On average integrated primary production rates were 177±177 mg C m^{-2} d^{-1} over the Mackenzie shelf (Fig. 6).
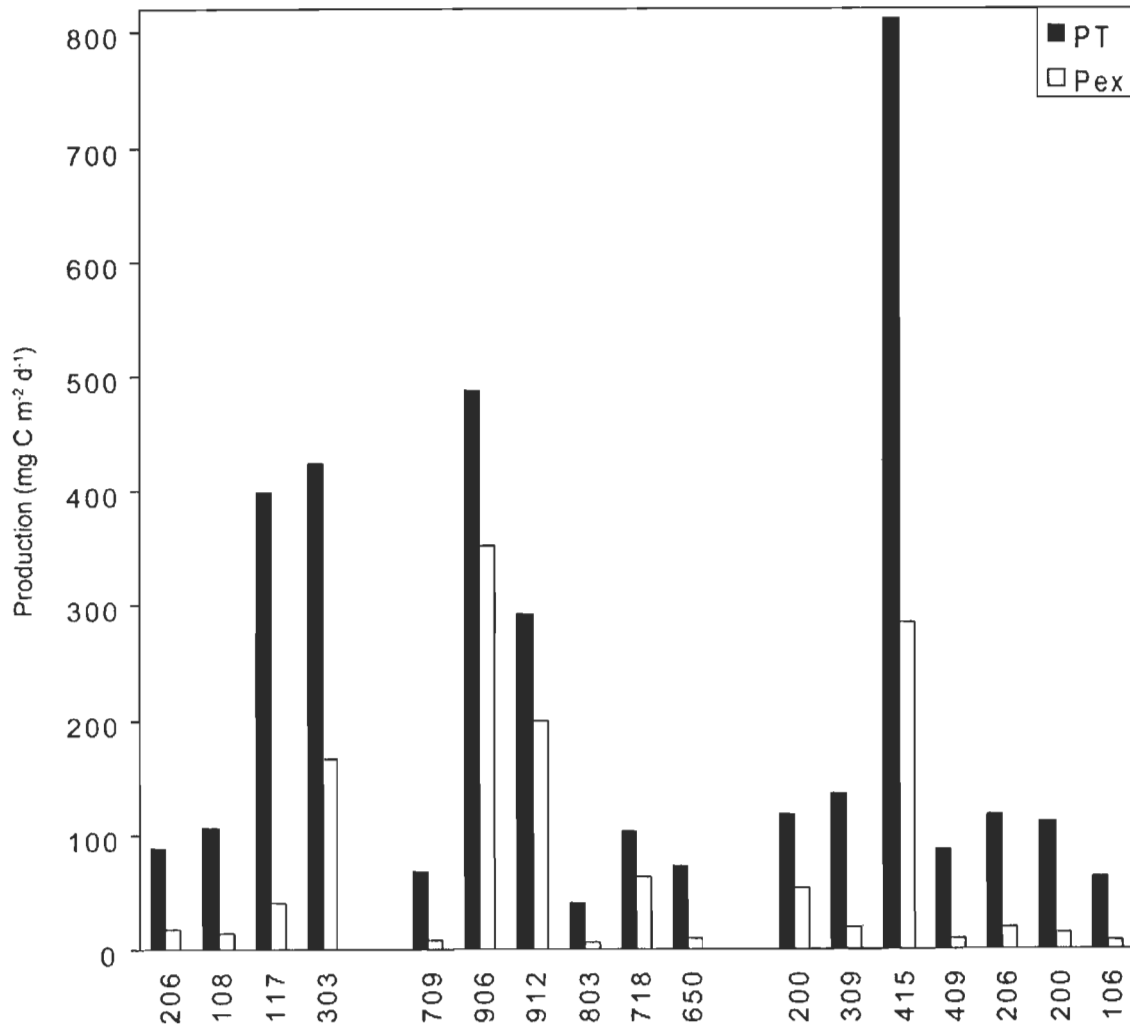
Figure 6: Rates of total particulate primary production (P_T) and estimates of maximum potential export of this particulate primary production (P_{ex}) (in mg C m^{-2} d^{-1}) integrated over the euphtotic zone from spring and summer 2004.

For all the sampling periods, f-ratios ranged from 0.10 to 0.58. The highest f-ratios corresponded to stations 303 in spring, 906 and 912 beyond the river plume in summer, and 415 and 200 in July. The potential export of primary production (P_{ex}) from the euphotic zone estimated from those f-ratios was variable throughout the sampling area and seasons (Fig. 6). In the Amundsen Gulf, P_{ex} accounted for 10 to 39 % of primary production in spring, as in summer (range of 11 to 46 %), and P_{ex} values were similar between seasons when station 303 was not considered. Over the Mackenzie shelf region, the river plume drove primary production potential export with high P_{ex} values from 40 to 281 mg C m^{-2} d^{-1} inshore (39 to 58 % of primary production) and low P_{ex} values from 6 to 10 mg C m^{-2} d^{-1} offshore (12 to 16 %).

DISCUSSION

Phytoplankton seasonal dynamics

Spring and summer periods were only sampled in the Amundsen Gulf area, therefore the seasonal dynamics could only be considered in this region. In spring, stations from the southern part of the Amundsen Gulf were sampled right after seasonal ice retreated, and the resulting phytoplankton biomass was low with variable contributions of >5 μm phytoplankton cells (Fig. 2). Moreover, nitrate concentrations at surface were close to the winter concentrations measured in Franklin Bay (Tremblay et al. 2008), suggesting that the phytoplankton community was in a pre-bloom stage. The exposure of phytoplankton cells to high light intensities could be responsible for the lag observed between ice retreat and phytoplankton growth, as cells were probably shade-adapted (Kirst & Wiencke 1995) and might take up to two weeks to be fully adapted to high light intensities (Tremblay et al. 2006). The station CA20 was sampled roughly two weeks after seasonal ice retreat, by that time phytoplankton formed a deep chlorophyll maximum (DCM) with relatively high chl a concentration (2.5 mg chl a m^{-3}), as well as a large contribution of >5 μm and >20 μm cells to biomass (96 % and 49 % respectively). Phytoplankton had consumed nutrients in the surface waters and the biomass accumulated above the PML where nutrients were still available. Diatoms dominated the DCM, with equal proportion of centric and pennate species. Pennate forms were represented by species (*Fragilariopsis cylindrus*, *Navicula pelagica* and *Pseudo-nitzschia delicatissima*), which were commonly growing in first-year sea ice in the area (M. Różańska, pers. comm.). This

suggests that a spring phytoplankton bloom developed following sea ice retreat and was probably seeded by ice algae. If we consider the time elapsed since ice retreat, the lag between ice retreat and phytoplankton growth and the biomass level measured at sampling time, the bloom duration could be reasonably approximated around two weeks, as was also estimated by nutrient draw-down (Simpson 2008).

In the middle of the Amundsen Gulf, the low phytoplankton biomass and contribution of large cells (>5 µm) (Fig. 2), together with the nitrate depletion, suggest that this area was already in post-bloom situation in early June, though no DCM was detected. Winds in the region typically force sea ice in and out of the area (Darnis et al. 2007) and the presence of sea ice prior to sampling may probably have led to unfavourable conditions for phytoplankton growth, through water column shading, melting and mixing, preventing phytoplankton to form DCM. Sea ice retreat and melting is not a continuous process in the Amundsen Gulf (Arrigo & van Dijken 2004, Barber & Hanesiak 2004), and sea ice can be occasionally forced into the area. Hence, spring blooms might not follow closely the seasonal ice retreat and be uncoupled in time and space in the Amundsen Gulf, as the persistence of DCM.

In summer, phytoplankton biomass formed a DCM, fuelled by nutrients from the Pacific halocline all over the Amundsen Gulf. The summer formation of DCM is also common in other arctic regions (Barents Sea, Owrid et al. 2000) and polynyas (North-East Water, Smith et al. 1995; North Water, Tremblay et al. 2006). Compared to spring DCM, summer DCM had lower sea ice signature, since most of sea-ice associated diatom species vanished. Although sea ice dynamic was less important in summer than in spring, the

presence of ice floes prior to sampling was associated to lower biomass and contribution of large cells (>5 µm) (Fig. 3). The shading of the water column during ice floes course was more likely responsible for the biomass decrease. The recurrent presence of sea ice in the Amundsen Gulf seemed to be the main factor of phytoplankton biomass variability in summer. Even if nitrates were still available at the DCM, the contribution of cells >5 µm and >20 µm to biomass were low or very low. Hence, the lack of accumulation of large cells, which were mostly diatoms, suggests an active grazing by mesozooplankton, which is consistent with the high flux of fecal pellets in the Amundsen Gulf (Juul-Pedersen 2007, Forest et al. 2008).

In the Amundsen Gulf, the summer vertical distribution of phytoplankton biomass differed from that of fall 2002. In October 2002, phytoplankton did not form DCM and was homogenously distributed in the first 30-40 m (Darnis et al. 2007, Chapitre I), whereas in October 2003, a DCM associated to bloom conditions formed at 30-35 m, and disappeared later in October to follow the same distribution as in fall 2002 (Chapitre I). The thinning of the euphotic zone, due to decreasing solar radiations, was more likely responsible for the DCM shoaling from summer to fall and its later disappearance. However, light availability was probably sufficient to sustain summer DCM until the end of August (Lee & Whitledge 2005).

Mackenzie River plume influence

The Mackenzie River waters form a buoyant layer that spreads over the Mackenzie shelf and responds quickly to wind stress and wind direction shift (Macdonald & Yu 2006).

Winds from the east tend to expand the river plume offshore toward the Canada Basin, whereas winds from the northwest force the plume eastward along the Tuktoyaktuk peninsula (Macdonald & Yu 2006). In June and July 2004, winds at Tuktoyaktuk came dominantly from the east with frequent strong winds from the northwest. At the end of June and beginning of July, winds came from the east, expanding the river plume offshore, and shifted to blow from southwest-northwest from 2 July and favoured the eastward expansion of the plume. The offshore station (906) was sampled soon after winds direction shifted and therefore presented the strongest river influence over the Mackenzie canyon, as shown by low salinity and high temperature (Fig. 4). The Mackenzie River plume was associated to high biomass, mostly comprising diatoms of nano- or microphytoplanktonic size, and high primary production (Fig. 4 and 6). However, phytoplankton communities in the river plume waters included numerous spores of the neritic centric diatom *Chaetoceros holsaticus*, indicating a decaying community as river plume waters aged or mixed with more saline waters. The high potential primary production export out of the euphotic zone, which corresponded to the river plume layer, was consistent with carbon flux measured at 25 m by Juul-Pedersen et al. (2008). This suggests that the Mackenzie River plume enhances primary production and carbon export on the shelf over short time periods depending on winds direction and strength.

Influence of winds on the shelf

Canyons crossing the Mackenzie shelf are sites of preferential upwelling (Macdonald et al. 1987) as the eastern corner of the Mackenzie shelf, where surface salinity

evidenced upwelling in June after two weeks of dominant easterlies at Tuktoyaktuk and Cape Parry. This upwelling event promoted high phytoplankton biomass over the eastern part of the shelf but also over the shelf slope. At station 303, the high biomass was mainly due to a thin DCM composed of diatoms. Nitrate concentration at DCM depth of station 303 was as low as concentrations at DCM depth during summer. Moreover, despite high primary production rate, the potential export was only of 39 %, suggesting that the bloom was already declining. Forest et al. (2008) estimated this bloom duration to less than five days, and explained its decline by shifts in wind direction. Wind-driven upwelling would thus favour short pulses of enhanced primary production and export.

The thinning of the PML over the Mackenzie and Kugmallit canyons, together with the strong easterlies that blew in the area prior to sampling, suggests that DCM observed at stations 906 to 912 and 712 to 718 was due to upwelling of nutrient-rich pacific waters over the shelf. At DCM, phytoplankton was actively growing, as evidenced by low phaeopigment concentration (<10 % of chl a concentration, data not shown), DCM were thus not related to phytodetritus resuspension. Over Kugmallit canyon, DCM were within the euphotic zone defined by the 1 % isolume at offshore stations, whereas at station 718 the DCM was laying between 1 and 0.1 % isolumes (Fig. 4). At stations 912 and 909, DCM were also situated between 1 and 0.1 % isolumes, while at station 906, light availability at DCM on sampling day was below 0.1 % of surface irradiance. Owing to the high variability in the Mackenzie River plume extension, light availability at DCM was likely variable from day to day, therefore light limitation would not occur for long periods. As the 1 % isolume was constraint to the surface brackish layer, primary production measurements at stations

718, 912 and 906 reflected only river plume production. Thus, upwelling related primary production was not assessed over the Mackenzie shelf. Furthermore, in turbid coastal waters of arctic shelves it would be interesting to estimate phytoplankton production until the 0.1 % isolume in June and July, when surface solar irradiance is maximal.

P/E parameters

From spring to summer, the P/E parameters measured in the Amundsen Gulf and over the Mackenzie shelf were close to that measured for other regions in the Arctic Ocean (Baffin Bay, Harrison & Platt 1986; Barents Sea, Rey 1991; Greenland Sea, Jensen et al. 1999), and also to those recorded in Antarctica (van Hilst & Smith 2002, Stambler 2003). Those parameters were characteristic of shade-adapted phytoplankton cells, i.e. high initial slope α, low maximal photosynthetic rate P^B_{max} and low optimal irradiance for photosynthesis E_k (Harrison & Platt 1986) (Table 4). In surface samples, E_k was generally close to irradiance at sampling time (early morning) and depth, therefore phytoplankton cells were light saturated roughly ten hours around midday, as they received more light energy than their absorption capacity (Kashino et al. 2002). In the Amundsen Gulf, E_k at surface was close or lower than E_k at depth, suggesting that surface communities were less adapted to their light environment than deep communities (from DCM or 1 % isolume). The surface nitrate depletion could limit phytoplankton acclimation to high irradiances at surface (Kashino et al. 2002). Moreover, Ralph et al. (2007) showed that during melting salinity stress could decrease the acclimation capacity of sea ice microalgae. Hence, the

presence of sea ice, melting throughout spring and summer in the Amundsen Gulf, could be an additional constrain to phytoplankton acclimation. Surface communities were dominated by flagellates and prasinophytes or chrysophytes, while in deep communities flagellates and diatoms dominated. Diatoms have high acclimation capacity, as they displayed a wide range of photoacclimation processes, and this could also have favoured the better acclimation of deep phytoplankton communities.

In the Mackenzie River plume, photosynthetic parameters in early July were close to that measured one month later at the river mouth by Retamal et al. (2008). However, E_k was slightly higher at the end of July when river sediment load was lower, thus high turbidity could have led to shade-adaptation of the river plume phytoplankton. Below the river plume, at depth where river plume waters mixed with shelf waters, photosynthetic parameters were the same as those from surface at the offshore station (Table 5). In addition, photosynthetic parameters values suggest that phytoplankton from marine shelf waters was acclimated to high irradiances before the river plume extension shaded the water column.

Phytoplankton biomass

In the Beaufort Sea, phytoplankton growth seemed to be mostly constrained by nitrate availability. The whole study area presented also high primary production to biomass ratios (5 to 18), which is common to other arctic regions, as the Barents Sea (Rey et al. 2000) or the central Arctic (Gosselin et al. 1997, Olli et al. 2007), and indicates a high

grazing pressure. Thus, in spring and summer, phytoplankton dynamics resulted from a complex combination of bottom-up and top-down controls.

During our study, the differences in phytoplankton communities of the Amundsen Gulf and the Mackenzie shelf were more likely due to the physical forcing prevailing in both regions. The Amundsen Gulf represented a stable environment, where the strong stratification could not be broken by winds during the sampling periods and the main factor of variability was sea ice dynamics. In contrast, the Mackenzie shelf was a highly variable environment strongly influenced by the Mackenzie River runoff and winds (river plume extension, shelf-break upwelling).

In the Amundsen Gulf, outside bloom periods, the phytoplankton biomass was relatively low and mostly due to small cells (<5 μm, ca. 70 % of biomass), consistent with measurements taken in the area in summer 2002 (Lee & Withledge 2005). These characteristics are common to the Barents (Not et al. 2005) and Greenland (Legendre et al. 1993) seas in summer or the central Arctic (Gosselin et al. 1997), but differed from other polynyas. In the Cape Bathurst polynya, the 2.5 to 3.5 fold lower phytoplankton biomass, compared to the Northeast water polynya (Smith et al. 1995) and the Northwater polynya (Klein et al. 2002) respectively, reflected probably the limited nutrient availability.

The Mackenzie shelf was characterized by a strong offshore gradient, with high biomass dominated by microphytoplankton (>20 μm) inshore, and low biomass dominated by small cells (<5 μm) over the continental slope. This gradient was already observed by Parsons et al. (1989) in the Beaufort Sea, but also on Russian shelves receiving large rivers outflow in the Kara (Deubel et al. 2003) and Laptev seas (Heiskanen & Keck 1996).

Furthermore, the Mackenzie shelf phytoplankton biomass was similar to previous measurements in the Beaufort Sea (Horner & Schrader 1982, Parsons et al. 1989) but also to biomass of the Russian Kara and Laptev Seas (Nöthig et al. 2003, Tuschling et al. 2000).

Primary production and export

In the Amundsen Gulf, spring and summer primary production rates (198 mg C m^{-2} d^{-1} and 105 mg C m^{-2} d^{-1} respectively) are lower than primary production measured in the Northwater polynya (1427 mg C m^{-2} d^{-1} in June and 414 mg C m^{-2} d^{-1} in July, Klein et al. 2002) and the Northeast water polynya (210 mg C m^{-2} d^{-1} in July, Smith 1995). This would place the Cape Bathurst polynya among the less productive polynyas in the Arctic. Meanwhile, the summer primary production is very similar to the rate of 106 mg C m^{-2} d^{-1} estimated in the Canada Basin and the Amundsen Gulf in late August 2002 (Lee & Whitledge 2005) and to the production measured in the Canada Basin north of the Chukchi Sea in late August (123 mg C m^{-2} d^{-1}, Cota et al. 1996). Finally, the Amundsen Gulf primary production compares well with production levels of the central Arctic (Gosselin et al. 1987, Olli et al. 2007) and the northern Barents Sea (Hegseth 1988), but remains at least twice lower than production in the Greenland Sea (Legendre et al. 1993, Richardson et al. 2005). Over the Mackenzie shelf, primary production was variable and exhibited an inshore-offshore gradient with lower rates offshore as observed in inner arctic shelf (Laptev Sea, Sorokin & Sorokin 1996). Primary production (40 to 487 mg C m^{-2} d^{-1}) falls in the range of previous estimates for the Beaufort Sea (Hsiao et al. 1977, Carmack et

al. 2004) and is similar to rates measured in the Laptev Sea (Sorokin & Sorokin 1996, Schmid et al. 2006).

We can build a composite annual primary production estimate and its potential export based on a composite productive period with fall measurements from 2002 and 2003 (Chapitre I) and spring and summer measurements in 2004 in the Amundsen Gulf. The productive period covered June to October. We extrapolated the gap in primary production measurements from mid-August to mid-September using summer and fall rates. A spring bloom of two weeks was estimated, however no measurement of this spring bloom were obtained, hence we used primary production rate measured during the upwelling-related bloom (spring 2004). Based on these conditions, the annual primary production reached 21 g C m^{-2} y^{-1}, of which 26 % could potentially be exported out of the euphotic zone. This estimate would be a lower estimate, since we did not measure the actual primary production during the spring bloom, and we could not include a fall bloom in the calculation. This annual primary production is in the same range as the estimate of 12-16 g C m^{-2} y^{-1} for the Beaufort Sea (Carmack et al. 2004) and 23-28 g C m^{-2} y^{-1} over the Mackenzie shelf slope (Lavoie et al. 2008), but 4 to 9 times lower than the satellite estimate of 90 to 175 g C m^{-2} y^{-1} in the Cape Bathurst polynya (Arrigo & van Dijken 2004). The annual primary production from Arrigo and van Dijken (2004) is comparable or higher than annual primary production of the Chukchi Sea (80 g C m^{-2} y^{-1}, Hill & Cota 2005; 55 g C m^{-2} y^{-1}, Lee et al. 2007), the Bering Sea (84-150 g C m^{-2} y^{-1}, Rho & Whitledge 2007) or the Northwater polynya (152 g C m^{-2} y^{-1}, Klein et al. 2002), which are systems with recurrent nutrients supply during the ice free season. Therefore, the actual annual primary production in the

Amundsen Gulf would probably lay between 20 and 90 g C m^{-2} y^{-1}. Based on the same calculation, the potential carbon export out of the euphotic zone would average 5 g C m^{-2} y^{-1}. However, for the same period the marine particulate organic carbon flux at 200 m in Franklin Bay reached 4 g C m^{-2} y^{-1} (Forest et al. 2008) and would account for 18 % of annual primary production. Considering the high stratification in the Amundsen Gulf, the flux measured in Franklin Bay further confirms that the annual primary production of 21 g C m^{-2} y^{-1} in the Amundsen Gulf is underestimated.

In the Amundsen Gulf, phytoplankton production seems mostly constrain by the winter nutrient inventory available when sea ice retreats, as over the Mackenzie shelf slope (Lavoie et al. 2008). Winter nutrients inventories have never been reported before for the Amundsen Gulf, therefore we cannot state if the low annual phytoplankton production is a general characteristic of the Cape Bathurst polynya. Over the Mackenzie shelf, enhanced phytoplankton production was associated to the river plume expansion and shelf-break upwelling, which promoted potential carbon export to depth. In a context of climatic change, with shorter sea ice covered season, winds could promote winter nutrients inventories build-up and increase shelf-break upwelling frequency, both favouring high phytoplankton production and potential export. However, the impact of reduced sea ice cover in the Beaufort Sea remains a matter of discussion.

CHAPITRE III

SPATIO-TEMPORAL DISTRIBUTION OF PICO- AND NANOPHYTOPLANKTON IN

THE SOUTHEASTERN BEAUFORT SEA

RESUME

La structure de taille du phytoplancton <20 µm a été étudiée dans le sud-est de la mer de Beaufort en automne 2003, ainsi qu'au printemps et en été 2004, par cytométrie en flux. Le picophytoplancton (<3 µm) dominait le phytoplancton <20 µm en abondance pendant toutes les saisons. Dans le golfe d'Amundsen, le picophytoplancton répondait plus rapidement au retrait printanier des glaces que le nanophytoplancton (>3 µm). De plus, les conditions de retrait des glaces (i.e. la vitesse) modelaient la structure de taille du phytoplancton <20 µm. En outre, en été, la circulation et la fonte de glace mobile favorisaient la croissance du pico- et du nanophytoplancton de 3-10 µm. En automne, la diminution de la disponibilité en lumière était probablement responsable de la chute de l'abondance du phytoplancton <20 µm. Cependant, le pico- et le nanophytoplancton de 3-10 µm étaient plus sensibles que le nanophytoplancton >10 µm, dont les abondances restaient constantes tout au long de l'automne. Sur le plateau continental du Mackenzie, le phytoplancton <20 µm était dominé, au large, par le picophytoplancton en été et en automne, alors que, près de la côte, le picophytoplancton était moins dominant en été qu'en automne. Le panache des eaux du fleuve Mackenzie était probablement une source de cellules de plus grande taille en été (nanophytoplancton) qu'à la fin de l'automne (pico- et nanophytoplancton de 3-10 µm). En général, les cellules picophytoplanctoniques étaient fortement retenues dans les eaux de surface, et entretenaient probablement un réseau trophique microbien très actif dans la mer de Beaufort.

ABSTRACT

Small phytoplankton (<20 μm) size structure was investigated in the southeastern Beaufort Sea in fall 2003 and during spring and summer 2004, using flow cytometry. Picophytoplankton (<3 μm) dominated <20 μm phytoplankton abundances over all the seasons. In the Amundsen Gulf, picophytoplankton responded faster to sea ice retreat than nanophytoplankton cells (>3 μm). Moreover, sea ice retreat conditions (i.e. speed) modelled the <20 μm phytoplankton size structure. In addition, mobile sea ice motion and melt during summer favoured pico- and small nanophytoplankton (3-10 μm) growth. In fall, decreasing light availability likely drove <20 μm phytoplankton abundance drop, however pico- and small nanophytoplankton (3-10 μm) were more sensitive than large nanophytoplankton (>10 μm), which maintained steady abundances throughout fall. Over the Mackenzie shelf, <20 μm phytoplankton was dominated by picophytoplankton offshore in summer and fall, whereas close to the shore, picophytoplankton was less dominant in summer than in fall. The plume of the Mackenzie River waters was likely a source of larger cells in summer (nanophytoplankton) than in late fall (pico- and small nanophytoplankton). Overall, there was a very high retention of picophytoplankton cells in the surface waters, probably sustaining the efficient microbial food web of the southeastern Beaufort Sea.

INTRODUCTION

The Arctic Ocean is more sensitive to ongoing warming trend than temperate latitude regions (ACIA 2005, IPCC 2007). Field and satellite observations indicate that the Arctic Ocean is warming faster than other oceans (Rigor et al. 2000, Comiso 2003). Furthermore, from 1978-2003 the arctic sea-ice minimum extent (i.e. summer) decreased by 7.4 % (Johanessen et al. 2004). Since 2002, the Arctic Ocean has experienced minimal sea-ice extent records with a new maximum in summer open water in September 2007 (Comiso et al. 2008), suggesting that sea ice shrinking is accelerating. In addition, numerical simulations predict that the Arctic Ocean could be free of ice in summer by the end of the 21st century (Serreze et al. 2007) or even by 2040 (Holland et al. 2006). The Arctic Ocean is also characterised by its large river inflow (Macdonald et al. 2004a), which would probably rise through the predicted intensification of the hydrological cycle under global warming trend (Peterson et al. 2002). Therefore, the arctic marginal seas would be particularly sensitive to climatic change impacts (ACIA 2005). Climatic change will likely affect arctic marine ecosystems, but the impact on food webs structure and carbon cycling remains uncertain (Walsh et al. 2004, Wassmann 2004, Hare et al. 2007). Prediction of climate-related changes, as well as model validation, requires the understanding of current functioning of arctic ecosystems. However, gaps still need to be filled in some biologically active regions and seasons in the Arctic Ocean (Carmack & Wassmann 2006).

Arctic pelagic ecosystems are characterized by large seasonal variations in solar radiation and sea ice cover (Sakshaug & Slagstad 1991). Phytoplankton productive season

is usually short, between spring sea ice melt and fall freeze-up, with high phytoplankton production and standing stocks restricted to even shorter periods of the ice-free season (Sakshaug 2004). Phytoplankton cell size is a critical factor in the fate of carbon through the food web, with large phytoplankton cells favoring carbon export and transfer to higher trophic levels (Chisholm 1992). The Arctic Ocean has traditionally been thought to be dominated by microphytoplankton (>20 μm) (von Quillfeldt 1997). However, recent studies focused on smaller phytoplankton forms (Wassmann et al. 2006) and showed active microbial food webs involving <3 μm phytoplankton (Lovejoy et al. 2002, Sherr et al. 2003, Lovejoy et al. 2007) and noteworthy carbon fixation by <5 μm phytoplankton (Gosselin et al. 1997, Lee & Whitledge 2005). Only a couple of studies focused on the size structure of small phytoplankton (Mostajir et al. 2001, Not et al. 2005, Schloss et al. 2008, Tremblay 2008), though microphytoplankton cells are often constrained to bloom periods, while smaller cells (i.e. nano- and picophytoplankton) often dominate outside these periods (Not et al. 2005).

The Beaufort Sea is an area of particular interest since it comprises the Mackenzie continental shelf and the Cape Bathurst polynya. Polynyas are considered as highly productive areas (Stirling 1997, Klein et al. 2002, Tremblay & Smith 2007), and represent preferential regions to study climatic change impacts owing to their reduced sea ice cover (Tremblay et al. 2006). Interior continental shelves, such as the Mackenzie shelf, are strongly influenced by river discharge (Carmack & Wassmann 2006), and the Beaufort Sea receives the 4th highest annual freshwater discharge in the Arctic from the Mackenzie River (Rachold et al. 2004). The Beaufort Sea exhibits a wide range of physical forcing, which

might strongly influence the size structure of <20 μm phytoplankton assemblages. Therefore, in the framework of the Canadian Arctic Shelf Exchange Study (CASES), the spatial and temporal variations in <20 μm phytoplankton, i.e. pico- and nanophytoplankton, was investigated in the southeastern Beaufort Sea in fall 2003 and in spring-summer 2004. This study focuses on the description of the <20 μm phytoplankton size structure and its seasonal and spatial variations in relation to physical forcing, and the importance of pico- and nanophytoplankton in the pelagic ecosystem of the Beaufort Sea.

MATERIALS AND METHODS

Study area

The shallow Mackenzie shelf is bounded by the Amundsen Gulf to the east, and the Canada Basin to the north (Fig. 1). The surface circulation in the Mackenzie shelf and its surrounding regions is mainly driven by wind forcing, the Mackenzie River discharge, and thermohaline convection (Carmack & Chapman 2003). The Mackenzie River strongly influences the Mackenzie shelf and its maximum discharge usually occurs at the end of June (Rachold et al. 2004). Over the sampling area, the water column is typically formed by the Polar Mixed Layer (0-50 m), overlying the Cold Halocline Layer (50-200 m) from Pacific origin, and the Atlantic Layer (>200 m) (Carmack et al. 1989, MacLaughlin et al. 1996). Beyond the shelf-break, the surface circulation is dominated by the south branch of the anticyclonic Beaufort gyre that drives the mobile permanent pack ice and the surface waters westward (Carmack & Macdonald 2002), below 50-85 m, the eastward Beaufort counter-current carries waters of Pacific origin along the slope (Pickart 2004).

The Cape Bathurst polynya is a large recurrent polynya generally located at the entrance of the Amundsen Gulf (Barber & Hanesiak 2004). Sea ice dynamics in this region exhibit a high interannual variability, and in spring, sea ice retreat can occur from April to late June (Arrigo & van Dijken 2004).
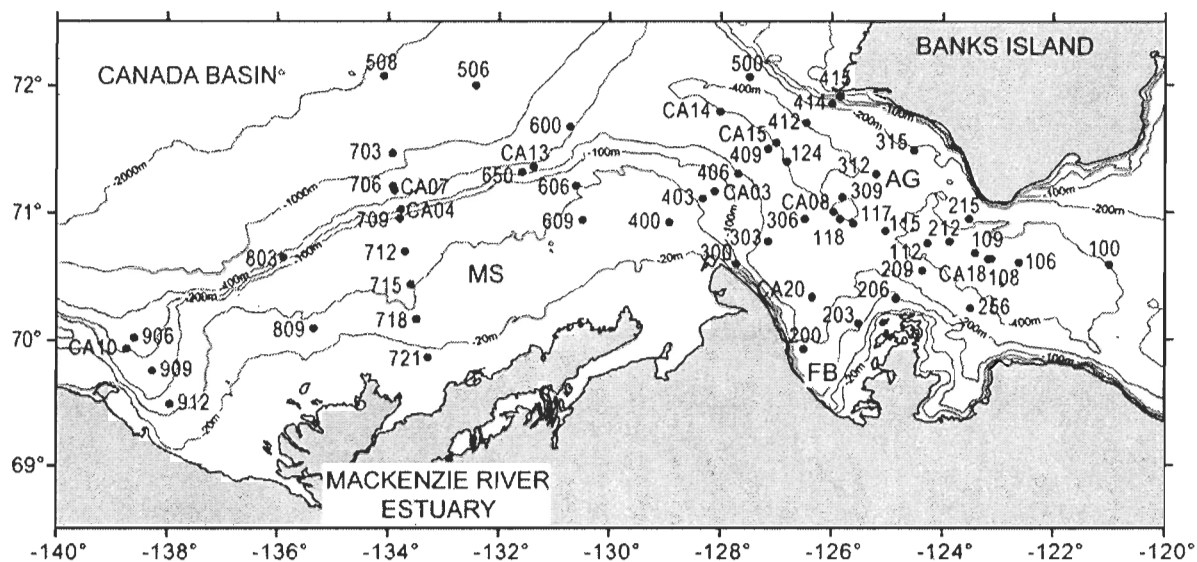
Figure 1: Location of stations sampled in the southeastern Beaufort Sea (AG: Amundsen Gulf; FB: Franklin Bay; MS: Mackenzie Shelf).

Sampling

In the framework of the Canadian Arctic Shelf Exchange Study (CASES), sampling took place in the southeastern Beaufort Sea (69-72°N, 120-140°W) during early (30 September – 13 October) and late fall 2003 (16 October - 14 November), and spring (4 – 21 June) and summer 2004 (26 June - 10 August) on board the CCGS *Amundsen* (Fig. 1 and Table 1). Water samples were collected with a rosette sampler SBE-carousel (Seabird) fitted with twenty-four 12 1 Niskin bottles (Ocean Test Equipment Inc.), a SBE-9plus CTD and a Seapoint chlorophyll fluorometer. Water samples were taken at 6 to 10 depths in the upper 100 meters (fixed depth: surface and ca. 5, 10, 15, 25, 50, 75 and 100 m; and fluorescence peaks). Samples for phytoplankton were pre-filtered onto a 333 μm mesh in order to remove large zooplankton.

Table 1: Location and periods of sampling in the southeastern Beaufort Sea.

Year	Season	Region	Sampling dates
2003	Early fall	Mackenzie shelf	30 September – 6 October
		Amundsen Gulf	9 – 13 October
2003	Late fall	Mackenzie shelf	19 – 22 October
		Amundsen Gulf	26 October – 19 November
2004	Spring	Amundsen Gulf and eastern Mackenzie shelf	4 – 21 June
2004	Summer	Mackenzie shelf	26 June – 27 July
		Amundsen Gulf	16 July – 10 August

Daily SMMR-SSM/I sea ice concentrations were calculated from daily ice concentration data provided by the National Snow and Ice Data Center (Cavalieri et al. 1996, updated 2006) for each 25×25-km pixel containing sampling stations from September 2003 to August 2004.

Downwelling PAR (Photosynthetically Active Radiation, 400–700 nm) irradiance was acquired using a GUV-510 surface radiometer (Biospherical Instruments). Underwater downwelling PAR profiles were collected at some stations during spring and summer 2004 using a PUV-500 radiometer (Biospherical Instruments) around noon. Irradiance profiles were recorded from the surface down to 60-75 m (or to the bottom at shallow stations). Underwater irradiance measurements were corrected for dark current measured in the field

using light-tight neoprene caps. The depth of the euphotic zone (1 % isolume) was further estimated by linear regression of the natural logarithm of underwater downwelling irradiance versus depth.

The depth of the Surface Mixed Layer (SML) was calculated according to Thomson and Fine (2003). The 31.6 isohaline defines the bottom of the Polar Mixed Layer (PML), and the 32.4 isohaline is characteristic of waters of Pacific origin (Carmack et al. 1989).

Samples for inorganic nutrient measurements were taken at the same depth than phytoplankton samples. Inorganic nutrient concentrations (nitrate + nitrite, phosphate and silicic acid) were measured on board using standard colorimetric methods (Grasshoff 1999) as described in Simpson et al. (2008).

Region definition

Stations were separated according to their locations relative to 128.35°W, which barely corresponds to the tip of the Cape Bathurst. Stations west of 128.35°W on the Mackenzie shelf and slope (depth < 400 m) were considered as Mackenzie shelf stations, and stations east of 128.35°W were considered to be in the Amundsen Gulf region. However, in early fall station CA13 was excluded from the shelf region owing to its closeness to the pack ice and the coastal station 415 was not considered in the Amundsen Gulf region.

Chlorophyll *a* determination

For the determination of phytoplankton chlorophyll *a* (chl *a*) concentration, water sub-samples of 0.5 to 1 l were filtered onto glass fibre filters (poresize 0.7 μm, Whatman GF/F) (total biomass) and 20 μm filters (Nitex) (>20 μm biomass). Chl *a* concentrations were determined with a 10-AU Turner Designs fluorometer following 24 hr extraction in 90 % acetone at 5°C in the dark without grinding (Parsons et al. 1984). Concentrations of chl *a* were corrected for phaeopigments by acidification of the extract (Knap et al. 1996). Chl *a* concentrations <20 μm was obtained by subtraction. All values were integrated over 50 m. The depth of 50 m was chosen for integration of chl *a* concentration values in order to include the euphotic zone, the PML and the deepest chl *a* peak for most of the stations.

Flow cytometry

Samples were preserved in 1 % paraformaldehyde final concentration (Marie et al. 2005) and frozen at 80°C for later counts of phytoplankton cells (<20μm) using a Epics Altra flow cytometer (Beckman-Coulter) equipped with a 488 nm laser (15 mW output). Prior to analysis, samples were pre-filtered on 40 μm mesh size. The flow rate was set on 100 μl min^{-1} and the acquisition time ranged from 5 to 20 min. The analyzed sample volume was determined from the change in mass corrected for a dead volume of 50 μl. One μm microspheres (0.96 μm Fluoresbrite YG, Polysciences) were added to each sample as an internal standard. Forward light scatter (FSC), side light scatter (SSC), orange fluorescence from phycoerythrin (575 ± 20 nm) and red fluorescence from chloprophyll (675 ± 10 nm) were measured. The orange fluorescence allows the discrimination of

phycoerythrin-containing cyanobacteria. Pico- and nanophytoplankton were discriminated based on FSC calibration with polystyrene microspheres of known size (3 μm Fluoresbrite YG, Polysciences, and Flow cytometry size calibration kit, Invitrogen). In this study, picophytoplankton corresponds to the <3 μm cells, small nanophytoplankton to 3-10 μm cells and large nanophytoplankton to >10 μm cells. All abundances were averaged over 50 m.

Statistical analyses

In order to investigate differences in pico- and nanophytoplankton abundances between the different regions and water masses, the non-parametric pair comparison Mann-Whitney U test was applied, as the data did not meet normal distribution and homoscedasticity (Zar 1999). The distribution of biological (<20 μm, <3 μm, 3-10 μm and >10 μm abundances) and physical (depth, salinity, temperature, nutrients and underwater PAR) variables was not normal and data could not be transformed so as to reach a normal distribution. Moreover depth, salinity, temperature and underwater PAR irradiance were all correlated (Spearman rank correlations, $p < 0.05$); therefore no statistical analysis could be performed to analyse the relationships between biological and physical variables. All statistical tests were carried out with the Statistica 7.0 program (StatSoft).

RESULTS

Physico-chemical conditions

In spring 2004, sea ice retreat occurred around the 16th May in the middle of the Amundsen Gulf and the eastern part of the Mackenzie shelf, whereas it started one week later in the southern part of the Amundsen Gulf about the 22nd May. All stations were sampled in open water (i.e. ice concentration < 50 %), however the delay between sea ice retreat and sampling was different. This delay was about 15 days for the group of stations south of the Amundsen Gulf (206, 256 and 108), while it ranged from 25 to 35 days for the other stations. Most of the sampling area was completely free of ice during summer 2004, however sea ice was observed at some stations in the Amundsen Gulf (315, 415, 412, 109, 215 and 109, concentration < 30 %). There, presence of sea ice was usually associated with low surface temperature. Sea ice (concentration < 50 %) was also present over the Mackenzie shelf slope and northward. In early fall 2003, stations were still in open water at sampling time. In late fall 2003, new sea ice formed over the entire sampling area and started to consolidate in November.

The daylength lasted 24 hours from June to August 2004, whereas it decreased from 13 hours on 30 September to 3 hours on 19 November 2003. Daily solar incoming PAR irradiance decreased from spring to summer 2004 (14.7 to 63.3 mol photon $m^{-2} d^{-1}$) and in fall 2003 (0.3 to 7.4 mol photon $m^{-2} d^{-1}$).

In spring 2004, low surface temperature (ca -1.2°C) characterised the group of stations south of the Amundsen Gulf, which was associated with thin SML (6 to 15 m) and

PML (< 26 m). Surface temperature were slightly higher in the middle of the Amundsen Gulf (-0.7 to -0.2°C), with thicker SML and PML (11 to 55m and > 36m, respectively). Over the eastern part of the Mackenzie shelf and slope, salinity data highlighted shelf-break upwelling. In this area, surface temperature was high (> 0°C) and the SML thickness ranged from 7 to 30 m and that of the PML from 0 to 55 m. In the Amundsen Gulf, surface temperature was generally higher in summer (ca 3.3°C). Low surface temperature and salinities were associated to recent sea ice melt (stations 109, 215, 212 and 106). The PML thickness ranged from 30 to 60 m, whereas the SML remained thin (4 to 11 m). In summer 2004, surface salinity and surface temperature followed an inverse trend over the Mackenzie shelf and slope, with high salinity and low temperature offshore, and low salinity and warm temperature inshore, associated to the Mackenzie River plume. River plume waters were found at stations 912, 909, 906, 809, 803, 718, 715 and 712. The SML and PML became thicker offshore (from 10 to 23 m and 15 to 60 m, respectively), inshore the SML corresponded to the river plume (ca. 5 m). Shelf-break upwelling was also evidenced by the high salinity at shallow depths over the shelf. In early fall 2003, surface temperature had decreased and was usually < 0.5°C, except at station 718 under the river plume influence. Later in fall, surface temperature declined under -1°C, even at station under the river plume influence (718, 715 and 712). During fall, the SML became thicker offshore over the Mackenzie shelf and slope (5 to 15 m), while its thickness ranged from 10 to 20 m in the Amundsen Gulf. The bottom of the PML usually laid between 30 and 50 m.

In spring and summer 2004, the depth of the euphotic zone (1 % isolume) generally matched the bottom of the PML about 40 to 60 m in the Amundsen Gulf. Over the

Mackenzie shelf, it followed and inshore-offshore gradient, with a deeper euphotic zone offshore (40 to 55 m) and a shallow euphotic zone close to the shore (3 to 20 m) associated with the Mackenzie River plume.

During all the sampling periods, nitrate was more likely the limiting nutrient in the upper 50 m (N/P < 6) (Simpson et al. 2008). Nitrate concentrations were generally low in the upper 50 m, though nitrate concentrations were still moderate at the bottom of the PML (> 1 µM). Nitrate inventories were low at most of the stations (ca. 100 mmol m^{-2} in the upper 50 m), however they were moderate to high (> 200 mmol m^{-2} in the upper 50 m) at stations south of the Amundsen Gulf in spring 2004 and at stations under shelf-break upwelling influence in spring and summer 2004.

Chl a biomass

Phytoplankton biomass exhibited high seasonal and spatial variations. In spring 2004, the biomass was low at stations south of the Amundsen Gulf (7 mg chl a m^{-2}) and increased in the middle of the gulf (16 mg chl a m^{-2}), however the contribution of phytoplankton <20 µm cells was roughly the same around 92 %. At stations close and over the eastern part of the Mackenzie shelf, the biomass reached 204 mg chl a m^{-2}, of which only 36 % were due to <20 µm cells. In summer, the biomass averaged 19 mg chl a m^{-2} in the Amundsen Gulf and was mostly due to <20 µm cells (94 %). Over the Mackenzie shelf and slope, the biomass decreased offshore, whereas the contribution of <20 µm cells increased. The average biomass was high (89 mg chl a m^{-2}) and the contribution of <20 µm cells low around 26 %. In early fall 2003, the biomass was lower over the Mackenzie shelf

(14 mg chl a m^{-2}), while the contribution of <20 μm cells increased to 96 %. Later in fall, the biomass remained roughly constant (at 14 mg chl a m^{-2}) and <20 μm cells contributed to 79 %. In the Amundsen Gulf, <20 μm cells represented about 63 % of the biomass (26 mg chl a m^{-2}) in early fall, but it was only estimated at 2 stations. The biomass further decreased to 10 mg chl a m^{-2} with 90 % due to <20 μm cells.

Pico- and nanophytoplankton

Pico- and nanophytoplankton populations

Over all the season sampled, several populations composed nanophytoplankton (3-10 μm and >10 μm), whereas the picophytoplankton (<3 μm) fraction was due to one single population. In spring and summer, the picophytoplankton population had a size mainly comprised between roughly 1 and 2.5 μm, while in fall the size of this population seemed smaller, with maximal size only slightly larger than 2 μm. Some phycoeryhtrin-containing cells with a small size were detected, however no distinct population was observed. Therefore, the question of the presence or absence of cyanobacteria could not be addressed, and picophytoplankton hereafter will only represent picoeukaryotes.

Pico- and nanophytoplankton distribution in the upper 50 meters

In spring 2004, picophytoplankton dominated the <20 μm phytoplankton abundance in the upper 50 meters over the entire sampled region (Table 2). Picophytoplankton abundances were an order of magnitude higher than that of 3-10 μm nanophytoplankton, which were in turn an order of magnitude higher than >10 μm nanophytoplankton

abundances (Table 2). Three groups of stations could be separated by the <20 μm phytoplankton size structure. Stations south of the Amundsen Gulf (group 1) were characterised by low concentrations of pico- and nanophytoplankton and a lower contribution of picophytoplankton to <20 μm phytoplankton abundance (Fig. 2 and Table 3). Stations in the middle of the Amundsen Gulf (group 2) showed the highest picophytoplankton abundances in spring and contributed to 97 % of <20 μm phytoplankton (Fig. 2 and Table 3). The last group consisted in stations close or over the eastern part of the Mackenzie shelf and slope (group 3). There higher abundances of nanophytoplankton coincided with higher <20 μm phytoplankton biomass (Fig. 2 and Table 3). In group 1 stations, pico- and nanophytoplankton were homogeneously distributed over the upper 15 m of the SML, with picophytoplankton abundances ranging from 600 to 3800 cells ml^{-1}. In the middle of the gulf, pico- and nanophytoplankton were evenly distributed over the entire PML. There picophytoplankton reached maximal abundance of 23900 cells ml^{-1}. At group 3 stations, the vertical distribution of pico- and nanophytoplankton was markedly different. At stations over or close to the shelf slope, pico- and nanophytoplankton formed a deep maximum of abundance at the bottom of the PML matching the chlorophyll maximum, whereas at shallow stations over the shelf two maxima of pico- and nanophytoplankton abundance were observed at the surface and at depth. In group 3 stations, maximal picophytoplankton abundance reached only 15300 cells ml^{-1}.

Table 2: Pico- (<3 μm), small nano- (3-10 μm) and large nanophytoplankton (>10 μm) abundances (averaged over the upper 50 m) and their relative contribution to <20 μm phytoplankton cell abundance for the different seasons, in the Amundsen Gulf and on the Mackenzie shelf, mean ± SD, the number of stations is in brackets.

Season	Region	Cell abundance (cells ml^{-1})			Contribution (%)		
		<3 μm	3-10 μm	>10 μm	<3 μm	3-10 μm	>10 μm
Spring	(n = 15)	7001 ± 4760	343 ± 219	103 ± 109	91	6	2
Summer	Shelf (n = 16)	1977 ± 1576	349 ± 176	130 ± 105	73	20	7
	Gulf (n = 21)	6363 ± 5207	356 ± 160	87 ± 47	92	6	2
Early fall	Shelf (n = 5)	2991 ± 878	227 ± 51	66 ± 17	91	7	2
	Gulf (n = 4)	2224 ± 402	210 ± 19	45 ± 11	90	9	2
Late fall	Shelf (n = 5)	2515 ± 422	158 ± 66	68 ± 30	89	6	2
	Gulf (n = 14)	1581 ± 523	178 ± 60	44 ± 29	87	10	3

Figure 2: Average (over 50 m) <20 μm phytoplankton and picophytoplankton (<3 μm) abundances and total (ChlT) and <20 μm (Chl<20 μm) chl *a* concentrations (integrated over 50 m) (a), average (over 50 m) small (3-10 μm) and large (>10 μm) nanophytoplankton cell abundances (b), and average contribution of pico- (<3 μm) and nanophytoplankton (3-10 μm and >10 μm) to <20 μm phytoplankton cell abundance (c) in spring 2004.

Table 3: Pico- (<3 µm), small nano- (3-10 µm) and large nanophytoplankton (>10 µm) abundances (averaged over the upper 50 m) (mean ± SD) and their relative contribution to <20 µm phytoplankton cell abundance, and sea ice conditions in spring for the different groups of stations.

	Group 1	Group 2	Group 3
Cell abundance (cells ml^{-1})			
<3 µm	958 ± 516	10382 ± 4321	6642 ± 2979
3-10 µm	117 ± 23	295 ± 78	504 ± 251
>10 µm	36 ± 5	36 ± 11	203 ± 114
Contribution to cell abundance (%)			
<3 µm	84	97	90
3-10 µm	12	3	7
>10 µm	4	0	3
Number of days from ice break-up	15 ±1	26 ± 2	32 ± 2
Number of days in open water	8 ± 3	7 ± 4	16 ± 4
Ice concentration (%)	38 ± 14	19 ± 21	14 ± 16
Number of stations	*3*	*6*	*6*

In summer 2004, the <20 µm phytoplankton of the Amundsen Gulf was also dominated by picophytoplankton which represented 92 % of <20 µm phytoplankton cells (Table 2). Pico- and nanophytoplankton formed a maximum in abundance at depth. Nanophytoplankton maximal abundances matched the chlorophyll maximum depth (i.e. the bottom of the PML and the euphotic zone), while picophytoplankton maximal abundances occurred at the chlorophyll maximum depth or slightly above. The spatial distribution of pico- and nanophytoplankton abundances was not very variable over the gulf, though extremely high picophytoplankton maximal abundances of 51000 and 63000 cells ml^{-1} were recorded at stations 212 and 109, respectively (Fig. 3). Higher chlorophyll biomass was associated to higher nanophytoplankton numbers, as in spring (Fig. 3). Maximum nanophytoplankton abundances were observed at the coastal station 415 with 5000 and 500 cells ml^{-1} of 3-10 µm and >10 µm cells respectively.
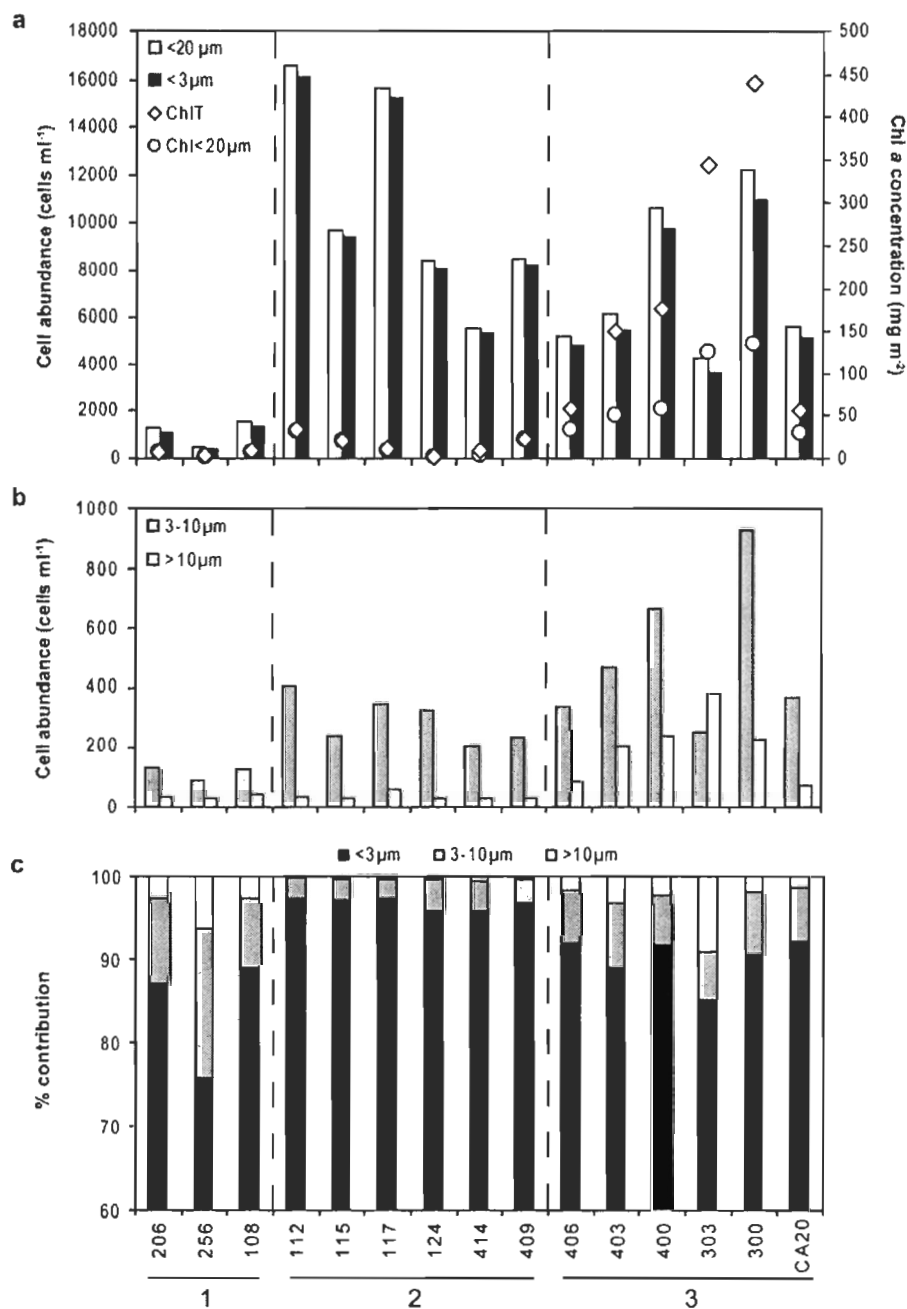
Figure 3: Average (over 50 m) <20 μm phytoplankton and picophytoplankton (<3 μm) abundances and total (ChlT) and <20 μm (Chl<20 μm) chl a concentrations (integrated over 50 m) (a), average (over 50 m) small (3-10 μm) and large (>10 μm) nanophytoplankton cell abundances (c), and average contribution of pico- (<3 μm) and nanophytoplankton (3-10 μm and >10 μm) to <20 μm phytoplankton cell abundance (c) in summer 2004 in the Amundsen Gulf region.

Contrary to the Amundsen Gulf, the spatial distribution of pico- and nanophytoplankton over the Mackenzie shelf and slope in summer 2004 was highly variable, and both picophytoplankton abundances and contribution to <20 µm phytoplankton abundance were significantly lower than in the adjacent Amundsen Gulf (Mann-Whitney U test, $p < 0.05$) (Table 2). Nanophytoplankton abundance followed an inshore-offshore gradient, as the chlorophyll biomass, with higher nanophytoplankton abundance and biomass close to the coast, while picophytoplankton showed the inverse trend with higher abundances offshore (Fig. 4). Maximum picophytoplankton numbers about 7000 cells ml^{-1} were observed at offshore stations 600 and 703, but also at station 400 with 8500 cells ml^{-1}. Nanophytoplankton (3-10 µm) exhibited the highest abundance in association to the river plume (1300 and 300 cells ml^{-1} of 3-10 µm and >10 µm cells, respectively, at station 906) or to shelf-break upwelling (2300 and 1200 cells ml^{-1} of 3-10 µm and >10 µm cells, respectively, at station 609). Offshore deep maximum of pico- and nanophytoplankton abundance corresponded to the chlorophyll maximum and the bottom of the PML. Inshore pico- and nanophytoplankton cells were generally concentrated in the surface layer, which corresponded to river plume waters. Over the Mackenzie shelf and slope, nanophytoplankton (3-10 µm and >10 µm) abundances were significantly higher in the river plume waters than in the underlying and adjacent surface waters of the PML (upper 10 m and whole PML) (Mann-Whitney U test, $p < 0.05$) (Table 4).
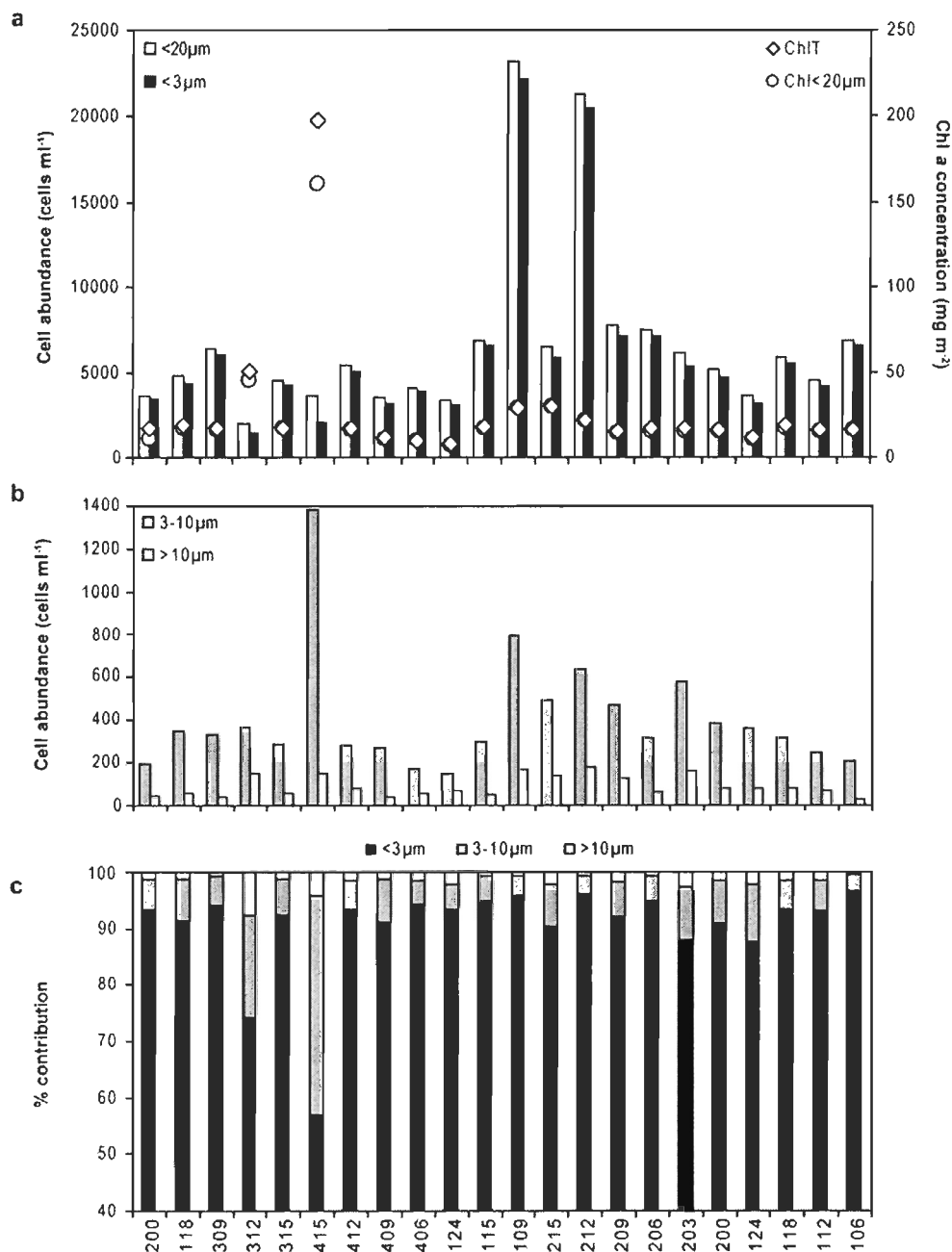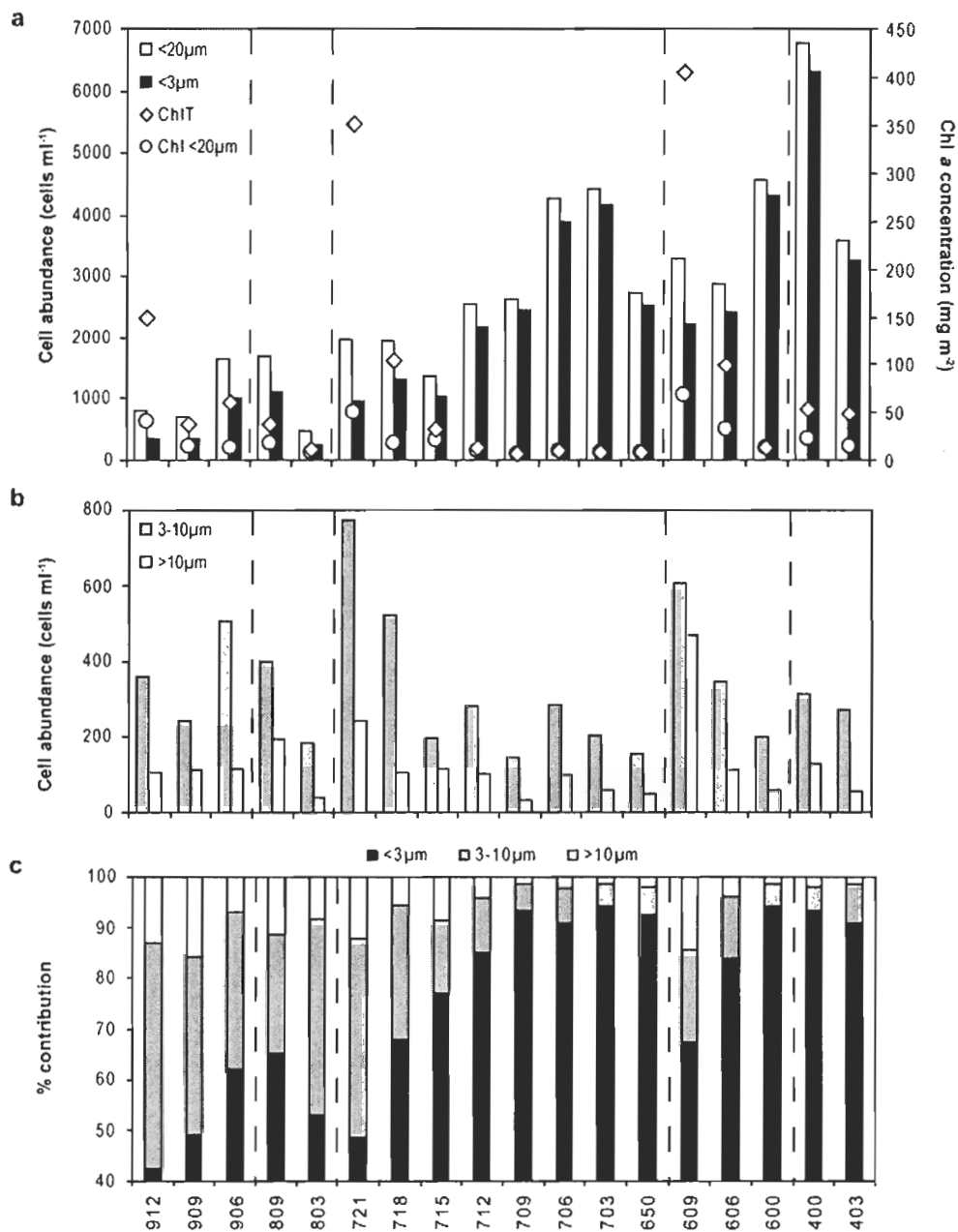
Figure 4: Average (over 50 m) <20 μm phytoplankton and picophytoplankton (<3 μm) abundances and total (ChlT) and <20 μm (Chl<20 μm) chl *a* concentrations (integrated over 50 m) (a), average (over 50 m) small (3-10 μm) and large (>10 μm) nanophytoplankton cell abundances (b), and average contribution of pico- (<3 μm) and nanophytoplankton (3-10 μm and >10 μm) to <20 μm phytoplankton cell abundance (c) in summer 2004 over the Mackenzie shelf and slope region.

Table 4: Pico- (<3 μm), small nano- (3-10 μm) and large nanophytoplankton (>10 μm) abundances (mean ± SD) and their relative contribution to <20 μm phytoplankton cell abundance over the Mackenzie shelf in the river plume and the upper 10 m and the whole Polar Mixed Layer (PML).

Season	Water layer	Cell abundance (cells ml⁻¹)			Contribution (%)		
		<3 μm	3-10 μm	>10 μm	<3 μm	3-10 μm	>10 μm
Summer	River plume (n = 16)	2172 ± 1077	907 ± 308[a, b]	182 ± 97[a, b]	64[a]	30[a]	6
	PML >10 m (n = 33)	2125 ± 1919	542 ± 338	115 ± 69	71	24	5
	PML (n = 79)	1887 ± 1828	452 ± 348	120 ± 137	64	28	8
Early fall	River plume (n = 3)	4979 ± 597[b]	392 ± 73[b]	82 ± 8	91	7	2
	PML >10 m (n = 10)	4685 ± 1319	300 ± 124	60 ± 21	93	6	1
	PML (n = 21)	3162 ± 1825	254 ± 104	67 ± 35	87	10	3
Late fall	River plume (n = 8)	7124 ± 1576[a, b]	435 ± 91[b]	67 ± 21[a, b]	93[b]	6[b]	1
	PML >10 m (n = 8)	5665 ± 811	342 ± 80	40 ± 14	94	6	0
	PML (n = 23)	3229 ± 2218	256 ± 89	47 ± 20	87	10	3

The number of samples is in brackets, a and b denote significant difference between River plume and the upper 10 m and the whole PML, respectively (Mann-Whitney U test, $p < 0.05$).

In early fall 2003, pico- and nanophytoplankton abundances and contribution to <20 µm phytoplankton abundance was similar in the Amundsen Gulf and the Mackenzie shelf regions (Fig. 5 and Table 2). Picophytoplankton contributed to 90 % of <20 µm phytoplankton abundance, as in spring and summer in the Amundsen Gulf, however pico- and nanophytoplankton numbers were lower compared to the spring and summer periods (Table 2). Picophytoplankton abundance reached a maximum of 7300 cells ml^{-1} at station CA18, and nanophytoplankton maximal abundances were attained at station CA20 (750 and 130 cells ml^{-1} of 3-10 µm and >10 µm cells, respectively). The vertical distribution of pico- and nanophytoplankton was similar in the Amundsen Gulf and over the Mackenzie shelf with cells concentrated in the upper 15 to 25 m. The Mackenzie River influence was only detected at station 718, which presented the highest nanophytoplankton abundance over the shelf (400 and 110 cells ml^{-1} of 3-10 µm and >10 µm cells, respectively). Pico- and small nanophytoplankton abundance in the river plume waters were similar to the surface 10 m of PML waters, but higher than the whole PML waters (Mann-Whitney U test, $p < 0.05$) (Table 4).
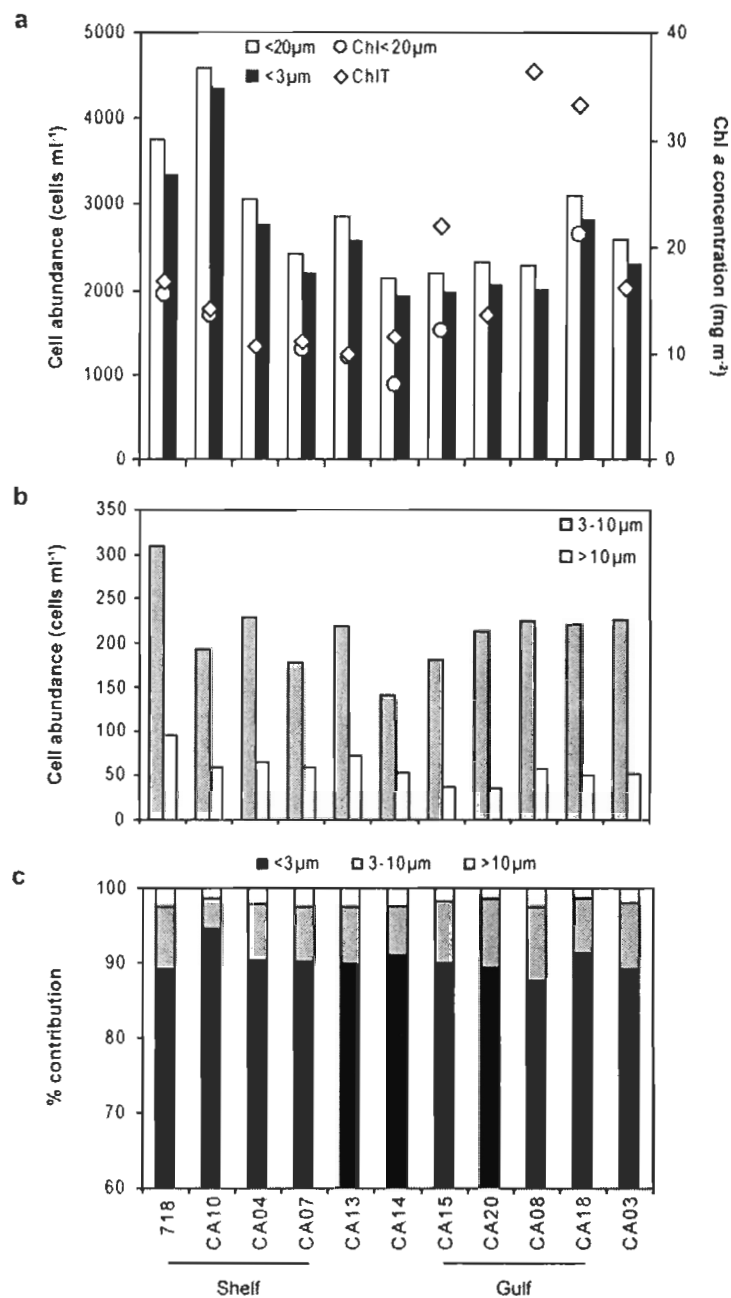
Figure 5: Average (over 50 m) <20 μm phytoplankton and picophytoplankton (<3 μm) abundances and total (ChlT) and <20 μm (Chl<20 μm) chl a concentrations (integrated over 50 m) (a), average (over 50 m) small (3-10 μm) and large (>10 μm) nanophytoplankton cell abundances (b), and average contribution of pico- (<3 μm) and nanophytoplankton (3-10 μm and >10 μm) to <20 μm phytoplankton cell abundance (c) in early fall 2003.

In late fall 2003, the Mackenzie shelf region was characterised by higher picophytoplankton abundances compared to the Amundsen Gulf (Mann-Whitney U test, $p < 0.05$) (Fig. 6 and Table 2). This difference was probably due to the Mackenzie River influence, since river plume waters had significantly higher pico- and nanophytoplankton abundances than underlying and adjacent PML waters (Mann-Whitney U test, $p < 0.05$) (Table 4). Pico- and nanophytoplankton cells were concentrated in the upper 10 m to 25 m over the Mackenzie shelf, and in the top 15 to 25 m in the Amundsen Gulf. Maximum picophytoplankton abundances were recorded at station 718 (8900 cells ml^{-1}) over the Mackenzie shelf, and at station 124 (7900 cells ml^{-1}) at the beginning of the sampling in the Amundsen Gulf. In the Amundsen Gulf, pico- and small nanophytoplankton abundance decreased over time, while large nanophytoplankton abundance remained stable (Fig. 6 and Fig. 7). The decrease was more pronounced for picophytoplankton than small nanophytoplankton, resulting in a lower contribution of picophytoplankton to <20 μm phytoplankton abundance (Fig. 6 and Table 2).
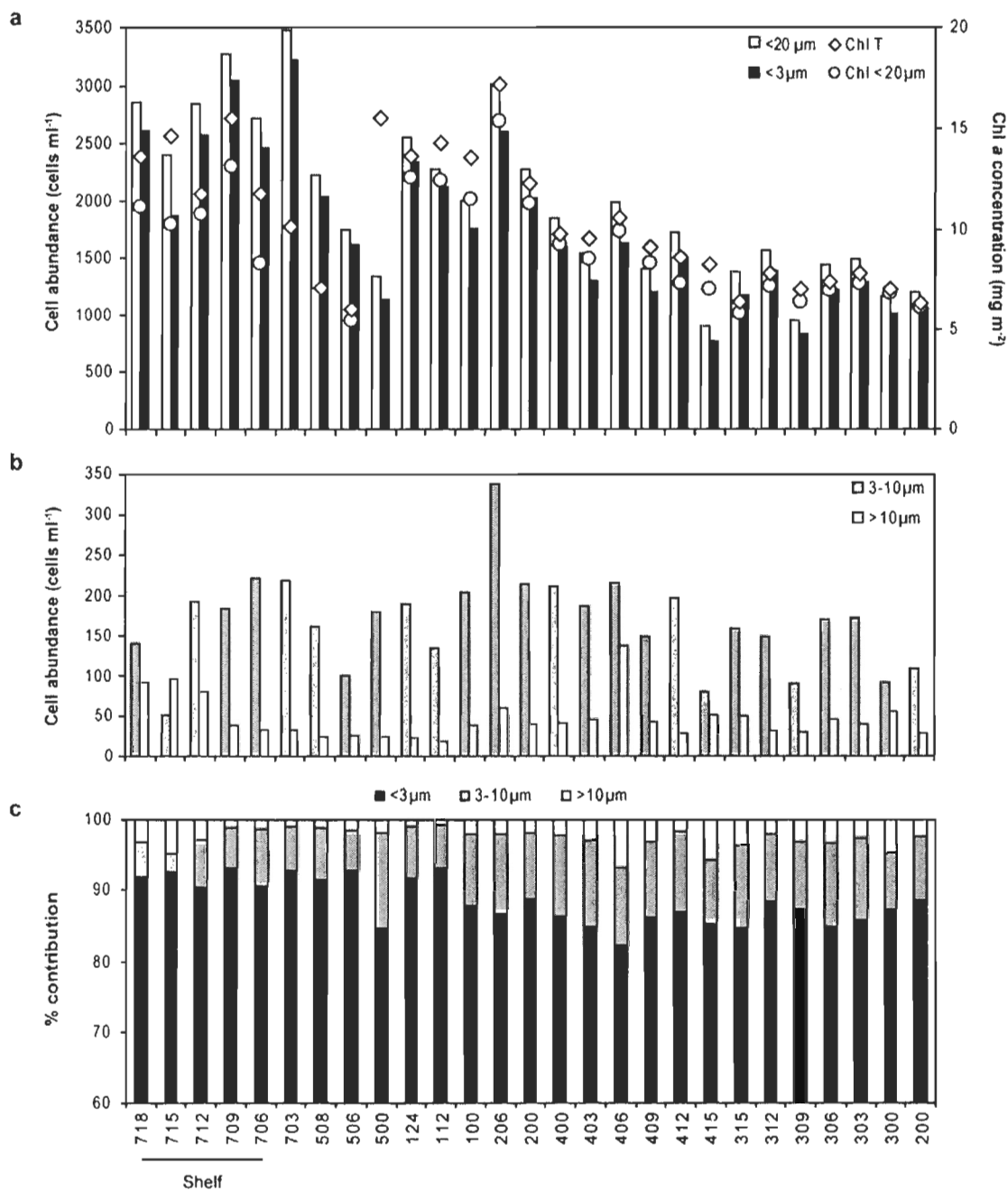
Figure 6: Average (over 50 m) <20 μm phytoplankton and picophytoplankton (<3 μm) abundances and total (ChlT) and <20 μm (Chl<20 μm) chl a concentrations (integrated over 50 m) (a), average (over 50 m) small (3-10 μm) and large (>10 μm) nanophytoplankton cell abundances (b), and average contribution of pico- (<3 μm) and nanophytoplankton (3-10 μm and >10 μm) to <20 μm phytoplankton cell abundance (c) in late fall 2003.
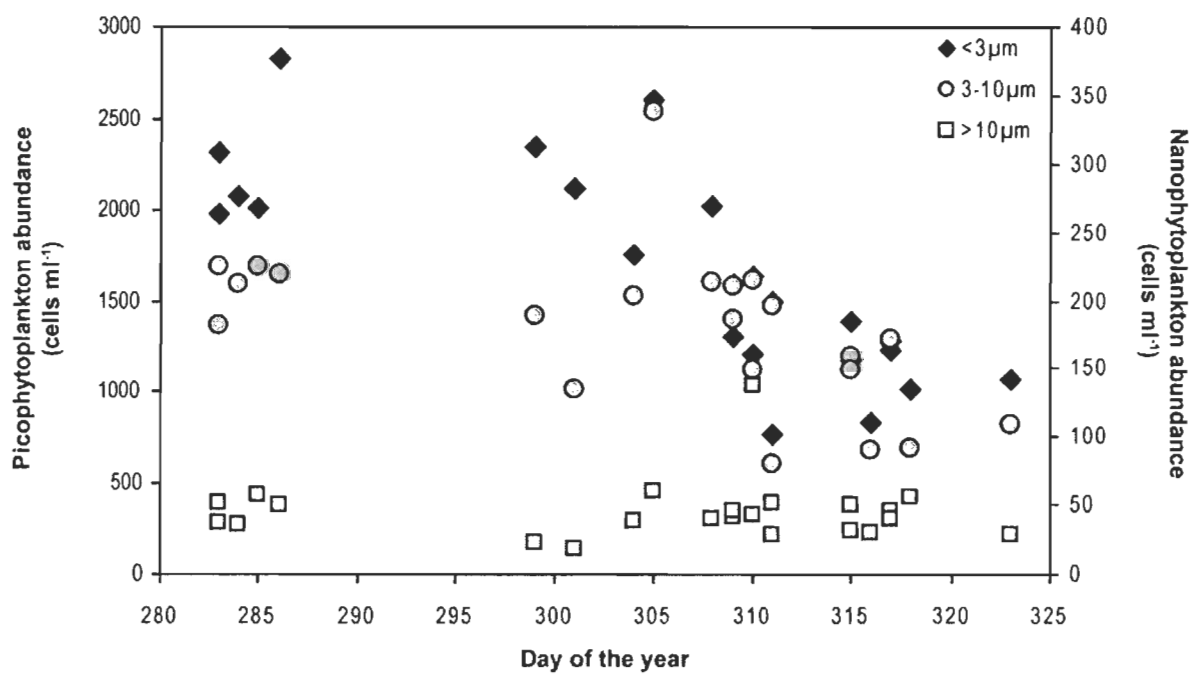
Figure 7: Average (over 50 m) picophytoplankton (<3 μm) and nanophytoplankton (3-10 μm and >10 μm) cell abundances as a function of the day of the year in fall 2003 in the Amundsen Gulf.

Pico- and nanophytoplankton in deep waters

Picophytoplankton dominated <20 μm phytoplankton abundance in the upper water column (top 50 m), with an average contribution of 81 % for all sampling periods and regions, whereas below 50 m in underlying waters of Pacific characteristics (salinity > 32.4), this contribution dropped to 45 %. The abundance of <20 μm phytoplankton cells below 50 m was compared to the <20 μm phytoplankton cells abundance of the upper 50 m. The proportion of <20 μm phytoplankton cells below the upper 50 m, i.e. out of the PML, was estimated for all size fractions (Table 5). The proportion of large nanophytoplankton cells below 50 m represented roughly half of their abundance in the upper 50 m, while 96 % of picophytoplankton cells would remained in the upper layer (Table 5). The proportion of picophytoplankton cells below 50 m was constant over the seasons, while the proportion of nanophytoplankton cells below 50 m was higher in fall.

Table 5: Proportion of pico- and nanophytoplankton cells below the upper 50 m for the different sampling seasons over the southeastern Beaufort Sea (in percentage of cell abundance of the upper 50 m).

	Proportion of cells below 50 m (%)		
	<3 μm	3-10 μm	>10 μm
Spring	2	13	21
Summer	5	22	45
Early fall	4	46	113
Late fall	8	42	113
Average	*4*	*25*	*55*

DISCUSSION

Picophytoplankton populations

Picophytoplankton showed high abundances throughout the seasons and regions in the southeastern Beaufort Sea. The predominance of picophytoplankton in cell abundance has previously been reported in other arctic regions. Regardless of the size threshold used to define picophytoplankton, our results fall in the range of picophytoplankton abundances observed in the Barents Sea (Throndsen & Kristiansen 1991, Not et al. 2005), the Baffin Bay (Mostajir et al. 2001, Tremblay 2008), the Greenland Sea (Booth & Smith 1997, Waniek et al. 2005), the central Arctic (Booth & Horner 1997, Sherr et al. 2003), the Bering Sea (Liu et al. 2002a, 2002b) and the Beaufort Sea (Różańska et al. 2007, Schloss et al. 2008, Tremblay 2008).

The presence of cyanobacteria in the Beaufort Sea has been reported by Waleron et al. (2007) using epifluorescence microscopy. The abundances of cyanobacteria reported (200 to 1400 cells ml^{-1}) would have been sufficient to be detected and form a distinct population by flow cytometry, but their estimates of picoeukaryotes abundance (<3 μm, 100 to 2400 cells ml^{-1}) was at least 2-fold lower than our picophytoplankton abundances for the same period one year later. The preservation protocol used in our study could have altered cyanobacteria fluorescence and prevented the detection of distinct populations, however our preservation protocol and the use of flow cytometry seemed to be more relevant for picoeukaryotes counting in the Beaufort Sea.

Only one population composed the picophytoplankton size fraction, its cell size seemed to vary from 1 µm to less than 3 µm for all seasons. The species *Micromonas pusilla* (Butcher) Manton and Parke has been identified as the main constituent of picophytoplankton in the Barents Sea (Throndsen & Kristiansen 1991, Not et al. 2005), but also in the Greenland Sea (Booth & Smith 1997) and the central Arctic (Sherr et al. 2003). Moreover, Terrado et al. (2008) identified *micromonas*-like cells by epifluorescence microscopy in the Beaufort Sea during winter and spring 2004, and Lovejoy et al. (2007) revealed the presence of a pan-Arctic *Micromonas* ecotype in the Beaufort Sea in 2002 and 2004. Therefore, the picophytoplankton population probably belonged to the genus *Micromonas*.

Picophytoplankton size

The upper size limit of the picophytoplankton varies according to phytoplankton studies. The historical definition of picophytoplankton set the upper limit at 2 µm (Sieburth et al. 1978), however the 3 µm one is also widely used (Li 1986, Not et al. 2005, Lovejoy et al. 2007). In a polar environment, Vanucci and Bruni (1998) addressed the question of picophytoplankton size definition using epifluorescence microscopy. They concluded that <2 µm and 2-3 µm phytoplankton size fractions had different ecological significance in the Ross Sea, and further separated these two size classes (Vanucci & Bruni 1999, Vanucci & Mangoni 1999). In our study, the use of the 2 µm threshold would have cut the picophytoplankton population, even if the part of the population >2 µm had likely the same ecological significance. Therefore, picophytoplankton relative abundance would have been

underestimated by about 15 %, increasing the relative importance of nanophytoplankton. Despite restrictions associated to FSC as an accurate size index, the flow cytometry allows choosing the threshold according to the size and red fluorescence characteristics of phytoplankton populations. As the arctic widespread *Micromonas* sp. can reach up to 2.5 μm in length (Throndsen & Kristiansen 1991), the use of 3 μm threshold and/or the counting of both <2 μm and 2-3 μm fractions would be relevant in the Arctic Ocean.

Seasonal variations

Seasonal variations will only be discussed in the Amundsen Gulf, as this region was not under the influence of the Mackenzie River and was the most extensively sampled region.

In spring, the phytoplankton size structure seemed to be related to sea ice dynamics (Table 3). South of the Amundsen Gulf (group 1), sea ice retreat occurred later compared to the northern areas, and was fast (one week). There, the biomass was due to <20 μm cells, of which picophytoplankton was dominant but in low numbers. Small nanophytoplankton abundance was similar to that reported under the ice in spring in the adjacent Franklin Bay, whereas picophytoplankton concentrations were almost 4 to 5-fold higher (Terrado et al. 2008). Moreover, nitrate inventories south of the Amundsen Gulf were close to the winter nitrate level in Franklin Bay (Tremblay et al. 2008). This suggests that the phytoplankton assemblage was still adapting to the environmental conditions related to ice retreat (e.g. increased light intensities), and that picophytoplankton would be faster adapted to these conditions than nanophytoplankton. In the middle of the Amundsen Gulf (group 2), <20 μm

cells dominated the biomass, with very high picophytoplankton abundances and moderate to low abundances of nanophytoplankton. Sea-ice retreat lasted 2.5 weeks and this area was in open water conditions only since one week prior sampling. At stations close the eastern part of the Mackenzie shelf and slope (group 3), sea-ice retreat was only slightly faster (two weeks), but the phytoplankton size structure was very different from the middle of the Amundsen Gulf and formed a deep maximum of biomass and <20 μm cells abundance. At least 40 % of the biomass was due to >20 μm cells, however <20 μm cells were abundant, and particularly nanophytoplankton. Stations close the eastern part of the Mackenzie shelf and slope were experiencing phytoplankton bloom situations, while at stations in the middle of the Amundsen Gulf nitrates were already depleted and no deep maximum formed. Whether a phytoplankton bloom happened in the middle of the Amundsen Gulf is not clear, even if research on arctic pelagic ecosystems proposed that surface nitrate depletion after sea ice break-up would be due to large blooming phytoplankton cells (large nano- and microphytoplankton, Smith & Sakshaug 1990, Wassmann et al. 2006). However if we assume that winter nitrate inventories were similar to the low inventories measured in the Franklin Bay (110 mmol m^{-2}, Simpson et al. 2008), a short bloom of large phytoplankton might have developed. Moreover, as nitrate reduction can be used to dissipate light energy when shade-adapted phytoplankton is transiently exposed to high light intensities (Lomas & Glibert 1999), which probably happened during sea ice retreat, nitrate consumption might have been even faster. Then, the slow sea ice retreat and/or the deep mixing would have prevented the accumulation of biomass at the bottom of the PML and favoured fast picophytoplankton growth over the whole PML. On the other hand, the

large nanophytoplankton abundance in the middle of the Amundsen Gulf was still similar to that at southern stations, therefore it can be hypothesized that the phytoplankton bloom was mainly due to pico- and small nanophytoplankton (i.e. cells <10 μm).

Overall, phytoplankton growth in spring in the Amundsen Gulf seemed closely linked to sea ice dynamics. The processes directly influencing phytoplankton growth (e.g. light availability, stratification/mixing, warming temperature) cannot be identified, though slow ice retreat seemed to favour high picophytoplankton growth, while fast sea ice retreat favoured the growth of pico- and nanophytoplankton and their accumulation at depth. Furthermore, picophytoplankton (presumably *Micromonas* sp.) responded faster to open water conditions than nanophytoplankton.

The spatial variability in <20 μm cells was very small over the Amundsen Gulf in summer. The <20 μm phytoplankton was dominated by picophytoplankton, present in abundances similar to those measured in late summer 2005 in the same region (Tremblay 2008). In the gulf, the main source of variability was attributed to sea ice motion and melt. Indeed, lower surface temperature and salinity were associated to the higher pico- and small nanophytoplankton abundances despite low nitrate concentrations (<1 μM). Hence, episodic sea ice motion and melt could favour pico- and small nanophytoplankton growth. On the other hand, temperature has been shown to be a major factor of picophytoplankton distribution in the north Atlantic (Li & Harrison 2001), but also in the Arctic (Mostajir et al. 2001, Tremblay 2008). In addition, Lovejoy et al. (2007) showed that an arctic strain of *Micromonas* sp. performed optimal growth at 6-8°C under moderate irradiances (50 and 100 μmol photon m^{-2} s^{-1}), while growth was minor and similar over 0 to 12°C at lower

irradiances (10 µmol photon $m^{-2}s^{-1}$). However, maximum picophytoplankton abundances corresponded to low temperature (< 0°C) and low to high irradiances (10 to 700 µmol photon $m^{-2}s^{-1}$) in spring, and to low temperature (-1 to 2°C) and low to moderate irradiances (10 to 100 µmol photon $m^{-2}s^{-1}$) in summer. Thus, in the Amundsen Gulf, even though the question of top-down control remains open, picophytoplankton growth did not seemed to be mainly driven by temperature but rather by a combination of physico-chemical and light conditions.

In early fall, pico- and nanophytoplankton abundances had decreased. Moreover, <20 µm phytoplankton was concentrated in the upper 15-25 meters. In spring maximum pico- and nanophytoplankton abundances coincided with temperatures < -0.5°C, and in fall maximum abundances were observed for similar temperatures (from -1.4 to 0.7°C). Hence, the vertical distribution of pico- and nanophytoplankton at surface in fall was probably more linked to light availability than water temperature. Later in fall, pico- and small nanophytoplankton abundance markedly decreased to 11th November two weeks prior continuous darkness of the polar night, however at that time, their abundances were still respectively 10 and 3-fold higher than winter abundances (Terrado et al. 2008). Both pico- and small nanophytoplankton abundances decreased through the end of the year (Fig. 7). In fall, decreasing solar incoming irradiance, daylength, light availability in the water column (due to sea ice) and temperature are linked to the day of the year; the effect of each parameter can therefore not be departed from the others. Since picophytoplankton and nanophytoplankton seemed to be able to growth fast at temperature < -1.1°C in spring when

light availability increases, light availability would be the major factor responsible for the decline of <20 μm phytoplankton abundance during fall.

In the Amundsen Gulf, sea ice dynamics was of major importance in driving seasonal variations in <20 μm phytoplankton growth mostly in spring and fall, even though direct effect of sea ice dynamics in fall could not be assessed owing to declining solar irradiance. Furthermore, in summer under low ambient nitrate concentrations, sea ice was a major factor driving spatial variability of <20 μm phytoplankton growth.

Spatial variability over the Mackenzie shelf

The spreading of Mackenzie River waters over the shelf is highly variable and mainly driven by wind speed and direction (Macdonald & Yu 2006), nevertheless the general inshore-offshore gradient was observed over most of the shelf in summer. Nanophytoplankton accumulation was favoured inshore, while picophytoplankton abundances were higher offshore resulting in a <20 μm phytoplankton size structure similar to that in the Amundsen Gulf. River plume waters seemed to be a source of nanophytoplankton (Table 4). This is consistent with the summer dominance diatoms inshore observed over the Mackenzie shelf (Hsiao et al. 1977, Parsons et al. 1989), but also with the picophytoplankton distribution from the Lena River/Laptev Sea, where picophytoplankton decreased along the salinity gradient from the river to the shelf, showing lower picophytoplankton abundances over the inshore shelf (Moreira-Turcq et al. 2001). At stations over the eastern part of the Mackenzie shelf (609 and 606), high abundances of both pico- and nanophytoplankton were observed; this area was not influenced by river

waters, but rather by shelf-break upwelling. In spring, over the eastern part of the Mackenzie shelf, shelf-break upwelling supported the growth of all <20 μm size fractions. Hence, over the shelf, shelf-break upwelling drove physico-chemical conditions supporting high abundances of all <20 μm phytoplankton size fractions, while river waters spreading promoted physico-chemical conditions selecting the larger size classes (i.e. nanophytoplankton).

In early fall, in the river plume all <20 μm phytoplankton size fractions showed abundances similar to the upper 10 m of the PML, but pico- and small nanophytoplankton had slightly higher abundances than over the whole PML (Table 4). The different <20 μm phytoplankton size structures between waters from the river plume and the entire PML reflected thus the vertical distribution of phytoplankton in the water column at the end of September rather than an actual import of phytoplankton cells from the Mackenzie River. Later in October, river plume waters exhibited higher abundances of large nanophytoplankton but also of picophytoplankton. The Mackenzie River seems to be a source of phytoplankton cells to the adjacent Mackenzie shelf, as previously observed by Garneau et al. (2006), Waleron et al. (2007) and Schloss et al. (2008). However, the size of <20 μm phytoplankton imported over the shelf varied from seasons, therefore tracking river waters spreading over the shelf would require more precise criterions than the simple <20 μm phytoplankton size structure.

Importance of <20 μm phytoplankton

Picophytoplankton dominated the <20 μm phytoplankton assemblage over all the sampled seasons. Together with the persistent low nitrate concentrations in the surface layer, this confirms the major importance of the microbial loop in the Beaufort Sea (Garneau et al. 2008, Simpson et al. 2008). Despite high abundances and dominance in the upper 50 m, picophytoplankton cell numbers were only slightly higher than that of nanophytoplankton in the Cold Halocline (Table 5). Only 4 % of picophytoplankton cells were sinking out of the upper 50 m. The retention of picophytoplankton in the surface layer is consistent with an active recycling food web and their small size preventing them to settle down. The proportion of picophytoplankton sinking cells did not vary much over the seasons, while this proportion increased over the year for nanophytoplankton cells. The lower export of nanophytoplankton cells in spring and summer was probably due to active grazing by zooplankton, and mostly copepods (Forest et al. 2008, Juul-Pedersen 2007). In fall, the proportion of <20 μm phytoplankton cells exported at depth were higher than in spring and summer, coinciding with the increasing export ratios of particulate phytoplankton production estimated in fall in the Amundsen Gulf (Juul-Pedersen 2007). The higher proportion of nanophytoplankton cells sinking out of the upper 50 m could result from cell death and/or resting spore formation as conditions became unfavourable for growth over the autumnal season (e.g. decreasing light availability and temperature).

In the Beaufort Sea, picophytoplankton likely represents a good food source for microzooplankton, as do bacteria. In a system with such high recycling efficiency, micrograzers probably control picophytoplankton abundance. Therefore, high abundances

were probably only reached in scarce occasion causing a mismatch between picophytoplankton and micrograzers, such as episodic sea ice motion and melt, as heterotrophic protists are more sensitive to decreasing temperature than autotrophic ones (Rose & Caron 2007). In spite of their major role in the microbial loop, picophytoplankton would not significantly contribute to direct carbon export at depth, while nanophytoplankton likely played an important role in vertical export, and were largely composed of diatoms (Chapitre II). In the climatic change context, community composition could shift from diatoms to flagellates with rising temperature (Hare et al. 2007). On the other hand, high temperature rise would lead to sub-optimal growth of the arctic *Micromonas* ecotype (Lovejoy et al. 2007). The potential impacts of climatic change on phytoplankton communities remain unclear. Therefore, understanding the arctic ecosystems functioning requires further investigations to deduce how the ongoing climate change would affect the phytoplankton communities and their trophic pathways.

CONCLUSION GENERALE

Le programme CASES a permis l'obtention de données pour l'ensemble des saisons de la période libre de glace en mer de Beaufort, et par conséquent la caractérisation du phytoplancton en termes de biomasse, production et structure de taille des communautés.

Dans le golfe d'Amundsen, la biomasse phytoplanctonique était dominée par des cellules de petite taille (<5 μm) (70%) pour l'ensemble des périodes d'échantillonnage, excepté début octobre 2003. En été, la biomasse phytoplanctonique s'accumulait pour former un maximum profond de chlorophylle au-dessus de la nitracline, alors qu'en automne, la biomasse phytoplanctonique était concentrée en surface en raison de la faible disponibilité en lumière. La communauté phytoplanctonique du golfe d'Amundsen présentait une succession typique des régions polaires (Dale et al. 1999, Rat'kova & Wassmann 2002), avec une dominance des diatomées lors d'efflorescences suivie d'une dominance de flagellés. La communauté phytoplanctonique du golfe d'Amundsen était constituée de flagellés et de prymnesiophycées après l'efflorescence printanière, de flagellés et de diatomées en été, puis de flagellés et de prymnesiophycées en automne ou de diatomées lors de l'efflorescence automnale en 2003. En outre, les dinoflagellés sans thèque représentaient toujours une proportion significative des abondances phytoplanctoniques. De plus, les variations saisonnières observées confirment l'occurrence

de deux périodes d'efflorescence dans la polynie du Cap Bathurst : au printemps après le retrait des glaces, et en automne.

La distribution spatiale du phytoplancton sur le plateau continental du Mackenzie correspondait à un gradient côte-large en raison de l'influence des eaux du panache du Mackenzie, les communautés les plus proches de la côte étant les plus soumises aux apports d'eau douce, notamment en été. Près de la côte, la biomasse phytoplanctonique élevée était dominée par des cellules de grande taille (>20 µm en été et >5 µm en automne), alors qu'au large, les cellules de petite taille dominaient la biomasse. De l'été à l'automne, les prasinophycées et les dinoflagellés ont succédé aux diatomées près de la côte, alors qu'au large les communautés étaient principalement composées de flagellés et de dinoflagellés. Le panache du Mackenzie représentait une zone de forte production de cellules de grande taille, ayant un potentiel élevé d'exportation en profondeur. De plus, le long du talus continental, ainsi qu'au niveau des canyons Kugmallit et Mackenzie, des phénomènes d'upwelling favorisaient également la forte production de cellules de grande taille, pouvant préférentiellement être exportée en profondeur. Contrairement au golfe d'Amundsen, où l'influence des vents sur la dynamique du phytoplancton n'a pas été mise en évidence, les vents modelaient la production phytoplanctonique sur le plateau continental du Mackenzie.

En mer de Beaufort, la période de production phytoplanctonique couvre les mois de juin à octobre. Au printemps, le retrait du couvert de glace débute la période productive alors qu'à la fin octobre la disponibilité réduite en lumière limite la production

phytoplanctonique. Hors de l'influence d'événements épisodiques, tels que l'expansion du panache du Mackenzie, les phénomènes d'upwelling et les périodes d'efflorescence, le phytoplancton de la mer de Beaufort est caractérisé par une biomasse relativement faible dominée par des cellules de petite taille, ainsi que par de forts rapports production/biomasse. Ceci suggère un broutage important, empêchant l'accumulation de biomasse due aux cellules de grande taille. En outre, l'importance relative des dinoflagellés sans thèque, ainsi que les faibles concentrations en éléments nutritifs, révèlent l'importance du réseau trophique microbien.

La production primaire annuelle estimée pour le golfe d'Amundsen (21 g C m^{-2}) est faible et constitue probablement une sous-estimation. En effet, la production liée à l'efflorescence automnale n'a pu être incluse dans le calcul et la production de l'efflorescence printanière a également été extrapolée. Cependant, cette estimation est proche des valeurs de production annuelle estimées pour la région du plateau continental du Mackenzie et le talus continental à partir de données in situ (Carmack et al. 2004, Lavoie et al. 2008). Cette faible valeur de production primaire pourrait être également due au faible réapprovisionnement hivernal de la couche de surface en nitrates (Tremblay et al. 2008), la disponibilité en nitrates lors du retrait des glaces pré-conditionnant le niveau de production primaire. En outre, la production primaire au niveau du maximum profond de chlorophylle ne peut pas toujours être prise en compte lorsque la production primaire est mesurée par incorporation de traceurs pour des profondeurs photiques prédéfinies. La production

phytoplanctonique des maxima profonds de chlorophylle devrait donc être mesurée pour pouvoir obtenir des estimations de production primaire plus représentatives.

Du printemps à l'été, le phytoplancton présentait des caractéristiques d'adaptation aux faibles intensités lumineuses. D'autre part, les paramètres photosynthétiques n'ont pu être mis en relation avec les variables environnementales. Ces tendances ont déjà été observées dans les mers polaires, où les variations des paramètres photosynthétiques demeurent généralement inexpliquées (Kirst & Wiencke 1995). Sous le couvert de glace, le phytoplancton, de même que les algues de glaces, étaient adaptés aux faibles intensités lumineuses (Ban et al. 2006), et suite au retrait des glaces, les cellules phytoplanctoniques s'accumulaient en profondeur formant un maximum profond de chlorophylle. L'adaptation aux faibles intensités lumineuses pourrait donc constituer un avantage à la formation rapide de maxima profonds de chlorophylle après le retrait des glaces.

Tout au long de la période libre de glace, le picophytoplancton présentait des abondances cellulaires relativement élevées, et dominait généralement le phytoplancton <20 µm en terme d'abondance. La dynamique des glaces modifiait la structure de taille du phytoplancton <20 µm dans le golfe d'Amundsen. En effet, la fraction picophytoplanctonique semblait répondre plus rapidement que le nanophytoplancton au retrait des glaces au printemps, et le passage de glace dérivante au cours de l'été favorisait également le développement du picophytoplancton. De plus, la vitesse de retrait des glaces au printemps semblait également modeler la structure de taille des communautés. Un retrait

lent favoriserait la croissance du picophytoplancton, alors qu'un retrait plus rapide favoriserait les deux fractions pico- et nanophytoplanctoniques. Sur le plateau continental, les eaux du panache conduisaient à des conditions favorables pour le nano- et du microphytoplancton en été, et pour le pico- et le nanophytoplancton en automne. En outre, en été les phénomènes d'upwelling favorisaient la croissance de l'ensemble des classes de taille (pico-, nano- et microphytoplancton). Sur le plateau continental du Mackenzie, la structure de taille des communautés phytoplanctoniques était dictée par la combinaison des variations du débit du fleuve Mackenzie et des vents. Au cours de la période libre de glace, la forte rétention des cellules picophytoplanctoniques dans les eaux de surface souligne l'importance du picophytoplancton au sein du réseau trophique microbien.

Les années échantillonnées dans le cadre du programme CASES correspondaient au début de la période d'accélération de la réduction du couvert de glace dans l'océan Arctique (Comiso et al. 2008). En outre, les écosystèmes des mers de Bering et de Barents subissent déjà des transformations sous l'effet des changements climatiques (Grebmeier et al. 2006, Hegseth et al. 2008, Wassmann et al. 2008). Les communautés phytoplanctoniques étudiées dans le cadre de cette thèse pourraient donc être sur le point de changer sous l'effet des changements climatiques. Les changements climatiques engendreraient des perturbations telles que : le réchauffement de l'océan Arctique, la réduction du couvert de glace, l'augmentation d'apports de matières dissoutes et particulaires due au dégel du pergélisol et à l'érosion côtière accrue, la fonte des glaciers, ainsi que la hausse des débits fluviaux suite à l'accroissement des précipitations (ACIA 2005). La réduction du couvert de glace

permettrait une exposition plus importante des eaux de surface à l'effet des vents, favorisant ainsi le mélange de la couche de surface. Ainsi, des phénomènes d'upwelling plus fréquents et l'augmentation du débit du Mackenzie pourraient conduire à une augmentation de la production primaire à fort potentiel d'exportation en profondeur sur le plateau continental du Mackenzie. Cependant, les apports d'eau douce accrus augmenteraient la stratification des eaux de surface, et l'augmentation des apports de matières dissoutes et particulaires diminueraient la pénétration de la lumière en profondeur. La diminution de la disponibilité en lumière en profondeur pourrait donc limiter la production des maxima profonds de chlorophylle dans le golfe d'Amundsen. Néanmoins, l'influence plus importante des vents pourrait favoriser le réapprovisionnement de la couche de surface en éléments nutritifs, augmentant ainsi la production primaire. Toutefois, au cours des périodes étudiées, les vents n'ont pas atteint des intensités suffisantes pour altérer la stratification des eaux de surface dans le golfe d'Amundsen. A partir des informations disponibles, il demeure toujours difficile de prévoir quels pourraient être les effets des perturbations climatiques sur la production primaire. Au niveau des communautés phytoplanctoniques, l'invasion d'espèces issues des latitudes plus basses semble être une conséquence probable du réchauffement (Hegseth et al. 2008), de même l'augmentation de température pourrait conduire à un changement des groupes dominant les communautés phytoplanctoniques (Hare et al. 2008). Le manque de séries temporelles plus fréquentes en mer de Beaufort constitue un obstacle majeur à la compréhension du fonctionnement de l'écosystème de la mer de Beaufort et à la prévision des effets potentiels des changements climatiques.

Dans un océan Arctique en cours de transformation, la composition du phytoplancton pourrait être altérée, et des espèces provenant des latitudes plus tempérées pourraient migrer dans l'océan Arctique. Cependant, pour les cellules phytoplanctoniques de petite taille la morphologie ne semble pas être révélatrice de la spécialisation des cellules à l'environnement arctique, comme c'est le cas pour le genre *Micromonas*. La caractérisation génétique des espèces présentes dans l'océan Arctique permettrait d'identifier les espèces ou les écotypes spécialistes de l'océan Arctique, et ainsi de suivre l'invasion vraisemblable d'espèces phytoplanctoniques d'origine pacifique ou atlantique.

La composition spécifique des assemblages phytoplanctoniques conditionne la production primaire et son transfert vers les niveaux supérieurs des réseaux trophiques. Au cours du programme CASES, l'échantillonnage n'a pas permis de caractériser les périodes d'efflorescence, les plus susceptibles de favoriser le transfert de carbone vers le réseau trophique herbivore et l'export de carbone en profondeur, dans la polynie du Cap Bathurst. La mise en place de programmes de recherche déployant une logistique permettant de laisser un brise-glace tout au long de l'hiver dans la région du golfe d'Amundsen serait donc appropriée pour permettre d'étudier la dynamique des efflorescences phytoplanctoniques dans la polynie du Cap Bathurst. De même, ceci permettrait d'évaluer l'influence de la dynamique du couvert de glace pour l'ensemble de la période printanière.

Au cours du programme CASES, seule la production phytoplanctonique particulaire a été estimée. Cependant, dans les régions polaires une part importante du carbone fixé par

le phytoplancton conduit à la formation de produits dissous (Carlson et al. 1998, Vernet et al. 1998). L'estimation de la production de carbone dissous permettrait donc de mieux comprendre le rôle du phytoplancton au sein du réseau trophique microbien. De même, la production primaire au niveau des maxima profonds de chlorophylle n'a pu être estimée dans certaines régions. Par exemple, au niveau du canyon Mackenzie, les maxima profonds de chlorophylle correspondaient à des profondeurs où la disponibilité en lumière représentait moins de 1 % de la lumière incidente. Au cours du printemps et de l'été, la profondeur de 0,1 % de lumière incidente serait probablement plus représentative de la limite de la zone euphotique. D'une manière générale, un effort particulier devrait être déployé afin d'estimer la production et l'écophysiologie des maxima profonds de chlorophylle, ainsi que leur importance dans le transfert de carbone dans l'écosystème de la mer de Beaufort. De plus, il serait intéressant d'estimer les pertes de production phytoplanctonique. Le broutage par le mesozooplancton et le microzooplancton est le mode de perte le plus fréquemment pris en considération. Cependant les pertes par lyse cellulaire due aux infections virales et à la mort cellulaire (programmée ou induite) semblent représenter une proportion significative de la production phytoplanctonique dans des environnements variés (e.g. régions oligotrophes, eutrophes, equatoriales, tropicales ou tempérées ; Brussaard et al. 1995, Agustí et al. 1998, Veldhuis et al. 2001, Agustí & Sánchez 2002, Brussaard 2004, Franklin et al. 2006, Baudoux et al. 2007) et devraient dorénavant être prises en compte afin d'élaborer les bilans de carbone dans l'océan Arctique.

Finalement, dans un environnement promis à d'importantes modifications sous l'effet des changements climatiques, où l'écosystème est enclin à subir des transformations abruptes, la poursuite de campagnes d'échantillonnage régulières est essentielle pour comprendre le fonctionnement des écosystèmes des régions où les données sont encore peu disponibles, suivre l'évolution de ces écosystèmes et permettre la prédiction des impacts éventuels des perturbations climatiques.

REFERENCES BIBLIOGRAPHIQUES

Aagaard K (1984) The Beaufort Undercurrent. In: Barnes PW, Schell DM, Reimnitz E (eds) The Alaskan Beaufort Sea: ecosystems and environments. Academic Press, New York, p 47-71

ACIA (2005) Arctic Climate Impact Assessment. Cambridge University Press, New York

Agawin NSR, Duarte CM, Agustí S (2000) Nutrient and temperature control of the contribution of picoplankton to phytoplankton biomass and production. Limnol Oceanogr 45:591-600

Agustí S, Sánchez MC (2002) Cell viability in natural phytoplankton communities quantified by a membrane permeability probe. Limnol Oceanogr 47(3):818-828

Agustí S, Satta MP, Mura MP, Benavent E (1998) Dissolved esteras activity as a tracer of phytoplankton lysis: evidence of high phytoplankton lysis rates in the northwestern Mediterranean. Limnol Oceanogr 43(8):1836-1849

Alexander V (1974) Primary productivity regimes of the nearshore Beaufort Sea, with reference to potential poles of ice biota. In: Reed JC, Sater JE (eds) The coast and the shelf of the Beaufort Sea. The Arctic Institute of North America, Arlington, p 609-635

AMAP (1998) AMAP Assessment report: Arctic pollution issues. Arctic Monitoring and Assessment Program (AMAP), Oslo, Norway

Arrigo KR, van Dijken GL (2004) Annual cycles of sea ice and phytoplankton in Cape Bathurst polynya, southeastern Beaufort Sea, Canadian Arctic. Geophys Res Lett 31:L08304, doi 10.1029/2003GL018978

Arzel O, Fichefet T, Goosse H (2006) Sea ice evolution over the 20th and 21st centuries as simulated by current AOGCMs. Ocean Modelling 12:401-415

Ban A, Aikawa S, Hattori H, Sasaki H, Sampei M, Kudoh S, Fukuchi M, Satoh K, Kashino Y (2006) Comparative analysis of photosynthetic properties in ice algae and phytoplankton inhabiting Franklin Bay, the Canadian Arctic, with those mesophilic diatoms during CASES 03-04. Polar Biosci 19:11-28

Barber DG, Hanesiak JM (2004) Meteorological forcing of sea ice concentrations in the southern Beaufort Sea over the period 1979 to 2000. J Geophys Res 109:C06014, doi 10.1029/2003JC002027

Baudoux A-C, Veldhuis MJW, Witte HJ, Brussaard CPD (2007) Viruses as mortality agents of picophytoplankton in the deep chlorophyll maximum layer during IRONAGES III. Limnol Oceanogr 52(6):2519-2529

Bérard-Therriault L, Poulin M, Bossé L (1999) Guide d'identification du phytoplancton marin de l'estuaire et du golfe du Saint-Laurent incluant également certains protozoaires. Publ Spéc Can Sci Halieut Aquat 128:1-387

Bessière A, Nozais C, Brugel S, Demers S, Desrosiers G (2007) Metazoan meiofauna dynamics and pelagic-benthic coupling in the Southeastern Beaufort Sea, Arctic Ocean. Polar Biol, doi 10.1007/s00300-007-0270-6

Booth BC, Horner RA (1997) Microalgae on the Arctic Ocean Section, 1994: species abundance and biomass. Deep-Sea Res II 44:1607-1622

Booth BC, Smith WO Jr (1997) Autotrophic flagellates and diatoms in the Northeast Water Polynya, Greenland: summer 1993. J Mar Syst 10:241-261

Borstadt GA, Gower FJR (1984) Phytoplankton chlorophyll distribution in the eastern Canadian Arctic. Arctic 37:234-243

Brussaard CPD (2004) Viral control of phytoplankton populations – a review. J Eukaryot Microbiol 51(2):125-138

Brussaard CPD, Riegman R, Noordeloos AAM, Cadée GC, Witte H, Kop AJ, Nieuwland G, van Duyl FC, Bak RPM (1995) Effects of grazing, sedimentation and phytoplankton cell lysis on the structure of a coastal pelagic food web. Mar Ecol Prog Ser 123:259-271

Canadian Ice Service of Environment Canada (http://ice-glaces.ec.gc.ca/)

Carlson CA, Ducklow HW, Hansell DA, Smith WO Jr (1998) Organic carbon partitioning during spring phytoplankton blooms in the Ross Sea polynya and the Sargasso Sea. Limnol Oceanogr 43(3):375-386

Carmack E, Barber D, Christensen J, Macdonald R, Rudels B, Sakshaug E (2006)Climate variability and physical forcing of the food webs and the carbon budget on panarctic shelves. Prog Oceanogr 7:145-181

Carmack E, Wassmann P (2006) Food webs and physical-biological coupling on pan-Arctic shelves: unifying concepts and comprehensive perspectives. Prog Oceanogr 71:446-477

Carmack EC, Chapman DC (2003) Wind-driven shelf/basin exchange on an Arctic shelf: The joint roles of ice cover extent and shelf-break bathymetry. Geophys Res Lett 30(14):1778, doi 10.1029/2003GL017526

Carmack EC, Macdonald RW (2002) Oceanography of the Canadian shelf of the Beaufort Sea: a setting for marine life. Arctic 55(supp 1):29-45

Carmack EC, Macdonald RW, Jasper S (2004) Phytoplankton productivity on the Canadian Shelf of the Beaufort Sea. Mar Ecol Prog Ser 277:37-50

Carmack EC, Macdonald RW, Papadakis JE (1989) Water mass structure and boundaries in the Mackenzie Shelf estuary. J Geophys Res 94:18043-18055

Cavalieri D, Parkinson C, Gloersen P, Zwally HJ (1996), updated 2006. Sea ice concentrations from Nimbus-7 SMMR and DMSP SSM/I passive microwave data, September 2003 to August 2004. Digital Media. National Snow and Ice Data Center, Boulder, CO, USA. URL: http://www.nsidc.org/data/nsidc-0051.htm

Cavalieri DJ, Gloersen P, Parkinson CL, Comiso JC, Zwally HJ (1997) Observed hemispheric asymmetry in global sea ice change. Science, 278:1104-1106.

Chisholm SW (1992) Phytoplankton size. In: Falkowski P, Woodhead A (eds) Primary productivity and biogeochemical cycles in the sea. Plenum press, p 213-237

Clarke KR (1993) Non-parametric analyses of changes in community structure. Aust J Ecol 18:117–143

Comiso JC (2003) Warming trends in the Arctic from clear sky satellite observations. J Clim 16:3498-3510

Comiso JC, Parkinson CL, Gersten R, Stock L (2008) Accelarated decline in the Arctic sea ice cover. Geophys Res Lett 35:L01703, doi 10.1029/2007GL031972

Cota GF, Pomeroy LR, Harrison WG, Jones EP, Peters F, Sheldon, WM, Weingartner TR (1996) Nutrients, primary production and microbial heterotrophy in the southeastern Chukchi Sea: Arctic summer nutrient depletion and heterotrophy. Mar Ecol Prog Ser 135:247-258

Dale T, Rey F, Heimdal BR (1999) Seasonal development of phytoplankton at a high latitude oceanic site. Sarsia 84: 419-435

Darnis G, Barber DG, Fortier L (2007) Sea ice and the onshore-offshore gradient in pre-winter zooplankton assemblages in southeastern Beaufort Sea. J Mar Syst, doi 10.1016/j.jmarsys.2007.09.003

Deser C, Walsh JE, Timlin MS (2000) Arctic sea ice variability in the context of recent atmospheric circulation trends. J Clim 13:617-633

Deubel H, Engel M, Fetzer I, Gagaev S, Hirche H-J, Klages M, Larionov V, Lubin P, Lubina O, Nöthig E-M, Okolodkov Y, Rachor E (2003) The southern Kara Sea ecosystem: phytoplankton, zooplankton and benthos communities influenced by river run-off. In: Stein R, Fahl K, Fütterer DK, Galimov EM, Stepanets OV (eds) Siberian river run-off in the Kara Sea, Proceedings in Marine Science 6, Elsevier, Amsterdam, p 237-265

Dittmar T, Kattner G (2003) The biogeochemistry of the river and shelf ecosystem of the Arctic Ocean: a review. Mar Chem 83:103-120

Dixon KW, Delworth TL, Knutson TR, Spelman MJ, Stouffer KJ (2003) A comparison of climate change simulations produced by two GFDL coupled climate models. Global Planet Change 37:81-102

DOE (1994) Handbook of methods for the analysis of the various parameters of the carbon dioxide system in sea water. In: Dickson AG, Goyet C (eds), Version 2, ORNL/CDIAC-74, http://www.mpl.ucsd.edu/people/adickson/CO2.QC/

Dower KM, Lucas MI, Phillips R, Dieckmann G, Robinson DH (1996) Phytoplankton biomass, P-I relationships and primary production in the Weddell Sea, Antarctica, during austral autumn. Polar Biol 16:41-52

Dugdale RC, Goering JJ (1967) Uptake of new and regenerated forms of nitrogen in primary productivity. Limnol Oceanogr 12:196-206

Environment Canada. Weather Archive of Environment Canada (http://www.climate.weatheroffice.ec.gc.ca/)

Eppley RW, Peterson BJ (1979) Particulate organic matter flux and planktonic new production in the deep ocean. Nature 282:677-680

Field JG, Clarke KR, Warwick RM (1982) A practical strategy for analyzing multispecies distribution patterns. Mar Ecol Prog Ser 8:37-52

Forest A, Sampei M, Makabe R, Sasaki H, Barber D, Gratton Y, Wassmann P, Fortier L (2008) The annual cycle of particulate organic carbon export in Franklin Bay (Canadian Arctic): environmental control and food web implications. J Geophys Res 113:C03S05, doi 10.1029/2007JC004262

Franklin DJ, Brussaard CPD, Berges JA (2006) What is the role and nature of programmed cell death in phytoplankton ecology. Eur J Phycol 41:1-14

Garneau M-E, Gosselin M, Klein B, Tremblay J-E, Fouilland E (2007) New and regenerated production during late summer bloom in an Arctic polynya. Mar Ecol Prog Ser 345:13-26

Garneau M-E, Roy S, Lovejoy C, Vincent WF (2008) Seasonal dynamics of bacterial biomass and production in a coastal arctic ecosystem: Franklin Bay, western Canadian Arctic. J Geophys Res 113:C07S91, doi: 10.1029/2007JC004281

Garneau M-E, Vincent WF, Alonso-Sáez L, Gratton Y, Lovejoy C (2006) Prokaryotic community structure and heterotrophic production in a river-influenced coastal arctic ecosystem. Aquat Microb Ecol 42:27-40

Gosselin M, Levasseur M, Wheeler PA, Horner RA, Booth BC (1997) New measurements of phytoplankton and ice algal production in the Arctic Ocean. Deep-Sea Res II 44(8):1623-1644

Gradinger R, Bluhm B (2005) Arctic Ocean exploration 2002. Polar Biol 28:169-170

Gradinger R, Ikävalko J (1998) Organism incorporation into newly forming Arctic sea ice in the Greenland Sea. J Plankton Res 20:871-886

Grasshoff K (1999) Methods of seawater analysis, 3 ed, Wiley-VCH, Weinheim, New York

Grebmeier JM, Overland JE, Moore SE, Farley EV, Carmack EC, Cooper LW, Frey KE, Helle JH, Mclaughlin FA, McNutt SL (2006) A major ecosystem shift in the northern Bering Sea. Science 311:1461-1464

Hare CE, Leblanc K, DiTullio GR, Kudela RM, Zhang Y, Lee PA, Riseman S, Hutchins DA (2007) Consequences of increased temperature and CO_2 for phytoplankton community structure in the Bering Sea. Mar Ecol Prog Ser 352:9-16

Harrison WG, Platt T (1986) Photosynthesis-irradiance relationships in polar and temperate phytoplankton populations. Polar Biol 5:153-164

Harrison WG, Wood LJE (1988) Inorganic nitrogen uptake by marine picoplankton: evidence for size partitioning. Limnol Oceanogr 33:468-475

Hegseth EN (1997) Phytoplankton of the Barents Sea – the end of a growth season. Polar Biol 17:235-241

Hegseth EN (1998) Primary production of the northern Barents Sea. Polar Res 17(2):113-123

Hegseth EN, Sundfjord A (2008) Intrusion and blooming of Atlantic phytoplankton species in the high Arctic. J Mar Syst, doi 10.1016/j.jmarsys.2007.11.011

Heimdal BR (1983) Phytoplankton and nutrients in the waters north-west of Spitsbergen in autumn of 1979. J Plankton Res 5(6):901-918

Heiskanen A-S, Keck A (1996) Distribution and sinking rates of phytoplankton, detritus, and particulate biogenic silica in the Laptev Sea and Lena River (Arctic Siberia). Mar Chem 53:229-245

Hill V, Cota G (2005) Spatial patterns of primary production on the shelf, slope and basin of the Western Arctic in 2002. Deep-Sea Res II 52:3344-3354

Holland MM, Bitz CM, Tremblay B (2006) Future abrupt reductions in the summer Arctic sea ice. Geophys Res Lett 33:L23503, doi 10.1029/2006GL028024

Holloway G, Sou T (2002) Has Arctic sea ice rapidly thinned? J Clim 15:1692-1701

Holmes MR, McClelland JW, Peterson BJ, Shiklomanov IA, Shiklomanov AI, Zhulidov AV, Gordeev VV, Bobrovitskaya NN (2002) A circumpolar perspective on fluvial sediment flux to the Arctic Ocean. Global Biogeochem Cycles 16/4, doi 10.1029/2002GB001920

Horner R (1984) Phytoplankton abundance, chlorophyll a, and primary productivity in the western Beaufort Sea. In: Barnes PW, Schell DM, Reimnitz E (eds) The Alaskan Beaufort Sea: ecosystems and environments. Academic Press, p 295-310

Horner R, Schrader GC (1982) Relative contributions of ice algae, phytoplankton, and benthic microalgae to primary production in nearshore regions of the Beaufort Sea. Arctic 35(4):485-503

Hsiao SIC, Foy MG, Kittle DW (1977) Standing stocks, community structure, species composition, distribution, and primary production of natural populations of phytoplankton in the southern Beaufort Sea. Can J Bot 55:685-694

IPCC (2007) Climate change 2007: the physical science basis; Contribution of Working Group I to the Fourth Assessment Report of the Intergovernmental Panel on Climate Change. Cambridge University Press, Cambridge and New York

IPCC (Intergovernmental Panel on Climate Change) (2001) Climate change 2001 ; synthesis report : contribution of working groups I, II and III to the third assessment report of the Intergovernmental Panel on Climate Change. Cambridge University Press, Cambridge and New York

Jakobsson M, Grantz A, Kristoffersen Y, Macnab R (2004) Physiography and bathymetry of the Arctic Ocean. In: Stein R, Macdonald RW (eds) The organic carbon cycle in the Arctic Ocean. Springer-Verlag, Berlin Heidelberg, p 1-5

Jensen F, Hansen BW (2000) Ciliates and heterotrophic dinoflagellates in the marginal ice zone of the central Barents Sea during spring. J Mar Biol Ass UK 80(1):45-54

Jensen HM, Pedersen L, Burmeister A, Hansen BW (1999) Pelagic primary production during summer along 65 to 72°N off West Greenland. Polar Biol 21:269-278

Jensen KG, Moestrup Ø (1998) The genus *Chaetoceros* (Bacillariophyceae) in inner Danish coastal waters. Opera Bot 133:1-68

Johannessen OM, Bengtsson L, Miles MW, Kuzmina SI, Semenov VA, Alekseev GV, Nagurnyi AP, Zakharov VF, Bobylev LP, Pettersson LH, Hasselmann K, Cattle HP (2004) Arctic climate change: observed and modelled temperature and sea-ice variability. Tellus A 56:328-341

Johannessen OM, Shalina E, Miles MV (1999) Satellite evidence far an Arctic sea ice cover in transformation. Science, 286:1937-1939

Johnson KM, Wills KD, Butler DB, Johnson WK, Wong CS (1993) Coulometric total carbon dioxide analysis for marine studies: maximizing the performance of an automated gas extraction system and coulometric detector. Mar Chem 44:167-187

Juul-Pedersen T (2007) Spatial and temporal patterns of sedimentation below the euphotic zone in the Canadian Beaufort Sea. Thèse de doctorat, Université du Québec, Rimouski

Juul-Pedersen T, Michel C, Gosselin M (2008) Influence of the Mackenzie River plume on the sinking export of particulate material on the shelf. J Mar Syst, doi 10.1016/j.jmarsys.2008.02.001

Kashino Y, Kudoh S, Hayashi Y, Suzuki Y, Odate T, Hirawake T, Satoh K, Fukuchi M (2002) Strategies of phytoplankton to perform effective photosynthesis in the North Water. Deep-Sea Res II 49:5049-5061

Kirst GO, Wiencke C (1995) Ecophysiology of polar algae. J Phycol 31:181-199

Klein B, LeBlanc B, Mei Z-P, Beret R, Michaud J, Mundy CJ, von Quillfeldt CH, Garneau M-E, Roy S, Gratton Y, Cochran JK, Bélanger S, Larouche P, Pakulski JD, Rivkin RB, Legendre L (2002) Phytoplankton biomass, production and potential export in the North Water. Deep-Sea Res II 49:4983-5002

Knap A, Michaels A, Close A, Ducklow H, Dickson A (1996) Protocols for the Joint Global Ocean Flux Study (JGOFS) core measurements. JGOFS Report Nr. 19. Reprint of the IOC Manuals and Guides No. 29, UNESCO, Bergen

Lavoie D, Macdonald RW, Denman KL (2008) Primary productivity and export fluxes on the Canadian shelf of the Beaufort Sea: a modelling study. J Mar Syst, doi 10.1016/j.jmarsys.2008.07.007

Lee SH, Whitledge TE, Kang S-H (2007) Recent carbon and nitrogen uptake rates of phytoplankton in Bering Strait and the Chukchi Sea. Cont Shelf Res, doi 10.1016/j.csr.2007.05.009

Lee SH, Withledge TE (2005) Primary and new production in the deep Canada Basin. Polar Biol 28:190-197

Legendre L (1990) The significance of microalgal blooms for fisheries and for export of particulate organic carbon in oceans. J Plankton Res 12:681-699.

Legendre L, Gosselin M, Hirche HJ, Kattner G, Rosenberg G (1993) Environmental control and potential fate of size-fractionated phytoplankton production in the Greenland Sea (75°N). Mar Ecol Prog Ser 98:297-313

Legendre L, Le Fèvre J (1991) From individual plankton cells to pelagic marine ecosystems and to global biogeochemical cycles. In: Demers S (ed) Particle analysis in oceanography. Springer Verlag, Berlin, p 261-300

Legendre L, Le Fèvre J (1995) Microbial food webs and the export of biogenic carbon in oceans. Aquat Microb Ecol 9:69-77

Levinsen H, Nielsen TG (2002) The trophic role of marine pelagic ciliates and heterotrophic dinoflagellates in arctic and temperate coastal ecosystems: a cross-latitude comparison. Limnol Oceanogr 47(2):427-439

Levinsen H, Nielsen TG, Hansen BW (1999) Plankton community structure and carbon cycling on the western coats of Greenland during stratified summer situation. II. Heterotrophic dinoflagellates and ciliates. Aquat Microb Ecol 16:217-232

Lewis MR, Smith JC (1983) A small volume, short-incubation-time method for measurement of photosynthesis as a function of incident irradiance. Mar Ecol Prog Ser 13:99-102

Li WKW (1986) Experimental approaches to field measurements: methods and interpretation. In: Platt T, Li WKW (eds) Photosynthetic picoplankton. Can Bull Fish Aquat Sci 214:251-286

Li WKW, Harrison WG (2001) Chlorophyll, bacteria and picophytoplankton in ecological provinces of the North Atlantic. Deep-Sea Res II 48:2271-2293

Liu H, Imai K, Suzuki K, Nojiri Y, Tsurushima N, Saino T (2002a) Seasonal variability of picophytoplankton and bacteria in the western subarctic Pacific Ocean at station KNOT. Deep-Sea Res II 49:5409-5420

Liu H, Suzuki K, Minami C, Saino T, Watanabe M (2002b) Picoplankton community structure in the subarctic Pacific Ocean and the Bering Sea during summer 1999. Mar Ecol Prog Ser 237:1-14

Lomas MW, Glibert PM (1999) Temperature regulation of nitrate uptake: a novel hypothesis about nitrate uptake and reduction in cool-water diatoms. Limnol Oceanogr 44(3):556-572

Lovejoy C, Legendre L, Martineau M-J, Bâcle J, von Quillfeldt CH (2002) Distribution of phytoplankton and other protists in the Noth Water. Deep-Sea Res II 49:5027-5047

Lovejoy C, Massana R, Pedrós-Alió C (2006) Diversity and distribution of marine microbial eukaryotes in the Arctic Ocean and adjacent seas. Appl Environ Microbiol 72(7):3085-3095

Lovejoy C, Vincent WF, Bonilla S, Roy S, Martineau M-J, Terrado R, Potvin M, Massana R, Pedrós-Alió C (2007) Distribution, phylogeny, and growth of cold-adpated picoprasinophytes in Arctic seas. J Phycol 43:78-89

Macdonald RW, Naidu AS, Yunker MB, Gobeil C (2004b) The Beaufort Sea: distribution, sources, fluxes and burial of organic carbon. In: Stein R, Macdonald RW (eds) The organic carbon cycle in the Arctic Ocean. Springer-Verlag, Berlin Heidelberg, p 177-192

Macdonald RW, Sakshaug E, Stein R (2004a) The Arctic Ocean: modern status and recent climate change. In: Stein R, Macdonald RW (eds) The organic carbon cycle in the Arctic Ocean. Springer-Verlag, Berlin Heidelberg, p 6-20

Macdonald RW, Soloman SM, Cranston RE, Welch HE, Yunker MB, Gobeil C (1998) A sediment and organic carbon budget for the Canadian Arctic Shelf. Mar Geol 144:255-273

Macdonald RW, Wong CS, Erickson P (1987) The distribution of nutrients in the southeastern Beaufort Sea: implications for water circulation and primary production. J Geophys Res 92(C3):2939-2952

Macdonald RW, Yu Y (2006) The Mackenzie Estuary of the Arctic Ocean. In: Wangersky PJ (ed) The handbook of environmental chemistry. Springer-Verlag, Berlin, p 91-120

Marie D, Simon N, Vaulot D (2005) Phytoplankton cell counting by flow cytometry. In: Andersen RA (ed) Algal culturing techniques, vol 17. Academic Press, London, p 253-267

McLaughlin FA, Carmack EC, Macdonald RW (1996) Physical and geochemical properties across the Atlantic/Pacific water mass front in the southern Canadian Basin. J Geophys Res 101(C1):1183-1197

Mingelbier M, Klein B, Claereboudt MR, Legendre L (1994) Measurement of daily primary production using 24h incubations with the ^{14}C method: a caveat. Mar Ecol Prog Ser 113:301-309

Moreira-Turcq PF, Cauwet G, Martin JM (2001) Contribution of flow cytometry to estimate picoplankton biomass in estuarine systems. Hydrobiologia 462:157-168

Mostajir B, Gosselin M, Gratton Y, Booth B, Vasseur C, Garneau M-E, Fouilland E, Vidussi F, Demers S (2001) Surface water distribution of pico- and nanophytoplankton in relation to two distinctive water masses in the North Water, northern Baffin Bay, during fall. Aquat Microb Ecol 23:205-212

Myers JL, Well AD (2003) Research design and statistical analysis. Lawrence Erlbaum Associates, London

Not F, Massana R, Latasa M, Marie D, Colson C, Eikrem W, Pedrós-Alió C, Vaulot D, Simon N (2005) Late summer community composition and abundance of photosynthetic picoeukaryotes in Norwegian and Barents Seas. Limnol Oceanogr 50(5):1677-1686

Nöthig E-M, Okolodkov Y, Larionov VV, Makarevich PR (2003) Phytoplankton distribution in the inner Kara Sea: a comparison of three summer investigations. In: Stein R, Fahl K, Fütterer DK, Galimov EM, Stepanets OV (eds) Siberian river run-off in the Kara Sea, Proceedings in Marine Science 6, Elsevier, Amsterdam, p 163-183

NSIDC (2007) Arctic sea ice shatters all previous record lows. http://nsidc.org/news/press/2007_seaiceminimum/20071001_pressrelease.html

Olli K (1999) Diel vertical migration of phytoplankton and heterotrophic flagellates in the Gulf of Riga. J Mar Syst 23:145-163

Olli K, Wassmann P, Reigstad M, Ratkova TN, Arashkevich E, Pasternak A, Matrai PA, Knulst J, Tranvik L, Klais R, Jacobsen A (2007) The fate of production in the central Arctic Ocean – top-down regulation by zooplankton expatriates? Prog Oceanogr 72:84-113

Overpeck J, Hughen K, Hardy D, Bradley R, Case R, Douglas M, Finney B, Gajewski K, Jacoby G, Jennings A, Lamoureux S, Lasca A, Macdonald G, Moore J, Retelle M, Smith S, Wolfe A, Zielinski G (1997) Arctic environmental change of the last four centuries. Science 278:1251-1256

Owrid G, Socal G, Civitarese G, Luchetta A, Wiktor J, Nöthig E-M, Andreassen I, Schauer U, Strass V (2000) Spatial variability of phytoplankton, nutrients and new production estimates in the waters around Svalbard. Polar Res 19(2):155-171

Palmisano AC, Beeler SooHoo J, Moe RL, Sullivan CW (1987) Sea ice microbial communities. VII. Changes in under-ice spectral irradiance during the development of Antarctic sea ice microalgal communities. Mar Ecol Prog Ser 35:165-173

Parsons TR, Maita Y, Lalli CM (1984) A manual of chemical and biological methods for seawater analysis. Pergamon Press, Toronto

Parsons TR, Webb DG, Dovey H, Haigh R, Lawrence M, Hopky GE (1988) Production studies in the Mackenzie River / Beaufort Sea Estuary. Polar Biol 8:235-239

Parsons TR, Webb DG, Rokeby BE, Lawrence M, Hopky GE, Chiperzak DB (1989) Autotrophic and heterotrophic production in the Mackenzie River/Beaufort Sea estuary. Polar Biol 9:261-266

Pesant S, Legendre L, Gosselin M, Smith REH, Kattner G, Ramseier RO (1996) Size-differential regimes of phytoplankton production in the Northeast Water Polynya (71°-81°N). Mar Ecol Prog Ser 142:75-86

Peterson BJ, Holmes RM, McClelland JW, Vörösmarty CJ, Lammers RB, Shiklomanov AI, Shiklomanov IA, Rahmstorf S (2002) Increasing river discharge to the Arctic Ocean. Science 298:2171-2173

Peterson BJ, McClelland J, Curry R, Holmes RN, Walsh JE, Aagaard K (2006) Trajectory shifts in the Arctic and Subarctic freshwater cycle. Science 313:1061-1066

Pickart RS (2004) Shelfbreak circulation in the Alaskan Beaufort Sea: Mean structure and variability. J Geophys Res 109, doi 10.1029/2003JC001912

Platt T, Gallegos CL, Harrison WG (1980) Photoinhibition of photosynthesis in natural assemblages of marine phytoplankton. J Mar Res 38(4):687-701

Rachold V, Eicken H, Gordeev VV, Grigoriev MN, Hubberten HW, Lisitzin AP, Shevchenko VP, Schirrmeister L (2004) Modern terrigenous organic carbon input to the Arctic Ocean. In: Stein R, Macdonald RW (eds) The organic carbon cycle in the Arctic Ocean. Springer-Verlag, Berlin Heidelberg, p 33-54

Ralph PJ, Ryan KG, Martin A, Fenton G (2007) Melting out of sea ice causes greater photosynthetic stress in algae than freezing in. J Phycol 43, doi 10.1111/j.1529-8817.2007.00382.x

Rat'kova TN, Wassmann P (2002) Seasonal variations and spatial distribution of phyto- and protozooplankton in the central Barents Sea. J Mar Syst 38:47-75

Retamal L, Bonilla S, Vincent WF (2008) Optical gradients and phytoplankton production in the Mackenzie River and the coastal Beaufort Sea. Polar Biol 31:363-379

Rey F (1991) Photosynthesis-irradiance relationships in natural phytoplankton populations of the Barents Sea. Polar Res 10(1):105-116

Rey F, Noji TT, Miller LA (2000) Seasonal phytoplankton development and new production in the central Greenland Sea. Sarsia 85:329-344

Rho T, Whitledge TE (2007) Characteristics of seasonal and spatial variations of primary production over the southeastern Bering Sea shelf. Cont Shelf Res 27:2556-2569

Richardson K, Markager S, Buch E, Lassen MF, Kristensen AS (2005) Seasonal distribution of primary production, phytoplankton biomass and size distribution in the Greenland Sea. Deep-Sea Res I 52:979-999

Rigor IG, Colony RL, Martin S (2000) Variations in surface air temperature observations in the Arctic, 1979-97. J Clim 13:896-914

Rose JM, Caron DA (2007) Does low temperature constrain the growth rates of heterotrophic protists? Evidence and implications for algal blooms in cold waters. Limnol Oceanogr 52(2):886-895

Rothrock DA, Yu Y, Maykut GA (1999) Thinning of the Arctic sea-ice cover. Geophysical Research Letter 26:3469-3472

Różańska M, Poulin M, Gosselin M (2007) Protist entrapement in newly formed sea ice in the Coastal Arctic Ocean. J Mar Syst, doi 10.1016/j.jmarsys.2007.11.009

Sakshaug E (2004) Primary and secondary production in the Arctic seas. In: Stein R, Macdonald RW (eds) The organic carbon cycle in the Arctic Ocean. Springer-Verlag, Berlin Heidelberg, p 57-81

Sakshaug E, Skjoldal HR (1989) Life at the ice edge. Ambio 18:60-67

Sakshaug E, Slagstad D (1991) Light and productivity of phytoplankton in polar marine ecosystems: a physiological view. Polar Res 10(1):69-85

Schloss IR, Nozais C, Mas S, van Hardenberg B, Carmack E, Tremblay J-E, Brugel S, Demers S (2008) Picophytoplankton and nanophytoplankton abundance and distribution in the southeastern Beaufort Sea (Mackenzie Shelf and Amundsen Gulf) during fall 2002. J Mar Syst, doi 10.1016/j.jmarsys.2008.01.004

Schmid MK, Piepenburg D, Golikov AA, von Juterzenka K, Petryashov VV, Spindler M (2006) Trophic pathways and carbon flux patterns in the Laptev Sea. Prog Oceanogr 71:14-330

Serreze MC, Holland MM, Stroeve J (2007) Perspectives on the Arctic's shrinking sea-ice cover. Science 315:1533-1536

Sherr EB, Sherr BF, Wheeler PA, Thompson K (2003) Temporal and spatial variation in stocks of autotrophic and heterotrophic microbes in the upper water column of the central Arctic Ocean. Deep-Sea Res I 50:557-571

Shindell DT, Miller RL, Schmidt GA, Pandolfo L (1999) Simulation of recent northern winter climate trends by greenhouse-gas forcing. Nature 399:452-455

Sieburth JMcN, Smetacek V, Lenz J (1978) Pelagic ecosystem structure: heterotrophic compartments of the plankton and their relationships to plankton size fractions. Limnol Oceanogr 23:1256-1263

Simpson KG (2008) Nutrient dynamics and nitrogen-based production in the Western Canadian Arctic Ocean. Thèse de maîtrise, Université McGill, Montréal

Simpson KG, Tremblay J, Gratton Y, Price NM (2008) An annual study of inorganic nitrogen and phosphorus, and silicic acid distribution in the southeastern Beaufort Sea. J Geophys Res, doi 10.1029/2007JC004462

Slagstad D, Støle-Hansen K (1991) Dynamics of plankton growth in the Barents Sea: model studies. Polar Res 10:173-186

Smith SD, Muench RD, Pease CH (1990) Polynyas and leads: an overview of physical processes and environment. J Geophys Res 95(C6):9461-9479

Smith WO Jr (1995) Primary productivity and new production in the Northeast Water (Greenland) Polynya during summer 1992. J Geophys Res 100(C3):4357-4370

Smith WO Jr, Marra J, Hiscock MR, Barber RT (2000) The seasonal cycle of phytoplankton biomass and primary productivity in the Ross Sea, Antarctica. Deep-Sea Res II 47:3119-3140

Smith WO Jr, Sakhaug E (1990) Polar phytoplankton. In: Smith WO Jr (ed) Polar oceanography, Part B: Chemistry, Biology and Geology, Academic Press, San Diego, p 477-525

Smith WO Jr, Walsh ID, Booth BC, Deming JW (1995) Particulate matter and phytoplankton and bacterial biomass distributions in the Northeast Water Polynya during summer 1992. J Geophys Res 100(C3):4341-4356

Sorokin YI, Sorokin PY (1996) Plankton and primary production in the Lena estuary and in the south-eastern Laptev Sea. Est Coast Shelf Sci 43:399-418

Stambler N (2003) Primary production, light absorption and quantum yields of phytoplankton from the Bellingshausen and Amundsen Seas (Antarctica). Polar Biol 26:438-451

Stirling I (1980) The biological importance of polynyas in the Canadian Arctic. Arctic 33:303-315

Stirling I (1997) The importance of polynyas, ice edges and leads to marine mammals and birds. J Mar Syst 10:9-21

Stroeve J, Markus T, Meier WN, Miller J (2006) Recent changes in the Arctic melt season. Ann Glaciol 44:367-374

Terrado R, Lovejoy C, Massana R, Vincent WF (2008) Microbial food web responses to light and nutrients beneath the coastal Arctic Ocean sea ice during winter-spring transition. J Mar Syst, doi 10.1016/j.marsys.2007.11.001

Thomson RE, Fine IV (2003) Estimating mixed layer depth from oceanic profile data. J Atmos Ocean Technol 20:319-329

Throndsen J, Hasle GR, Tangen K (2003) Norsk Kystplanktonflora. Almater Forlag AS, Oslo

Throndsen J, Kristiansen S (1991) *Micromonas pusilla* (Prasinophyceae) as part of pico- and nanoplankton communities of the Barents Sea. Polar Res 10(1):201-207

Tomas CR (1997) Identifying marine phytoplankton. Academic Press, San Diego

Topham DR, Perkin RG, Smith SD, Anderson RJ, den Hartog G (1983) An investigation of a polynya in the Canadian Archipelago, 1, introduction and oceanography. J Geophys Res 88(C5):2888-2899

Tremblay G (2008) Répartition spatiale du pico-, nano- et du microphytoplancton dans le haut arctique canadien en fin de saison estivale. Thèse de maîtrise, Université du Québec, Rimouski

Tremblay J-E, Klein B, Legendre L, Rivkin RB, Therriault J-C (1997) Estimation of f-ratios in ocean based on phytoplankton size structure. Limnol Oceanogr 42(3):595-601

Tremblay J-E, Michel C, Hobson KA, Gosselin M, Price NM (2006) Bloom dynamics in early opening waters of the Arctic Ocean. Limnol Oceanogr 51(2):900-912

Tremblay J-E, Simpson K, Martin J, Miller L, Gratton Y, Barber D, Price NM (2008) Vertical stability and the annual dynamics of nutrients and chlorophyll fluorescence in the coastal, southeast Beaufort Sea. J Geophys Res 113:C07S90, doi 10.1029/2007JC004547

Tremblay J-E, Smith W Jr (2007) Primary production and nutrient dynamics in polynyas. In: Smith W Jr, Barber DG (eds) Polynyas: windows to the world. Elsevier, Berlin, p 239-270

Tuschling K, von Juterzenka K, Okolodkov YB, Anoshkin A (2000) Composition and distribution of the pelagic and sympagic algal assemblages in the Laptev Sea during autumnal freeze-up. J Plankton Res 22(5):843-864

Van Hilst CM, Smith WO Jr (2002) Photosynthesis/irradiance relationships in the Ross Sea, Antarctica, and their control by phytoplankton assemblage composition and environmental factors. Mar Ecol Prog Ser 226:1-12

Vanucci S, Bruni V (1998) Presence or absence of picophytoplankton in the western Ross Sea during spring 1994: a matter of size definition? Polar Biol 20:9-13

Vanucci S, Bruni V (1999) Small nanoplankton and bacteria in the western Ross Sea during sea-ice retreat (spring 1994). Polar Biol 22:311-321

Vanucci S, Mangoni O (1999) Pico- and nanophytoplankton assemblages in a subantarctic ecosystem: the Strait of Magellan. Bot Mar 42:563-572

Veldhuis MJW, Kraay GW, Timmermans KR (2001) Cell death in phytoplankton: correlation between changes in membrane permeability, photosynthetic activity, pigmentation and growth. Eur J Phycol 36:167-177

Vernet M, Matrai PA, Andreassen I (1998) Synthesis of particulate and extracellular carbon by phytoplankton at the marginal ice zone in the Barents Sea. J Geophys Res 103(C1):1023-1037

Vinnikov KY, Robock A, Stouffer RJ, Walsh JE, Parkinson CL, Cavalieri DJ, Mitchell JFB, Garrett D, Zakharov VF (1999) Global warming and northern hemisphere sea ice extent. Science 286:1934-1937

von Quillfeldt CH (1997) Distribution of diatoms in the Northeast Water Polynya, Greenland. J Mar Syst 10:211-240

Waleron M, Waleron K, Vincent WF, Wilmotte A (2007) Allochtonous imputs of riverine picocyanobacteria to coastal waters in the Arctic Ocean. FEMS Microbiol Ecol 59:356-365

Walsh JJ, Dieterle DA, Maslowski W, Whitledge TE (2004) Decadal shifts in biophysical forcing of Arctic marine food webs: numerical consequences. J Geophys Res 109:C05031, doi 10.1029/2003JC001945

Waniek JJ, Holiday NP, Davidson R, Brown L, Henson SA (2005) Freshwater control of onset and species composition of Greenland shelf spring bloom. Mar Ecol Prog Ser 288:45-57

Wassmann P (2004) Particulate organic carbon flux to the seafloor of the Arctic Ocean: quantity, seasonality and processes. In: Stein R, Macdonald RW (eds) The organic carbon cycle in the Arctic Ocean. Springer-Verlag, p 131-138

Wassmann P, Carroll J, Bellerby RGJ (2008) Carbon flux and ecosystem feedback in the northern Barents Sea in an era of climate change: an introduction. Deep-Sea Res II, doi 10.1016/j.dsr2.2008.05.025

Wassmann P, Reigstad M, Haug T, Rudels B, Carroll ML, Hop H, Gabrielsen GW, Falk-Petersen S, Denisenko SG, Arashkevich E, Slagstad D, Pavlova O (2006) Food webs and carbon flux in the Barents Sea. Progr Oceanogr 71:232-287

Wheeler PA, Gosselin M, Sherr E, Thibault D, Kirchman DL, Benner R, Whitledge TE (1996) Arctic cycling of organic carbon in the central Arctic Ocean. Nature 380:697-699

Wheeler PA, Watkins JM, Hansing RL (1997) Nutrients, organic carbon and organic nitrogen in the upper water column of the Arctic Ocean: implications for the sources of dissolved organic carbon. Deep-Sea Res II 44:1571-1592

Williams WJ, Carmack EC, Shimada K, Melling H, Aagaard K, Macdonald RW, Ingram RG (2006) Joint effects of wind and ice motion in forcing upwelling in Mackenzie Trough, Beaufort Sea. Cont Shelf Res 26(19):2352-2366

Williams WJ, Melling H, Carmack EC, Ingram RG (2008) Kugmallit Valley as a conduit for corss-shelf exchange on the Mackenzie Shelf in the Beaufort Sea. J Geophys Res 113, C02007, doi 10.1029/2006JC003591

Zar JH (1999) Biostatistical analysis. Prentice-Hall, Upper Saddle River, NJ

Zhang X, Walsh JE (2006) Toward a seasonally ice-covered Arctic Ocean: scenarios from the IPCC AR4 model simulations. J Clim 19:1730-1747